

# Adsorption of an Organic Dye with Cellulose Nanocrystals

by

Rasim Batmaz

A thesis  
presented to the University of Waterloo  
in fulfillment of the  
thesis requirement for the degree of  
Master of Applied Science  
in  
Chemical Engineering

Waterloo, Ontario, Canada, 2013

© Rasim Batmaz 2013

I hereby declare that I am the sole author of this thesis. This is a true copy of the thesis, including any required final revisions, as accepted by my examiners.

I understand that my thesis may be made electronically available to the public.

## Abstract

In developing countries many industries use dyes to colour their products, such as textiles, rubber, paper, cosmetics, leather, plastics, and food industries. Such a wide range of using dyes in many industries increases the demand of dye, and currently 100,000 dyes are commercially available with a rough estimated production of  $10^6$  tones/year. Without proper treatment, dye effluent can be mixed with surface and ground water system and it may finally enter the drinking water system. Therefore, the treatment of dye effluents before discharge to the environment has become an global challenge due to the stability and adverse effects of dyes. Among the present methods, adsorption has been preferred to other conventional techniques due to the simple design and operation, low initial investment, effectiveness and insensitivity to toxic substances.

The high surface area and the presence of permanent negative charge on the surface makes cellulose nanocrystal (CNC) an excellent candidate for the adsorption of basic (cationic) dyes. The objective of this project is to evaluate the adsorption properties of CNC for the removal of methylene blue from aqueous solution by changing the parameters such as adsorbent dosage, initial dye concentration, pH, temperature and salt concentration. It was found that the adsorption is independent of pH, however increase in temperature and ionic strength decreased the removal percentage slightly. The Langmuir and Freundlich isotherms were used to evaluate the feasibility of the adsorption process. The adsorption capacity of CNC was determined using the linearized form of Langmuir model. It possessed a value of 118 mg/g at pH 9 and 25 °C. To enhance the adsorption, CNC was oxidized with TEMPO reagent to convert primary hydroxyl groups to carboxyl groups that provides more negative charge. After the oxidation, the adsorption capacity increased from 118 to 769 mg/g.

## **Acknowledgements**

I would like to express my deepest gratitude to my supervisor, Dr. K.C. Tam who gave me the opportunity to study such an exciting project and patiently guided me throughout my master's studies. I would also like to thank Masuduz Zaman, Parinaz Akhlaghi, Baoliang Peng, Gagan Minhas and all of my labmates for their constant help and motivation. I wish to express my immense gratitude to my loving family for their guidance and mental support. Most of all I like to thank Sümeyye Batmaz, my wife who never stopped supporting me.

# Table of Contents

List of Tables	x
List of Figures	xii
<b>1 Introduction</b>	<b>1</b>
1.1 Background . . . . .	1
1.2 Objective . . . . .	4
1.3 Organization of Thesis . . . . .	4
<b>2 Literature Review</b>	<b>5</b>
2.1 Introduction . . . . .	5
2.2 Types of Dyes . . . . .	6
2.2.1 Chemical Classification of Dyes . . . . .	7
2.2.2 Usage Classification of Dyes . . . . .	7
2.2.2.1 Reactive Dyes . . . . .	7
2.2.2.2 Disperse Dyes . . . . .	9
2.2.2.3 Direct Dyes . . . . .	9

2.2.2.4	Vat Dyes . . . . .	9
2.2.2.5	Sulfur Dyes . . . . .	9
2.2.2.6	Basic (Cationic) Dyes . . . . .	9
2.2.2.7	Acid Dyes . . . . .	10
2.2.2.8	Solvent Dyes . . . . .	10
2.3	Current Technologies for Dye Removal . . . . .	10
2.3.1	Biological Methods . . . . .	10
2.3.1.1	Aerobic Treatment . . . . .	12
2.3.1.1.1	Fungi . . . . .	12
2.3.1.1.2	Bacteria . . . . .	13
2.3.1.2	Anaerobic Degradation . . . . .	14
2.3.2	Chemical Methods . . . . .	15
2.3.2.1	Oxidation . . . . .	15
2.3.2.1.1	Hydrogen Peroxide . . . . .	15
2.3.2.1.2	Sodium Hypochlorite . . . . .	17
2.3.2.1.3	Ozonation . . . . .	17
2.3.2.2	Photocatalysis . . . . .	18
2.3.3	Electrochemical Methods . . . . .	19
2.3.3.1	Electrocoagulation . . . . .	19
2.3.3.2	Electrochemical Oxidation . . . . .	19
2.3.3.3	Electrochemical Reduction . . . . .	20
2.3.4	Physicochemical Methods . . . . .	21
2.3.4.1	Ion-exchange . . . . .	21

2.3.4.2	Coagulation/Flocculation . . . . .	21
2.3.4.3	Filtration . . . . .	22
2.3.4.4	Adsorption . . . . .	23
2.3.4.5	Adsorption Isotherms . . . . .	23
2.4	Disadvantages of Current Dye Removal Technologies . . . . .	25
2.5	Adsorbents . . . . .	26
2.5.1	Activated Carbon . . . . .	28
2.5.2	Low-cost Adsorbents . . . . .	30
2.5.2.1	Agricultural Waste Products . . . . .	30
2.5.2.2	Industrial Waste Products . . . . .	30
2.5.2.3	Biosorbents . . . . .	32
2.5.2.3.1	Chitin and Chitosan: . . . . .	32
2.5.2.3.2	Biomass . . . . .	33
2.5.2.4	Clays . . . . .	35
2.6	Cellulose Nanocrystals (CNC) . . . . .	36
2.6.1	Preparation of Cellulose Nanocrystal . . . . .	39
2.6.2	Properties of CNC Suspensions . . . . .	42
2.6.3	Modifications of CNC . . . . .	44
2.6.3.1	Non-covalent Modification . . . . .	45
2.6.3.2	Covalent Modification . . . . .	45
2.6.3.2.1	Tempo-Mediated Oxidation: . . . . .	45
2.6.3.2.2	Cationization: . . . . .	46
2.6.3.2.3	Acetylation: . . . . .	48

2.6.3.2.4	Silylation: . . . . .	50
2.6.3.2.5	Aldehyde Functionalization: . . . . .	51
2.6.3.2.6	Polymer Grafting: . . . . .	51
<b>3</b>	<b>Materials and Methods</b>	<b>54</b>
3.1	Materials . . . . .	54
3.2	Carboxylation of CNC . . . . .	54
3.3	Characterization of Unmodified and Carboxylated CNC . . . . .	55
3.3.1	Fourier Infrared Transform Spectroscopy . . . . .	55
3.3.2	Potentiometric Titration . . . . .	56
3.3.3	Transmission Electron Microscopy . . . . .	56
3.4	Experimental Setup and Procedure . . . . .	57
3.4.1	Sampling Procedure . . . . .	57
3.4.2	Dye Uptake ( $q_e$ ) . . . . .	57
3.4.3	Effect of Adsorbent Dosage . . . . .	58
3.4.4	Effect of Initial Dye Concentration . . . . .	58
3.4.5	Effect of pH . . . . .	58
3.4.6	Effect of Ionic Strength . . . . .	58
3.4.7	Adsorption Isotherms and Thermodynamic Parameters . . . . .	59
<b>4</b>	<b>Results and Discussions</b>	<b>60</b>
4.1	Characterization of Unmodified and Carboxylated CNC . . . . .	60
4.1.1	Transmission Electron Microscopy . . . . .	60
4.1.2	Fourier Transform Infrared (FT-IR) Spectroscopy . . . . .	60



4.1.3	Potentiometric Titration (Determination of Carboxyl Acid Content on CNC) . . . . .	63
4.2	Wavelength of Maximum Absorbance and Calibration Curve . . . . .	64
4.3	Adsorption of Methylene Blue on Unmodified CNC . . . . .	65
4.3.1	Effect of Adsorbent Dosage . . . . .	65
4.3.2	Effect of Initial Dye Concentration . . . . .	66
4.3.3	Effect of pH . . . . .	68
4.3.4	Effect of Ionic Strength . . . . .	69
4.3.5	Adsorption Isotherms . . . . .	70
4.3.5.1	Langmuir Isotherm . . . . .	70
4.3.5.2	Freundlich Isotherm . . . . .	73
4.3.5.3	Comparison of Isotherms . . . . .	74
4.3.6	Thermodynamic Parameters . . . . .	75
4.4	Activation of CNC by Oxidation . . . . .	77
<b>5</b>	<b>Conclusions</b>	<b>80</b>
5.1	Summary . . . . .	80
5.2	Future Direction . . . . .	81
	<b>References</b>	<b>82</b>

# List of Tables

2.1	Classification of dyes according to the structure (Hunger,2003). . . . .	8
2.2	Various strains applied for decolorization. . . . .	13
2.3	Bacterial strains capable of degrading dyes in the absence of additional source.	14
2.4	Percentage decolorization of dyes using different anodes (Martínez-Huitle and Brillas, 2009). . . . .	20
2.5	Comparison of current dye removal methods ( Robinson et al. (2001), Crini (2006), Verma et al. (2012), Singh and Arora (2011)). . . . .	27
2.6	Adsorption capacities $q_m$ (mg/g) of agricultural and commercial activated carbons for methylene blue (Rafatullah et al. (2010)). . . . .	29
2.7	Adsorption capacities $q_m$ (mg/g) of agricultural waste products for methylene blue (Rafatullah et al. (2010)). . . . .	31
2.8	Adsorption capacity $q_m$ (mg/g) of chitosan for various dyes (Crini (2006)).	34
2.9	Adsorption capacities $q_m$ (mg/g) of biomass for various dyes (Crini (2006)).	35
2.10	Categories of nanocellulose materials (Klemm et al., 2011). . . . .	37
4.1	Langmuir constants, equation and regression coefficient of linearized plots for the adsorption of methylene blue on unmodified CNC. . . . .	73
4.2	Freundlich constants, equation and regression coefficient of linearized plots for the adsorption of methylene blue on unmodified CNC. . . . .	74

4.3	Freundlich constants, equation and regression coefficient of linearized plots for the adsorption of methylene blue on unmodified CNC. . . . .	75
4.4	Thermodynamic parameters for the adsorption of methylene blue on unmodified CNC. . . . .	77
4.5	Langmuir constants, equations and regression coefficients of linearized plots for the adsorption of methylene blue on carboxylated CNC. . . . .	77

# List of Figures

2.1	Current dye removal technologies. . . . .	11
2.2	Activation of hydrogen peroxide with Fe(II) and UV (Singh and Arora, 2011). . . . .	16
2.3	Degradation mechanism of azo dyes with ozone (Reife and Freeman, 1996). . . . .	18
2.4	Molecular structure of cellulose (Habibi et al., 2010). . . . .	36
2.5	TEM pictures of a) MFC and b) CNC c) SEM picture of BNC (Klemm et al., 2011). . . . .	37
2.6	a) High-pressure homogenizer b) Interior view of a high-pressure microfluidizer (Klemm et. al., 2011). . . . .	38
2.7	TEM images of cellulose nanocrystals prepared from (a) tunicate, (b) bacterial, (c) ramie, (d) sisal (Habibi et al., 2010). . . . .	39
2.8	(a) Hydrolysis mechanism of cellulose (b) Surface esterification of cellulose nanocrystal (Hsieh and Lu, 2010). . . . .	41
2.9	Model of the formation of individual crystallites. . . . .	42
2.10	(a) Orientation of nanocellulose crystals in the isotropic and anisotropic phases (Habibi et al., 2010). . . . .	43
2.11	Phase separation of CNC suspensions. The concentrations are 8.78, 7.75, 6.85 and 5.78 wt% from left to right (Dong et al., 1996). . . . .	44

2.12	a) AFM image of CNC films prepared under electrical field at 10 V with a frequency of $2.5 \times 10^5$ Hz (Habibi et. al, 2008) b) Effect of magnetic field on the orientation of cholesteric layers (Revol et al., 1994). . . . .	45
2.13	TEM images of (a) cotton microcrystals and (b) tunicate microcrystals in toluene (Heux et al., 2000). . . . .	46
2.14	Scheme of TEMPO-mediated oxidation of cellulose (Shibata and Isogai, 2003).	47
2.15	Cross-sectional representation of CNC showing the available hydroxyl groups for TEMPO-mediated oxidation (Habibi et. al 2006). . . . .	47
2.16	a)Reaction scheme showing the functionalization of CNC with EPTMAC b)Thixotropic behaviour of HPTMAC-CNC hydrogel (4.9% w/w) before agitation and after agitation (Hasani et al., 2008). . . . .	48
2.17	TEM images of tunicin microcrystals (a) before acetylation (b) after partial acetylation possessing DS value of 0.17 (Sassi and Chanzy, 1995). . . . .	49
2.18	(A) Dispersibility of (a) unmodified whiskers (b) acetylated whiskers in 1,4-dioxane (c) Suspension of acetylated whiskers viewed through crossed polars (B) TEM image of ASA-modified cellulose whisker (DS $\approx$ 0.02) dispersed in thin polystyrene film (Yuan et al., 2006). . . . .	50
2.19	Reaction scheme representing the simultaneous occurrence of acid hydrolysis and esterification of cellulose (Braun and Dorgan, 2009). . . . .	50
2.20	(A) Suspensions of silylated tunicin whiskers in THF (a) Suspension of original tunicin whisker (b) Suspension of silylated sample possessing DS value of 0.4 (c) Suspension of silylated sample possessing DS value of 0.6 (B) Model of the surface silylation of cellulose whiskers (Gousse et al., 2002).	51
2.21	Aldehyde functionalization of CNC ( Drogat et al.,2011). . . . .	52
2.22	Growth of PDMAEMA on CNC by surface initiated ATRP (Yi et al., 2009).	53
4.1	TEM image of CNC. . . . .	61

4.2	FTIR spectra of unmodified CNC. . . . .	62
4.3	FTIR spectra of unmodified CNC and carboxylated CNC. . . . .	62
4.4	Potentiometric titration curve for CNC. . . . .	63
4.5	Potentiometric titration curve for carboxylated CNC. . . . .	64
4.6	UV-vis spectrum of methylene blue. . . . .	65
4.7	Calibration curve of methylene blue. . . . .	66
4.8	Effect of adsorbent dosage on the removal of methylene blue (dye concentration=200 mg/L). . . . .	67
4.9	Effect of initial dye concentration ( $C_0$ ) on the percentage removal of methylene blue (adsorbent dosage=12.17mg/ml). . . . .	68
4.10	Effect of pH on the percentage removal of methylene blue (adsorbent dosage=12.17 mg/ml, dye concentration=500 mg/L). . . . .	69
4.11	Effect of ionic strength on percentage dye removal (adsorbent dosage=12.17mg/ml, dye concentration=500 mg/L). . . . .	70
4.12	Effect of ionic strength on dye uptake (mg/g) at various initial dye concentrations. . . . .	71
4.13	Linearized Langmuir plots for the adsorption of methylene blue on unmodified CNC at 25 °C and 50 °C. . . . .	72
4.14	Plot of separation factor at various dye concentrations. . . . .	73
4.15	Linearized Freundlich plot for the adsorption of methylene blue on unmodified CNC at 25 °C and 50 °C. . . . .	75
4.16	Comparison of experimental data with Langmuir and Freundlich model. . .	76
4.17	Linearized Langmuir plot for the adsorption of methylene blue on carboxylated CNC. . . . .	78

4.18 Comparison of the adsorption capacity of CNC with commercial activated carbons and agricultural wastes (Rafatullah et al., 2010). . . . .	79
---	----

# Chapter 1

## Introduction

### 1.1 Background

Earth is a unique planet endowed with water and the necessary elements capable to support life. Even though 71% of the earth's surface is covered with water, only 2.5% is fresh and available for use. This is because 97.5% of available water is salt water that is unsuitable for human consumption. Out of this 2.5%, only 0.27% of fresh water is accessible because the rest is in frozen polar ice cap, underground and marsh (Korzoun and Sokolov, 1978).

The rapid increase in population and industrial activities doubles the water demand every 21 years (Ahuja, 2009). On the other hand, there is a reduction in the rainfall in the previous decade (Humphreys, 2009), and the pollution of fresh water is a major problem encountered by more than half of the world's population. More than 80 countries are facing water crisis (Ahuja, 2009). UN estimates that 1.2 billion people do not have access to clean water for their domestic consumption (Rijsberman, 2006) and 2.7 billion people will be affected by water shortage by 2025 (Ahuja, 2009). Thus, keeping water sources safe to address the scarcity of water is a global challenge. Governmental organizations and industries are searching for cost effective technologies for water and wastewater treatments.



Wastewater can be treated from different sources, such as industry, municipality and agriculture using various treatment methodologies. The criterion for selecting the appropriate treatment method is the types of contaminants present in the wastewater. Industrial wastewaters usually possess organic and inorganic contaminants, such as dyes, phenolic compounds and heavy metals (Al-Asheh et al., 2003). Among these materials, the annual production of dyes is becoming a major concern. It is roughly estimated that  $10^6$  tons of dyes are produced annually (Hunger, 2003). The amounts of dyes discharged from such a large production are not precisely known. However, it was reported that 10-15% of the dyes used in industry is lost during the dyeing process (Hai et al., 2007; Husain, 2006). Without proper treatment, dye effluent can be mixed with surface and ground water system and it may finally enter the drinking water system (Acemioglu, 2004). Such large amounts of dye effluent discharge into the environment are worrying for both toxicological and esthetical reasons (Métivier-Pignon et al., 2003). Firstly, even a dye lacks any adverse effect on environment; the presence of colour in the receiving stream may cause public concern. Furthermore, dyeing industry effluents contain toxic and oxygen-demanding substances whose oxidation by bacteria and other organisms may result in the depletion of oxygen in the receiving stream, which may adversely impact aquatic life (Hubbe et al., 2012). It was reported that dyes can cause some diseases on humans, such as dysfunction of kidneys, reproductive system, dermatitis, liver, skin irritation, allergy and cancer (Ozcan and Ozcan, 2004). Dyes may also affect aquatic life by reducing the light penetration, which is essential for photosynthetic activity. Since most of the dyes used in industry are synthetically derived that possess complex molecular aromatic structure, they are difficult to biodegrade when discharged into waste streams (Aksu, 2005). Besides this, degradation of azo dyes may result in more toxic byproducts under anaerobic conditions (Song et al., 2009). Thus, the treatment of industrial effluents before discharge is crucial and many governmental organisation have introduced strict legislations on the removal of dyes from effluents (Robinson et al., 2001). These strict laws force industry and academic institutions to find new and economical methods for dye removal (Rai et al., 2005).

During the past three decades, various physical, chemical and biological treatment

methods have been reported for dye removal (Crini, 2006). Among them, adsorption has been considered superior over other conventional techniques in terms of economic and environmental reasons, such as simple design and operation, low initial investment, effectiveness and insensitivity to toxic substances (Sharma et al., 2011; Unuabonah et al., 2008). Furthermore, adsorption offers the best results, and with a correctly designed system it will yield high quality treated water (Crini, 2006; Ho and McKay, 2003; Jain et al., 2003a).

Activated carbon is the most widely used adsorbent for water treatment due to its high surface area and excellent adsorption. However, the high cost of activated carbon restricts its widespread use, which reveals the need of low-cost adsorbents for the removal of dyes (Sharma et al., 2011). Various materials have been studied to find cheap alternative adsorbents, such as natural clay (Gürses et al., 2004), zeolite (Wang et al., 2006), perlite (Doğan et al., 2004), by-product from agriculture (Hamdaoui, 2006), waste material from industry (Gulnaz et al., 2004), biomass (dead/living) (Marungrueng and Pavasant, 2007), chitin and chitosan (Wong et al., 2004).

Cellulose is the most abundant material found in the nature. Native cellulose consists of crystalline and amorphous regions. The amorphous region makes it sensitive to acid hydrolysis that disrupts the amorphous regions and forms individual rod-like crystallites called cellulose nanocrystals (CNC) that possess high mechanical strength (Angles and Dufresne, 2001; Landry et al., 2011). Sulphuric acid hydrolysis of native cellulose introduces negative charges on the surface of CNC due to the formation of sulfate ester groups (Samir et al., 2005). Increasing the content of negative charge on the surface is possible by oxidizing CNC with TEMPO (2,2,6,6-Tetramethyl-1-piperidinyloxy) (Habibi et al., 2006). There is an increasing interest in CNC over the last decade due to its exciting properties, such as high surface area, availability, hydrophilicity, chirality, mechanical strength, broad chemical-modifying capacity, biodegradability and biocompatibility (Klemm et al., 2006). The presence of negative charge on the surface of CNC makes it a possible candidate for the adsorption of positively charged dyes. Besides the ionic interaction, hydrogen bonding, van der Waals and hydrophobic forces will promote the adsorption of dyes on the surface of

CNC. To the best of my knowledge, the application of CNC for dye removal has not been previously reported, and it is expected to provide an alternative adsorbent for treating the dye effluents.

## 1.2 Objective

The objective of this research is to demonstrate the adsorption properties of CNC for the removal of methylene blue dye from aqueous solution. To achieve this objective we focus on two key issues:

- Varying the parameters such as adsorbent dosage, initial dye concentration, pH, temperature and salt concentration.
- Establishing adsorption isotherms.

## 1.3 Organization of Thesis

This thesis consists of 5 chapters. The second chapter provides a literature review on dyes, current dye removal technologies, adsorption phenomena, adsorbents and cellulose nanocrystal. The third chapter provides the materials used in this project and the techniques employed for the characterization of CNC. It also discusses the experimental procedures for the modification of CNC and for adsorption studies. The fourth chapter focuses on the characterization of CNC and the parameters affecting the adsorption performance. The adsorption data will be evaluated by Langmuir and Freundlich isotherm models. The fifth chapter provides an overview of the whole research and it briefly discusses the future steps of this project.

# Chapter 2

## Literature Review

### 2.1 Introduction

Dye is a substance that introduces color to the substrate to which it is applied, such as textile, leather, fiber, hair, plastic or solution (Zollinger, 1991). Dyes appeared to be coloured due to presence of chromophores in their structures that absorbs a certain wavelength of light within the range of visible region of the electromagnetic spectrum. This absorption occurs due to the electronic transitions between the different orbitals within the dye molecule, and the energy levels of the orbitals determine the absorbed wavelengths (Allen, 1971).

Humans have been using dyes for thousands of years and it is believed that Neanderthal man first used colorant 180,000 years ago (Gupta and Suhas, 2009). Blue indigo is the first known organic colourant that was found in the wrappings of mummies in Egyptian tombs 4000 years ago (Gordon and Gregory, 1983). Till the late nineteenth century, the dyes were more or less natural and prepared on small scale (Gupta and Suhas, 2009). It was only after the discovery of the first synthetic dye by Perkin in 1856 that dyes were manufactured synthetically and on a large scale (Hunger, 2003; Venkataraman, 1965). Today, many industries use dyes to colour their products, such as textiles, rubber, paper,

cosmetics, leather, plastics, and food. Such a wide range of dyes used in many industry increases the demand of dye and currently 100,000 dyes are commercially available with a rough estimated production of  $10^6$  tones/year (Chrisite, 2007; Hunger, 2003; Husain, 2006). This enormous production and use of dye is causing severe damage to the environment due to non-biodegradability and toxicity of these compounds.

Few decades earlier, environmental impacts of dyes were not considered as an important issue. It was estimated that the chemical composition of half of the dyes used in industry was not known. With the growing health concerns, people started to pay more attention to dyes (Gupta and Suhas, 2009). This led to the formation of an international association, ETAD (Ecological and Toxicological Association of the Dyestuffs Manufacturing Industry) in 1974 to mitigate the public concerns over the toxicological impact of dyes (Anliker, 1979). It was found that basic and diazo dyes possess highest toxicity (Shore, 1996). With increasing information on the environmental consequences of dyestuff, government legislations are becoming more and more stringent especially in developed countries (O'Neill et al., 1999).

Adsorption is one of the effective methods for wastewater treatment. The key role and the major cost for an efficient adsorption process are the adsorbent. So far, many different adsorbents have been used to demonstrate the significant removal of dyes from aqueous systems. The most widely used adsorbent is activated carbon; however its high cost motivates researchers to search for new adsorbents.

## 2.2 Types of Dyes

Dyes have considerable structural diversity allowing them to be classified in several ways. One of them is the solubility: soluble dyes including acid, mordant, metal complex, direct, basic and reactive dyes; insoluble dyes including azoic, sulfur, vat and disperse dyes (Gupta and Suhas, 2009). However, dyes are mainly classified according to their chemical structures or their application methods. The former approach is used by dye chemists,

whereas the second approach is used by the user of dyes, and the dye technologist who speaks of disperse dyes for polyester and reactive dyes for cotton (Hunger, 2003).

### **2.2.1 Chemical Classification of Dyes**

Classifying the dyes according to the chemical structures has many advantages. Firstly, it shows the functional groups which has the characteristic properties, for example, anthraquinone dyes (weak, expensive) and azo dyes (strong, good all-round properties, cost effective). Secondly, the number of the chemical groups is manageable to classify the dyes (Hunger, 2003). Table 2.1 shows the classification of dyes according to the chemical structure.

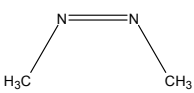
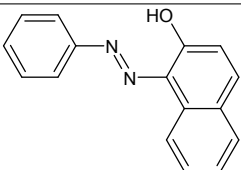
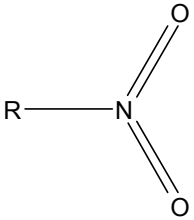
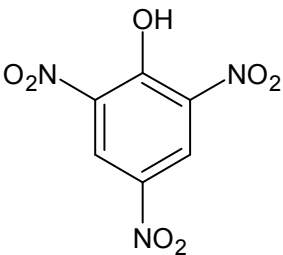
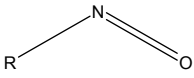
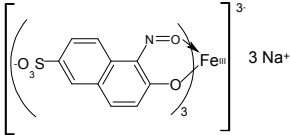
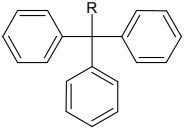
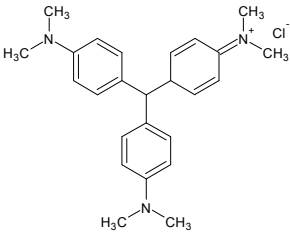
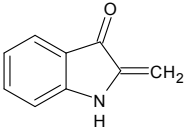
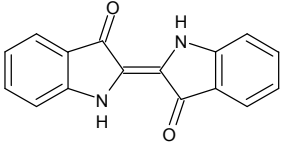
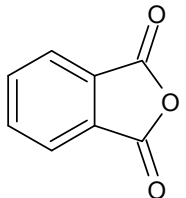
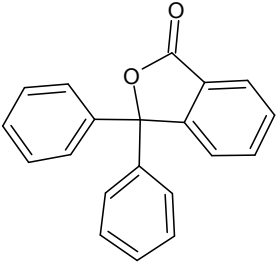
### **2.2.2 Usage Classification of Dyes**

Dyes can also be classified according to their applications, and the classification system using the Color Index is used by the Society of Dyers and Colorists and the American Association of Textile Chemists and Colorists (Hubbe et al., 2012). Some of the groups of dyes are described below (Hunger, 2003):

#### **2.2.2.1 Reactive Dyes**

Reactive dyes form a covalent bond with the fiber. They show extremely high wash-fastness properties using relatively simple dyeing methods to yield brighter colors. They find their uses especially for cotton; however they are also used to a small extent on wool and nylon. Their principle chemical structures are azo, triphendioxazine, phthalocyanine, formazan, and anthraquinone.

**Table 2.1:** Classification of dyes according to the structure (Hunger,2003).

Type of Chromophore	Structural Unit	Example	Related Information
Azo Group			Largest group of commercial dye
Nitro Group			Interest for their small molecular structure, minor commercial importance
Nitroso Group			The iron complexes of sulfonated 1-nitroso-2-naphthol are commercially important dyes in this group
Triarylmethane Group			Obtained by introducing amine or hydroxyl groups into the triphenylmethane rings
Indigoid Group			One of the oldest class of dye
Phthalein Group			Prepared by treating phenol with phthalic anhydride

#### **2.2.2.2 Disperse Dyes**

They are non-ionic dyes that are not soluble in water, which are applied to hydrophobic fibers from aqueous dispersion. They are mainly used for polyester, and to a lesser extent on nylon, cellulose, cellulose acetate and acrylic fibers.

#### **2.2.2.3 Direct Dyes**

They are anionic water-soluble dyes that are mainly used to dye cotton and regenerated cellulose, paper, leather and nylon. These dyes are mainly polyazo compounds, along with some phthalocyanines, oxazines and stilbenes.

#### **2.2.2.4 Vat Dyes**

These water-insoluble dyes are not capable directly dyeing fibers. However, their affinity for the textile fiber can be enhanced by reducing them to soluble leuco salts in alkaline bath. The main chemical classes of vat dyes are anthraquinone and indigoid, which are mostly used for cotton, wool and rayon.

#### **2.2.2.5 Sulfur Dyes**

They are applied to cotton fibers from an alkaline reducing bath using sodium sulfide as reducing agent. Although they are relatively small groups of dyes, their low cost and good washfastness properties make them important from an economic point of view.

#### **2.2.2.6 Basic (Cationic) Dyes**

They are water-soluble cationic dyes that are mainly used for paper, polyacrylonitrile, modified nylons and modified polyesters.



#### **2.2.2.7 Acid Dyes**

They are water-soluble anionic dyes and possess affinity for amphoteric fibers. They are applied to nylon, wool, silk and small extent to paper, leather, food and cosmetics.

#### **2.2.2.8 Solvent Dyes**

They are either non-polar or little polar water-insoluble dyes due to the absence of polar solubilizing groups in their structure. They are used for gasoline, plastics, oils and waxes.

### **2.3 Current Technologies for Dye Removal**

Various methods have been proposed and developed for the removal of dye for past two decades. Even though some of these techniques have found some practical applications, it is still limited to using these techniques in industrial processes due to their high cost and low efficiency. The methods to remove dye can be categorized as: biological, chemical and physicochemical methods. Figure 2.1 shows the current dye removal methods that will be discussed in this chapter.

#### **2.3.1 Biological Methods**

Biological treatment is a widely used method to remove pollutants from wastewater. It is very effective in terms of purifying wastewater contaminated with organic constituents. Mineralization of complex organic molecules and xenobiotic compounds is performed by microorganisms. 70% of the organic substances determined by COD (chemical oxygen demand) analysis could be converted to biosolids (Anjaneyulu et al., 2005). The degradation of dyes by the application of microorganisms for dye removal was initiated almost

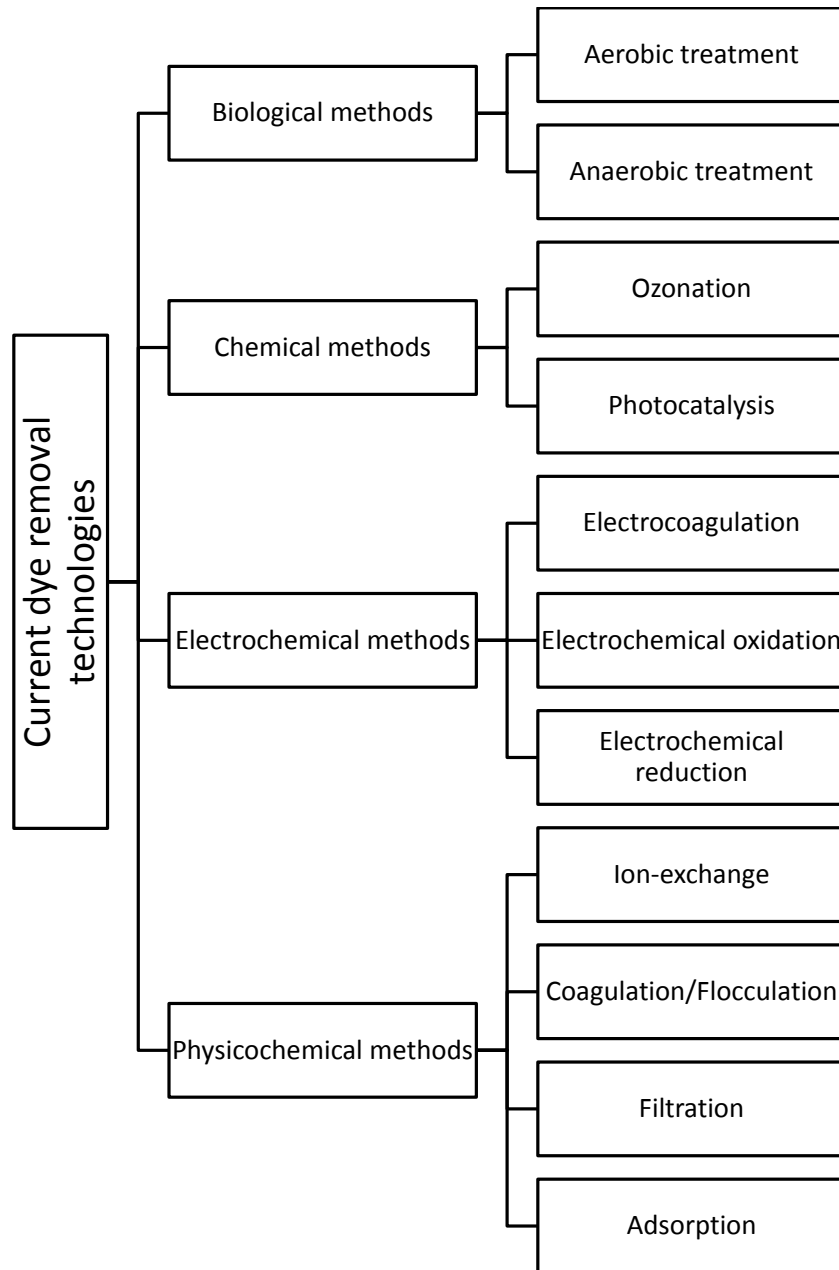


**Figure 2.1:** Current dye removal technologies.

two decades ago (Paszczynski et al., 1986). It is a simple method to operate but it involves a complex biological mechanism, however it offers some advantages, such as low-cost operation (Forgacs et al., 2004).

The biodegradation of dyes is more difficult than other organic pollutants because the dyes are usually stable organic molecules. Other factors affecting the biodegradation are high water solubility and high molecular weight of dyes, which makes permeation through cell membranes difficult (Singh and Arora, 2011). Biological treatment of dyes can be broadly classified into two groups: aerobic treatment and anaerobic treatment. Any of these methods are not sufficient to decolorize the dye wastewater alone, thus they could be combined with chemical pretreatment (Reife and Freeman, 1996).

### **2.3.1.1 Aerobic Treatment**

In aerobic treatment, free oxygen molecules dissolved in wastewater are used by microorganisms to degrade organic constituents. Fungi and bacteria are two classes of microorganism that have been widely used to treat dye wastewater.

**2.3.1.1.1 Fungi** Various fungal strains have been tested to evaluate their decolorization capacities (Table 2.2). Because of its high enzyme production, white-rot fungi; *Phanerochaete Chrysosporium* has been studied in detail for the removal of dyes (Capalash and Sharma, 1992; Cripps et al., 1990; Glenn and Gold, 1983). It was reported that *Phanerochaete chrysosporium* was able to decolorize azo dyes such as orange II, Congo red, and tropaeolin O, under aerobic conditions (Cripps et al., 1990). Although 93-100% decolorization of dyes was achieved, the degradation took place within 6-9 days, which is very slow. Almost 40% decolorization of sulphonated azo dyes were achieved in 21 days (Paszczynski et al., 1992). High decolorization capability of *Phanerochaete chrysosporium* stems from the production of extracellular enzyme, such as *lignin peroxidase*. This enzyme has a non-specific nature, thus can decolorize a wide range of dyes (Rai et al., 2005). However, it was reported that the practical application of *Phanerochaete chrysosporium* is not possible due

to two major problems (Wong and Yu, 1999). First, the release of *lignin peroxidase* is inhibited by the presence of carbon and nitrogen nutrient in industrial effluent (Zhen and Yu, 1998). Second, *lignin peroxidase* consumes considerable amounts of other reagents such as veratryl alcohol and hydrogen peroxide for the degradation of dyes (Young and Yu, 1997). However, it would be difficult to find large quantity of *lignin peroxidase*, veratryl alcohol and hydrogen peroxide simultaneously in most industrial effluents for dye decolorization. Due to these facts, Wong and Yu proposed the use of another fungus (*Trametes versicolor*) to decolorize azo and indigo dyes. (Wong and Yu, 1999). The responsible enzyme, *laccase*, for the dye decolorisation was an extracellular oxidase. Compared to the *lignin peroxidase*, *laccase* can be produced in the presence of carbon and nitrogen nutrients (Moldes et al., 2003) and it does not require hydrogen peroxide and secondary metabolites to catalyze the oxidation (Thurston, 1994). Anthroquinone dye can be directly oxidized by *laccase* but azo and indigoid dyes require redox mediators for the decolorization (Rai et al., 2005). Campos et al. (2001) reported that no decolorization of indigo dye was observed by *laccase* alone however complete decolorization was achieved after the addition of redox mediator (Campos et al., 2001).

In the light of these facts, it can be concluded that the decolorization of dye by fungus depends on dye structure, presence of carbon and nitrogen nutrients in the media and enzymatic activity.

**Table 2.2:** Various strains applied for decolorization.

Strain	Dye	Reference
<i>Schizophyllum commune</i>	Cibacron Red FN-2BL	Bhatti et al. (2008)
<i>Pleurotus ostreatus</i>	Disperse orange3, disperse yellow3	Zhao and Hardin (2007)
<i>Bjerkandera adusta strain</i>	CI Acid Orange 10	Eichlerova et al. (2007)

**2.3.1.1.2 Bacteria** Similar efforts have been conducted to identify the bacteria capable of degrading dyes for more than two decades. Ogawa et al. (1978) reported that a

bacterium, isolated from the sewerage system of a dyestuff factory, could degrade various dyes (Idaka et al., 1978). However, it was observed that the growth and respiration of these organisms were inhibited by the dyes. Several other bacterial strains have been employed for the decolorization of dyes, such as *Aeromonas hydrophilia* (Jiang and Bishop, 1994), *Pseudomonas luteola* (Hu, 1994), *Pseudomonas* (Kulla et al., 1983), *Bacillus subtilis* (Azmi and Banerjee, 2001). All the bacterial strains involved in these studies needed additional carbon and energy sources. The availability of these additional carbon and energy sources are suspected to lead to the formation of micro anaerobic zones within an aerobic system. Furthermore, a similar role of anaerobic zones might have facilitated the anaerobic reduction of azo dyes in anaerobic biofilm reactors, when additional substrate was provided (Costerton et al., 1994). On the other hand, some other strains have been shown to be successful in the mineralization of dyes in the absence of additional energy source and they are presented in Table 2.3.

**Table 2.3:** Bacterial strains capable of degrading dyes in the absence of additional source.

Strain	Dye	Reference
Sphingomonas sp strain 1CX	Acid orange 8, Acid orange 10	Coughlin et al. (1999)
S5	Sulfonated azo compound	Blumel et al. (1998)
MI2	Acid orange 7, Acid orange 8	Coughlin et al. (1997)

### 2.3.1.2 Anaerobic Degradation

The decolorization of dyes under anaerobic conditions has been studied since 1970 (Walker and Ryan, 1971) and the potential of anaerobic microorganisms to degrade azo dyes is well established (Brown, 1981; Carliell et al., 1995). However, because the phenomenon of azo dye reduction is not clearly understood yet (Rai et al., 2005), the degradation mechanism may be enzymatic (Haug et al., 1991), nonenzymatic (Gingell and Walker, 1971), extracellular (Carliell et al., 1995), or intracellular (Wuhrmann et al., 1980). It has been understood from these studies that decolorization mechanism is not due to the

degradation of azo dye by microorganisms, but the reduction of azo dye by the reoxidation of reduced flavin nucleotides (Carliell et al., 1998). The electron donors for this process are the cosubstrates such as glucose, hydrolyzed starch, acetate, yeast extract and propionate. The structure of cosubstrate has an important effect on the degree and rate of decolorization (Rai et al., 2005). Apart from the cosubstrates, mediators can also increase the rate of azo reduction by facilitating the transport of electrons (van der Zee et al., 2000). In addition to cosubstrates, reaction conditions such as temperature, pH, etc. have an effect on the decolorization process (Rai et al., 2005). On the other hand, Bromley-Challenor et al. showed that without using any external cosubstrate, unadapted activated sludge effectively decolorized an azo dye under anaerobic conditions (Bromley-Challenor et al., 2000). The sludge utilized its endogenous energy reserves which are sufficient to decolorize high concentrations up to 400 mg/L of azo dye.

## **2.3.2 Chemical Methods**

### **2.3.2.1 Oxidation**

Oxidation is a widely studied chemical decolorization method due to the simplicity of the process (Singh and Arora, 2011). During the oxidation process, oxidizing agents attack the chromophores (Letterman, 1999). When dye molecules are oxidized, they are broken down into small colorless molecules such as water, carbon dioxide, nitrogen, aldehydes, acids and sulfates. The oxidation products depend on molecular structure of dye and the strength of oxidant (Uygur, 1997). Oxidizing agents such as ozone, chlorine and chlorine dioxide, hydrogen peroxide, and permanganate are used for conventional chemical oxidation of dyes (Xu et al., 2005).

**2.3.2.1.1 Hydrogen Peroxide** Hydrogen peroxide is widely used for the decolorization of wastewater (Singh and Arora, 2011). Most of the water-insoluble dyes such as vat dyes, chrome dyes and sulfur dyes are decolorized by this treatment (Uygur, 1997).

The dyes are oxidized through an increase in the amount of oxygen in wastewater, which results in the reduction of COD (chemical oxygen demand) (Singh and Arora, 2011). The oxidation by-products of hydrogen peroxide are harmless compared to the by-products of chlorine and ozone treatments (Uygur, 1997). If the oxidation process is not activated, it can only destroy certain colorants but fails to destroy dyes that are harder to oxidize, and only degradation of dye molecules in wastewater was observed. Oxidation without the activation is limited by long reaction time, more space for the equipment and high operational cost (Singh and Arora, 2011). The low efficiency of both color and COD removal were overcome by the development of advanced oxidation processes (AOP). In AOP, the activation of hydrogen peroxide oxidation is usually done by UV light; ozone; inorganic salts such as Fe(II), Cu(II); or ultrasound, that helps to generate hydroxyl radicals (Figure 2.2).

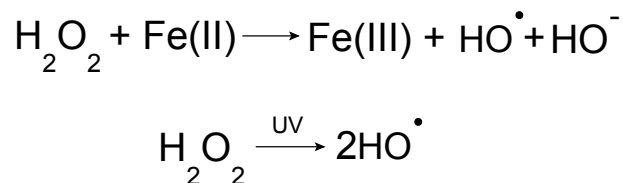


**Figure 2.2:** Activation of hydrogen peroxide with Fe(II) and UV (Singh and Arora, 2011).

Hydrogen peroxide is commonly known as Fenton's reagent when it is activated by inorganic Fe(II) salts. Eren and Acar (2006) reported the decolorization of CI Reactive Yellow 15, which resists degradation, with Fenton's reagent (Eren and Acar, 2006). The results suggested that the best pH was 3, which lead to 98.7% average decolorization. Xu et al. (2004) reported on the degradation of 20 dyes belonging to reactive, acid, cationic, direct, disperse, and vat dye classes using Fenton's reagent (Xu et al., 2004). Reactive, acid, cationic, direct dyes were decolorized in the range of 87-100%, whereas the decolorization of the water-insoluble dyes such as disperses and vat dyes were found to be 30-56%. The major drawback of using Fenton's process is sludge formation and the requirement of acidic medium (Robinson et al., 2001).

Hydrogen peroxide can also be activated by the application of UV radiation that en-

hances the generation of hydroxyl radicals (Figure 2.2) (Huang et al., 2008). Activation by UV offers the advantage over the Fe(II) catalyzed process because it is not restricted to the acidic pH, and sludge formation is eliminated. However, this system faces the problem of UV absorption by colored effluent, which decreases the efficiency of dye removal (Singh and Arora, 2011). The application of UV radiation to Fenton's reagent instead of H<sub>2</sub>O<sub>2</sub> alone is another option in dye decolorization. Xu et al. (2004) reported that Fe(II)/H<sub>2</sub>O<sub>2</sub>/UV is more effective than H<sub>2</sub>O<sub>2</sub>/UV and H<sub>2</sub>O<sub>2</sub>/Fe(II) for the removal of water-soluble and water-insoluble dyes (Xu et al., 2004).

**2.3.2.1.2 Sodium Hypochlorite** Oxidation of textile wastewater containing water-soluble dyes (direct, acid, metal complex, reactive) has been widely oxidized with chlorine in the form of sodium hypochlorite (NaOCl) for dye removal (Singh and Arora, 2011). Cl<sup>+</sup> ion attacks on the amino group of a dye, resulting in azo-bond cleavage (Slokar and Le Marechal, 1998). However, this method is not suitable for water-insoluble vat and disperse dyes, and the decolorization of reactive dyes took a long time (Singh and Arora, 2011). The use of chlorine for dye removal should be less frequent due to the release of aromatic amines that are carcinogenic (Robinson et al., 2001).

**2.3.2.1.3 Ozonation** Ozone is a very effective oxidizing reagent due to its high reactivity (oxidation potential, 2.07 V) compared to chlorine (1.36 V) and H<sub>2</sub>O<sub>2</sub> (1.78 V). It reacts rapidly with many dye classes and usually provides good color removal efficiencies (Alaton et al., 2002). In ozonation, ozone molecule selectively attacks the unsaturated bonds of chromophores, thus color removal occurs rapidly but the mineralization of chromophore is low (Figure 2.3). Ozonation of dye usually results in the partially oxidized by-products such as aldehydes, ketones, and organic acids (Singh and Arora, 2011). The decolorisation of dyes such as Congo red (Khadhraoui et al., 2009), CI Reactive Red 194 and CI Reactive Yellow 145 (Gul et al., 2007) were achieved by ozonation, however effective mineralization was not observed. The major disadvantage of the ozonation is the possible formation of toxic by-products, which requires additional toxicity and the phytotoxicity tests on the



effluent before discharged to the environment (Zhang et al., 2004). Another disadvantage of the ozonation is the short half-life of ozone, which can be influenced by salts, pH and temperature (Slokar and Le Marechal, 1998). Therefore, continuous ozonation is necessary for decolorisation (Robinson et al., 2001).

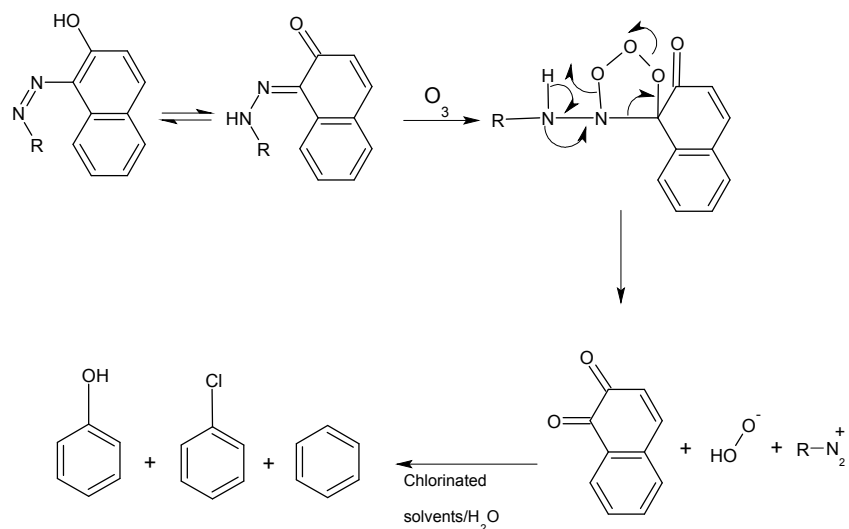


**Figure 2.3:** Degradation mechanism of azo dyes with ozone (Reife and Freeman, 1996).

### 2.3.2.2 Photocatalysis

Commercial dyes are made to be resistant to photodegradation due to the required standards of light fastness of dyeing (Singh and Arora, 2011). Thus, various catalysts and irradiation conditions have been studied to find the optimal conditions for decolorization. The effect of  $\text{TiO}_2$  as a catalyst has been well established in the literature (dos Santos et al., 2007; Forgacs et al., 2004). Liakou et al. tested the decomposition of Basic Yellow 15, Acid Blue 40, Direct Blue 160, Direct Blue 87, and Reactive Red 120 in the presence of UV and  $\text{TiO}_2$  (Liakou et al., 1997). The results demonstrated that the structure of dyes and

pH have an impact on the oxidation mechanism. Two azo dyes, namely CI Acid Orange 7 and CI Direct Red 28 were decolorized under UV and sunlight in the presence of TiO<sub>2</sub>. After 2 hours of photolysis, 95% and 93% of decolorization was achieved (Singh and Arora, 2011).

Recently, solar technologies have attracted some attention. Xia et al. (2008) studied the photocatalytic degradation of methyl violet and methylthionine chloride over cobalt doped mesoporous SBA-15 under sunlight (Xia et al., 2008).

### **2.3.3 Electrochemical Methods**

#### **2.3.3.1 Electrocoagulation**

Conventional coagulation process involves the addition of coagulating agents such as Fe<sup>3+</sup> and Al<sup>3+</sup> to the wastewater. The difference of electrocoagulation is that the coagulating agents are generated by the anodes immersed in the wastewater (Martínez-Huitle and Brillas, 2009). This can lower the sludge formation as excess use of coagulating agents could be avoided (Singh and Arora, 2011). The efficiency of dye removal depends on the current density, anode material, initial pH and etc. (Daneshvar et al., 2007). It was reported that 98% removal of C.I. Acid Yellow was achieved using iron anode at pH 6 (Daneshvar et al., 2007). On the other hand, Can et al. reported 92.5% removal of Remazol Red RB 133 using aluminum anode at pH 9 (Can et al., 2003).

#### **2.3.3.2 Electrochemical Oxidation**

Electrochemical oxidation is widely used for the removal of organic pollutants from the wastewater (Martínez-Huitle and Brillas, 2009). It has been recently used for the decolorisation of dyes. Oxidation of dyes in an electrolytic cell may take place in two ways. The first one is by direct anodic oxidation of dye molecules where electrons are transferred directly to the anode, however, the degradation was low (Panizza and Cerisola, 2007). The

**Table 2.4:** Percentage decolorization of dyes using different anodes (Martínez-Huitle and Brillas, 2009).

Anode	Dye	Concentration	Time(h)	% colour removal	Reference
PbO <sub>2</sub>	Blue reactive 19	25 mg/L	2.0	100	Andrade et al., 2007
PbO <sub>2</sub>	Basic brown 4	100 mg/L	0.5	100	Awad and Galwa, 2005
Ti/Sb <sub>2</sub> O <sub>5</sub> -SnO <sub>2</sub>	Reactive red 120	1500 mg/L	6.25	95	Chen et al., 2003
Ti/Ru <sub>0.3</sub> Ti <sub>0.7</sub> O <sub>2</sub>	Direct black 36	0.1 mM	3.0	40	Socha et al., 2006
Pt Anode	Acid red 27	100 mg/L	3.0	100	Hattori et al., 2003
Graphite anode	Vat blue 1	200 mg/L	0.5	14	Cameselle et al., 2005
ACF anode	Acid red 27	80 mg/L	8.0	99	Fan et al., 2006

second way is the oxidation of dye molecules by electrogenerated species from wastewater (Martínez-Huitle and Brillas, 2009), which yielded complete or partial degradation. The choice of anode is the most important factor determining the extent of dye mineralization (Martínez-Huitle and Brillas, 2009). Table 2.4 provides the percentage color removal of different anodes.

### 2.3.3.3 Electrochemical Reduction

Electrochemical reduction is not as popular as electrochemical oxidation because it is less effective (Martínez-Huitle and Brillas, 2009). Several parameters, such as potential difference and current intensity, nature and number of electrodes and distance between them, pH, and salt concentration determine the efficiency of the process (Josji and Purwar, 2004). Jain et al. (2003) investigated the electrochemical reduction of Active Yellow 23 (Jain et al., 2003b). Complete decolorization took approximately 4 hours using Pt cathode

and 2 hours using steel cathode.

## **2.3.4 Physicochemical Methods**

### **2.3.4.1 Ion-exchange**

Ion exchange is a process used to remove ionic species from the medium. The sample is passed over the column of ion exchange resin until the active sites are saturated. It has been widely used for softening the hard water (Greenleaf et al., 2006), whereas it has not been applied to dye removal probably due to the general opinion that ion exchangers could not accommodate a wide range of dyes (Slokar and Le Marechal, 1998). However, it was reported that acid, direct, and sulphur dyes could be eliminated using an anion exchange column in a column containing nonpolar resin (Slokar and Le Marechal, 1998). The disadvantage of using ion exchange process is its cost due to the use of organic solvents for regeneration (Anjaneyulu et al., 2005).

### **2.3.4.2 Coagulation/Flocculation**

Coagulation is a well-known method for the treatment of wastewater. As discussed previously, it involves the addition of coagulating agents to the wastewater to alter the physical state of particles and facilitate sedimentation (Verma et al., 2012). One of the major problems of coagulation is that water-soluble dyes resist coagulation (Hai et al., 2007). It is usually observed that direct, vat, acid, mordant and reactive dyes coagulate but the quality of resulting floc is poor and does not settle well (Anjaneyulu et al., 2005). Polyelectrolytes can be added to enhance the coagulation by promoting the formation of large and rapid settling flocs (Verma et al., 2012). Coagulation-flocculation method was successfully used to remove water-insoluble sulfur and disperse dyes (Singh and Arora, 2011). The other major problem of coagulation is the toxicity of sludge produced after dye removal. The sludge may be rich in ferrous/ferric salts, which is a potential danger to

the aquatic biota (Sotero-Santos et al., 2007). Therefore the sludge should also be treated before disposal; however this increases the cost of the process.

### **2.3.4.3 Filtration**

In filtration technique, membranes have a crucial role by creating a physical barrier to specific components depending on their size. There are different filtration techniques such as microfiltration (MF), ultrafiltration (UF), nanofiltration (NF), and reverse osmosis (RO). They have found applications in textile industry for the recovery of sizing agent from the effluent (Singh and Arora, 2011). These techniques principally differ in the size of pores of membranes used in the separation process. To operate the separation process successfully at high flux rates at different pHs, temperature and solvent, the membranes should have reasonable mechanical, thermal and chemical stability (Josji and Purwar, 2004).

The removal of water-soluble dyes from textile effluent using reverse osmosis and nanofiltration is well documented (Cooper, 1995). Nanofiltration can be used for the recovery of dyes such as CI Reactive Red 24, CI Reactive Orange 12, CI Reactive Blue 19, CI Reactive Black 5 (Petricic et al., 2007; Vishnu and Joseph, 2007). Hydrolyzed reactive dyes are the most challenging to be removed by conventional methods, however they have been removed from textile effluent using nanofiltration (Tang and Chen, 2002) and reverse osmosis techniques (Josji and Purwar, 2004). The major drawback of this method is the high cost and short life of membranes. Membranes are suffering from clogging and need to be frequently regenerated (Robinson et al., 2001). Another problem of the filtration technique is the subsequent disposal of dyes since the dyes from the separation process are not degraded but only concentrated (Singh and Arora, 2011).

#### **2.3.4.4 Adsorption**

Among previously described processes, adsorption is a well-known dye removal method, where dissolved molecules are concentrated on the solid surface. Polar or non-polar molecules can be retained at the specific sites on the surface due to chemical bonding, Columbic, and van der Waals forces.

Adsorbent choice has an important role on the performance of dye removal. Whereas inorganic adsorbents possess properties such as good mechanical and chemical stability, high specific area, and resistance to microbial degradation, organic adsorbents have renewable sources such as wastes or by-products of industrial processes (Forgacs et al., 2004). Adsorption properties of various organic and inorganic adsorbents have been well studied and their dye removal capacities have been reported in the literature.

Adsorption process is affected by the parameters such as initial dye concentration, adsorbent dosage, contact time, pH, temperature and the presence of other substances. Equilibrium data are studied by changing these parameters to evaluate the adsorption isotherms that describe the correlation between amount of dye molecules adsorbed and concentration of dye molecules in the solution. Adsorption isotherm is very important for the design and optimization of the adsorption process for dye removal. The most commonly used adsorption isotherms are the Langmuir and Freundlich isotherms (Dogan et al., 2008).

Adsorption has been gaining popularity due to the advantages, such as simple design and operation, low initial investment, effectiveness, insensitivity to toxic substances. Adsorption process does not generate toxic pollutants (Crini, 2006). Besides this, a wide range of low-cost adsorbents is available (Gupta and Suhas, 2009).

#### **2.3.4.5 Adsorption Isotherms**

Adsorption isotherms are used to describe the adsorption capacity of an adsorbent. This facilitates the selection of the most appropriate adsorbent for a process and evaluating the feasibility of the process for a given application (Kaushik and Malik, 2009). There are

two widely used and easily linearized adsorption isotherm models that were proposed by Langmuir (Langmuir, 1918) and Freundlich (Freundlich, 1906).

Langmuir model basically assumes that (Wong et al., 2003):

- Adsorption takes place at specific sites.
- Adsorption energy of all sites is identical and independent of the surface coverage.
- Once a dye molecule is bound to an active site, no further adsorption can occur at that site.
- Adsorption is restricted to monolayer.

The equation of Langmuir isotherm can be represented as:

$$q_e = \frac{q_m K_a C_e}{1 + K_a C_e} \quad (2.1)$$

where  $q_e$  is the equilibrium amount of dye adsorbed per g of adsorbent (mg/g),  $q_m$  is the maximum amount of dye which can be adsorbed per g of adsorbent (mg/g),  $C_e$  is the equilibrium concentration of free dye molecules in the solution (mg/L),  $K_a$  is a constant related to the energy of adsorption (L/mg) which shows the affinity between dye and adsorbent.

The values of  $K_a$  and  $q_m$  can be extracted using the linearized form of Langmuir isotherm.

$$\frac{1}{q_e} = \frac{1}{K_a q_m C_e} + \frac{1}{q_m} \quad (2.2)$$

The linearized form of Langmuir isotherm is represented by a plot of  $1/q_e$  vs.  $1/C_e$ , where  $q_m$  and  $K_a$  can be determined from the interception and slope, respectively.

Freundlich isotherm model is usually used to describe heterogeneous systems and involves the formation of multilayer adsorption (Wong et al., 2003). It can be represented as:

$$q_e = kC_e^{1/n} \quad (2.3)$$

where  $q_e$  is the amount of dye adsorbed per g of adsorbent (mg/g) in equilibrium,  $k$  is related to the adsorption capacity,  $1/n$  is heterogeneity factor which ranges from 0 to 1 and  $C_e$  is the equilibrium concentration of free dye molecules in the solution (mg/L).

The linearized form of Langmuir isotherm is

$$\ln q_e = \ln k + 1/n \ln C_e \quad (2.4)$$

The intercept of a linear plot of  $\ln(q_e)$  vs  $\ln(C_e)$  plot is represented by  $\ln(k)$  and the slope yields  $1/n$ .

## 2.4 Disadvantages of Current Dye Removal Technologies

**Adsorption:** The major drawback of adsorption process is the high cost of adsorbent (activated carbon).

**Biological Treatment:** Most of the dyes resist biodegradation so it is difficult to degrade them biologically (Singh and Arora, 2011). Degradation is sensitive to the toxicity of some chemicals (Bhattacharyya and Sarma, 2003) and it usually takes long time (several days) (Pagga and Brown, 1986). Its application is limited due to requirement of large land area, which limits the options in the design and operation of such process (Bhattacharyya and Sarma, 2003).



**Chemical Methods:** Decolorization of dyes using hydrogen peroxide is suffering from its low oxidation power. The oxidation when uncatalyzed (i.e. activation) fails to degrade the dyes that are harder to oxidize. Furthermore, it needs long reaction time, larger space for the equipment and the high operating cost (Singh and Arora, 2011). On the other hand, the activation of hydrogen peroxide (Fenton's reagent) faces the problem of sludge formation through the flocculation of reagents and dye molecules (Robinson et al., 2001). The major drawback in oxidizing dyes with sodium hypochlorite is the production of carcinogenic aromatic amines (Robinson et al., 2001) and toxic chlorinated organic compounds (Singh and Arora, 2011). Ozonation is another method for oxidizing the dyes that is restricted due to the possible formation of toxic by-products (Zhang et al., 2004) and short half-life of ozone (Slokar and Le Marechal, 1998). Analyzing the toxicity of these by-products before disposal and the requirement of continuous ozonation for the oxidizing process increases the cost.

**Electrochemical Methods:** The major drawback of electrochemical methods is the requirement of high energy.

**Physicochemical Methods:** Coagulation and flocculation produce large amounts of sludge that requires subsequent disposal. Filtration technology is expensive due to the short life of membranes that are susceptible to clogging. The major drawback of ion-exchange method is the high cost of regeneration due to the use of organic solvents.

Table 2.5 summarizes the advantages and disadvantages of current dye removal techniques to provide an overview that allow us to make the necessary comparison.

## 2.5 Adsorbents

Adsorbent plays a key role in the adsorption process due to provision of active sites to bind the molecules. On the other hand, the major drawback of adsorption process is the cost or low adsorption capacity of adsorbents. Recently, a wide range of adsorbents, such as natural clay (Gürses et al., 2004), zeolite (Wang et al., 2006), perlite (Doğan et al.,

**Table 2.5:** Comparison of current dye removal methods ( Robinson et al. (2001), Crini (2006), Verma et al. (2012), Singh and Arora (2011)).

Method	Advantages	Disadvantages
<b>Physicochemical</b>		
Adsorption	Effective removal of wide range of dyes	Cost of adsorbent and regeneration difficulties
Ion exchange	Effective regeneration with no loss of adsorbent	Cost of regeneration and not applicable for disperse dyes
Filtration	Capable of removing all dyes and producing high quality treated effluent	High cost and concentrated sludge formation
Coagulation	Simple	Sludge formation
<b>Biological</b>		
	Low-cost operation	Slow process
<b>Chemical</b>		
Fenton's reagent	Effective for water soluble and insoluble dyes	Sludge formation and requirement of acidic medium
Sodium Hypochlorite	Effective for water-soluble dyes	Production of aromatic amines
Ozonation	Applied in gaseous state; no volume change, rapid and efficient process	Short half-life of ozone, possible formation of toxic by-products
Photocatalysis	No sludge formation	Expensive method and formation of hazardous by-products
<b>Electrochemical</b>		
Electrocoagulation	No requirement for additional chemicals: lower sludge formation	High energy requirement
Electro (oxidation/reduction)	Nonhazardous breakdown compounds	High energy requirement

2004), by-product from agriculture (Hamdaoui, 2006), waste material (Gulnaz et al., 2004), biomass (dead/living) (Marungrueng and Pavasant, 2007), chitin and chitosan (Wong et al., 2004) have been studied to find the cheaper and effective adsorbents.

### 2.5.1 Activated Carbon

Activated carbons are amorphous carbon-based materials exhibiting high degree of porosity that correspond to a large surface area (McKay, 1996). Adsorption capacity of activated carbons depends on factors, such as source of raw material and preparation conditions including pyrolysis temperature and activation time (Crini, 2006). Other than surface area, pore structure (Crini, 2006) and the presence of functional groups like carboxylic ( $-\text{COOH}$ ) and phenolic ( $\text{Ph}-\text{OH}$ ) also affect the adsorption capacity (Purkait et al., 2007). In addition, molecular size and solubility of dyes also affect the adsorption process, and the nonpolar nature of carbon results in poor adsorption of water-soluble dyes (Josji and Purwar, 2004). In general, low adsorption occurs with acid and reactive dyes having low molecular mass, whereas high adsorption has been reported for basic and direct dyes that are usually of higher relative molecular mass and medium to high adsorption for disperse dyes having hydrophobic character (Singh and Arora, 2011). Table 2.6 presents the adsorption capacities of activated carbon for methylene blue.

Activated carbons, available in the market, are usually prepared from coal, lignite, coconut shell, and wood. Coal is the most widely used precursor for activated-carbon production due to its abundance and low cost (Crini, 2006). Activated carbon has been widely studied to adsorb dyes for wastewater treatment; however high cost of activation and raw material restricts their application. To make the process economically feasible, one has to find ways to reduce the operational cost of regeneration or developed low cost adsorbents, such as waste products to eliminate the need for regeneration. Because regeneration process of activated carbon is expensive and often results in loss of adsorbent, it becomes necessary to develop low-cost adsorbents (Purkait et al., 2007).

**Table 2.6:** Adsorption capacities  $q_m$  (mg/g) of agricultural and commercial activated carbons for methylene blue (Rafatullah et al. (2010)).

Adsorbent	$q_m$ (mg/g)	Reference
<b>Commercial</b>		
Activated carbon	980.3	Kannan and Sundaram (2001)
Activated carbon	588	El Qada et al. (2008)
Activated carbon	380	El Qada et al. (2008)
Activated carbon	238	Marungrueng and Pavasant (2007)
Activated carbon	9.81	Basava Rao and Ram Mohan Rao (2006)
<b>Agricultural</b>		
Bamboo	454.2	Hameed et al. (2007)
Rice husk	343.50	Kannan and Sundaram (2001)
Coconut shell	277.90	Kannan and Sundaram (2001)
Apricot	102	Basar (2006)
Rosa canina seed	47.2	Gurses et al. (2006)
Date pit	12.9	Banat et al. (2003)
Walnut shell	3.53	Aygün et al. (2003)
Almond shell	1.33	Aygün et al. (2003)

## **2.5.2 Low-cost Adsorbents**

The problems mentioned above have led to the development of low-cost adsorbents. According to Bailey et al. (1999) a low-cost adsorbent should be available in nature or be a waste or by-product of another industry, and it requires less pre-treatment (Bailey et al., 1999). Various waste products from agricultural and industrial operations, natural materials and biosorbents have been tested for dye removal.

### **2.5.2.1 Agricultural Waste Products**

Sawdust and bark are two raw agricultural solid wastes that are available in large quantities and they may be used as adsorbents due to their physicochemical characteristics and low-cost (Crini, 2006). The cell walls of sawdust mainly consist of cellulose and lignin which contain tannins or other phenolic compounds capable of binding dyes through different mechanisms, such as ion-exchange or hydrogen bonding (Shukla et al., 2002). Adsorption of basics (Khattari and Singh, 2000), acidic (Ho and McKay, 1998) and metal complex (Ozacar and Sengil, 2005) dyes was reported. It was also reported that chemical pre-treatment improves the adsorption capacity of sawdust (Garg et al., 2003).

Bark is another waste product that is found to be effective for dye removal. It contains polyhydroxy polyphenol groups, which are thought to be active sites for the adsorption process (Crini, 2006). MacKay et al. reported the promising adsorption of Basic blue 9 and Basic red 2 on bark of about 914 mg/g and 1119 mg/g, respectively (McKay et al., 1999). Other than bark and sawdust there are also other available sources such as date pits, rice husk, hazelnut shell, wheat straw and orange peel which have been successfully employed for the removal of dyes from aqueous solution (Table 2.7).

### **2.5.2.2 Industrial Waste Products**

Fly ash, metal hydroxide sludge and red mud are three important industrial by-products due to their low-cost and local availability (Acemioglu, 2004; Namasivayam and Arasi,

**Table 2.7:** Adsorption capacities  $q_m$  (mg/g) of agricultural waste products for methylene blue (Rafatullah et al. (2010)).

Adsorbent	$q_m$ (mg/g)	Reference
Teak wood bark	914.59	McKay et al. (1999)
Cedar sawdust	142.36	Hamdaoui (2006)
Meranti sawdust	120.48	Ahmad et al. (2009)
Teak wood bark	84	McKay et al. (1986)
Raw date pits	80.3	Banat et al. (2003)
Rice husk	40.59	Vadivelan and Kumar (2005)
Hazelnut shell	38.22	Dogan et al. (2008)
Orange peel	18.6	Annadurai et al. (2002)
Fine grinded wheat straw	2.23	Batzias et al. (2009)

1997; Namasivayam and Sumithra, 2005).

Metal hydroxide sludge is produced by precipitating the metal ions with calcium hydroxide in wastewater. It contains insoluble metal hydroxides,  $M(OH)_n$ , and other salts such as  $CaSO_4$ ,  $CaCO_3$ ,  $NaCl$ ,  $NaHCO_3$  (Netpradit et al., 2003). Netpradit et al. (2003) studied the adsorption properties of metal sludge waste obtained from an electroplating industry for the removal of reactive dyes (Netpradit et al., 2003). The authors reported that the sludge has maximum adsorption capacity in the range of 48-62 mg/g.

Fly ash is another industrial by-product generated by thermal power plants and it is generally available at no cost. It may be used in the construction of roads, bricks and cement (Rafatullah et al., 2010). It may contain some hazardous substances such as heavy metals; however it is widely used in industry (Crini, 2006). Approximately 6.74 million metric tons of coal fly ash was used in cement and concrete products in the United States (Manz, 1999). However, this amount of utilization is not sufficient to exploit all the fly ash generated, thus it is needed to develop new alternative environmental friendly applications (Janoš et al., 2003). Bagasse fly ash has been widely used for dye removal because it

does not contain large amounts of toxic metals (Crini, 2006). Acemioglu (2004) studied the adsorption of Congo red onto calcium-rich fly ash and reported that the adsorption increased with increased temperature but decreased with increasing pH. Wang et al. (2005) reported that the applicability of fly ashes depended strongly on its origin (Wang et al., 2005).

Red mud, an aluminum industry by-product, is generated during the processing of bauxite ore (Namasivayam and Arasi, 1997). It is mainly composed of fine particles of silica, aluminum, iron, calcium, and titanium oxides and hydroxides (Wang et al., 2005). Red mud is relatively toxic due to the high calcium and sodium hydroxide content and thus utilizing red mud has been considered for solving solid waste disposal problem (Namasivayam et al., 2002; Wang et al., 2005). Namasivayam and Arasi (1997) studied the adsorption of Congo red onto red mud and reported that the maximum adsorption capacity was 4.05 mg/g (Namasivayam and Arasi, 1997). It was also evaluated that chemical and physical pre-treatment can affect the adsorption capacity (Tor and Cengeloglu, 2006; Wang et al., 2005).

### **2.5.2.3 Biosorbents**

**2.5.2.3.1 Chitin and Chitosan:** Chitin and chitosan are abundant, renewable and biodegradable biopolymers that can be used to adsorb dyes for wastewater treatment. Chitosan is obtained by (partial) deacetylation of chitin which is a natural polysaccharide found in a wide range of natural sources such as crustaceans, fungi, insects, annelids and mollusks. Chitin is the most abundant polymer after cellulose. Despite the availability of wide range of sources, chitin and chitosan are commercially obtained from crab and shrimp shells because crustaceans exoskeleton is available as a by-product of food processing. It has been estimated that the annual crustacean shells production is about  $1.2 \times 10^6$  tones and utilization of such a large amount of solid waste for dye removal could be helpful to the environment and economy (Crini, 2006; Rinaudo, 2006).

Various studies have been conducted to demonstrate the adsorption properties of chi-

tosan (Table 2.8). These studies showed that chitosan is an efficient biosorbent for the removal of different classes of dyes. It can be used in different forms such as flake-types, gels, bead-types and fibers. Bead-type of chitosan has larger adsorption capacities than other forms, which is attributed to their larger surface area. Beads containing chitosan could be produced by crosslinking chitosan chains with gluteraldehyde or epichlorohydrin (Crini, 2006).

It was reported that 1 g of chitosan adsorbed 2498 mg of reactive blue 2 (Chiou et al., 2004). Such an excellent performance for the adsorption of an acidic dye could be due to other factors other than surface area since chitosan has low affinity to basic (cationic) dyes (Chao et al., 2004). This performance is attributed to the  $\text{NH}_3^+$  groups on chitosan which attract anionic dyes however repel the cationic dyes. This means that dye uptake is strongly dependent on pH for acidic and basic dyes. In addition to this, other factors such as source of chitin, molecular weight, degree of deacetylation, crystallinity, and amino group content affect the adsorption properties (Guibal, 2004; Ravi Kumar, 2000; Varma et al., 2004).

**2.5.2.3.2 Biomass** Living or dead biomass can be used as adsorbent for wastewater treatment. The use of biomass is attractive due to their availability and low price. They are the by-products of fermentation and activated sludge processes. The physicochemical characteristics of biomass such as bacteria, yeasts, fungi and algae afford them the ability to remove different kinds of dyes. Adsorption takes place principally at the cell wall (Aksu, 2005). Cell walls contain polysaccharides, proteins and lipids that possess many functional groups that are capable of binding to dyes. The use of dead biomass is more advantageous because they are not affected by the toxic wastes and they do not need the supply of nutrients (Crini, 2006).

Aksu and Tezer (2000) reported that *Rhizopus arrhizus* has an adsorption capacity of 588.2 mg/g for the removal of reactive black 5 (Aksu and Tezer, 2000). Table 2.9 summarizes the adsorption capacities of other microorganisms for different types of dyes. Pre-



**Table 2.8:** Adsorption capacity  $q_m$  (mg/g) of chitosan for various dyes (Crini (2006)).

Biosorbent	Dye	$q_m$ (mg/g)	Reference
Crosslinked chitosan bead	Reactive blue 2	2498	Chiou et al. (2004)
Crosslinked chitosan bead	Reactive red 2	2422	Chiou et al. (2004)
Crosslinked chitosan bead	Direct red 81	2383	Chiou et al. (2004)
Crosslinked chitosan bead	Reactive red 189	1936	Chiou and Li (2002)
Crosslinked chitosan bead	Reactive yellow 86	1911	Chiou et al. (2004)
Chitosan bead	Reactive red 189	1189	Chiou and Li (2002)
Chitosan (bead,crab)	Reactive red 222	1106	Wu et al. (2000)
Chitosan (bead,lobster)	Reactive red 222	1037	Wu et al. (2000)
Chitosan	Acid orange 12	973.3	Wong et al. (2004)
Chitosan	Acid orange 10	922.9	Wong et al. (2004)
Chitosan	Acid red 73	728.2	Wong et al. (2004)
Chitosan	Acid red 18	693.2	Wong et al. (2004)
Chitosan	Acid green 25	645.1	Wong et al. (2004)
Chitosan (flake,lobster)	Reactive red 222	398	Wu et al. (2000)
Chitosan (flake,crab)	Reactive red 222	293	Wu et al. (2000)

**Table 2.9:** Adsorption capacities  $q_m$  (mg/g) of biomass for various dyes (Crini (2006)).

Biosorbent	Dye	$q_m$ (mg/g)	Reference
<i>Rhizopus arrhizus</i> biomass	Reactive black 5	588.2	Aksu and Tezer (2000)
<i>Chlorella vulgaris</i> biomass	Reactive red 5	555.6	Aksu and Tezer (2005)
Activated sludge biomass	Basic red 18	285.71	Gulnaz et al. (2004)
Activated sludge biomass	Basic blue 9	256.41	Gulnaz et al. (2004)
Yeasts	Reactive black 5	88.5	Aksu (2003)
Dead fungus <i>Aspergillus niger</i>	Acid blue 29	13.82	Fu and Viraraghavan (2001b)

treatment of microorganisms can enhance the adsorption properties. Fu and Viraraghavan (2001) used pretreatment methods such as autoclaving and reacting with some chemicals (Fu and Viraraghavan, 2001). They reported that effective pretreatment was different for different types of dyes.

The disadvantage of using biomass is that they are not appropriate for used in column systems in powdered form. Although biomass can be immobilized on a support to address this problem, it will however increase the cost (Aksu, 2005).

#### 2.5.2.4 Clays

Clays are strong candidates as adsorbent due to their low cost, abundance and adsorption capacities (Monvisade and Siriphannon, 2009). They are lamellar aluminosilicates exhibiting different physicochemical properties such as swelling, adsorption, ion exchange and surface acidity (Yang et al., 2006). They are classified according to their layered structures (Crini, 2006). Adsorption capacities stem from the negative charge on the structure and relatively high surface area (QU, 2008). Various types of clays such as bentonite (Ozcan et al., 2007), kaolin (Nandi et al., 2009), montmorillonite (Damardji et al., 2009), clinoptilolite (Alpat et al., 2008), sepiolite (Alkan et al., 2005), smectite (Czímerová et al., 2004) and zeolite (Wang et al., 2006) have been widely studied for the removal of dyes .

## 2.6 Cellulose Nanocrystals (CNC)

As the most important skeletal component in plants, cellulose is a fascinating natural polymer because it is an almost inexhaustible and sustainable raw material with exciting properties such as hydrophilicity, chirality, biodegradability, broad chemical-modifying capacity, and its formation of versatile semi-crystalline fiber morphologies (Klemm et al., 2006). The molecular structure of cellulose is shown in Figure 2.4. It is a carbohydrate polymer consisting of repeating  $\beta$ -D-glucopyranose molecules that are covalently linked by acetal functions between the equatorial OH group of C4 and the C1 carbon atom ( $\beta$ -1,4-glucan), which is the manner in which cellulose is biogenetically formed (Klemm et al., 2005). Cellulose, in the cell walls of plants and trees and in its native state (cellulose-I), forms a crystalline structure whereby chains aggregate by extensive hydrogen bonding (Klemm et al., 1998). There are two forms of crystalline celluloses known to occur in plants: cellulose I  $\alpha$  and I  $\beta$  (Atalla and VanderHart, 1999). However, the entire structure of cellulose is not crystalline. There is a significant amount of paracrystalline and amorphous regions that make the structure sensitive to acid hydrolysis, and eventually breakdown into individual crystallites.

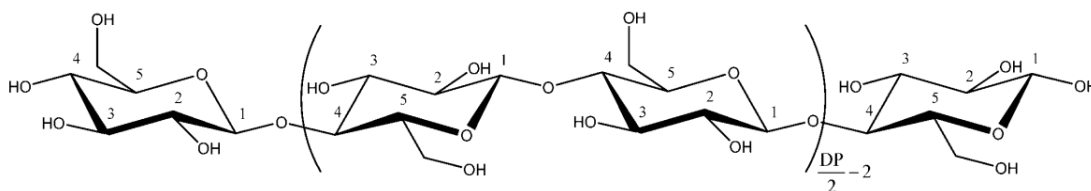


**Figure 2.4:** Molecular structure of cellulose (Habibi et al., 2010).

Currently the isolation, characterization and search for applications of new forms of nanocellulose are creating much activity. New methods for the production of nanocellulose ranges from top-down production to bottom-up production. Top-down methods involve enzymatic, chemical and physical methodologies to isolate the nanocellulose from wood and forest/agricultural residues, whereas bottom-up production of nanocellulose fibrils is produced by bacteria using glucose. These isolated cellulosic materials at least have one

dimension in the range of nanometers, which is the reason for the nomenclature of nanocellulose. The advantage of nanocellulose is that they combine their cellulosic properties such as hydrophilicity, chemical-modifying capacity and larger surface area. Based on their functions, dimensions and preparation methods (which depend on processing conditions) and on the source of cellulose, nanocelluloses can be classified into three categories (Table 2.10) (Klemm et al., 2011). Figure 2.5 shows the general structures of these cellulose types observed in the electron micrographs.

**Table 2.10:** Categories of nanocellulose materials (Klemm et al., 2011).

Types of nanocellulose	Synonyms	Typical sources	Formation and average size
Microfibrillated cellulose (MFC)	Microfibrillated cellulose, nanofibrils and microfibrils, nanofibrillated cellulose	wood, sugar beet, potato tuber, hemp flax	delamination of wood pulp by mechanical pressure before and/or after chemical or enzymatic treatment diameter: 5-60 nm length: several micrometers
nanocrystalline cellulose (NCC)	Cellulose nanocrystals, crystallites, whiskers, rodlike cellulose microcrystals	wood, cotton, hemp, flax, wheat straw, mulberr bark, ramie, avicel, tunicin, cellulose from algae and bacteria	acid hydrolysis of cellulose from many sources diameter: 5-70 m length: 100-250 nm ( from plant celluloses); 100nm-several micrometers (from cellulose of tunicates and algae, bacteria)
bacterial nano-cellulose (BNC)	bacterial cellulose, microbial cellulose, biocellulose	low-molecular-weight sugars and alcohols	bactrial synthesis diameter: 20-100 nm, diferent type of nanofiber networks

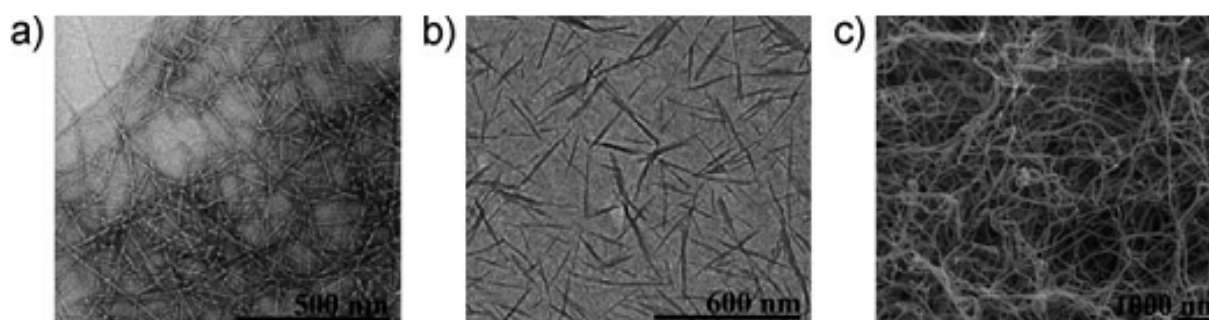


**Figure 2.5:** TEM pictures of a) MFC and b) CNC c) SEM picture of BNC (Klemm et al., 2011).

Nanocellulose can be derived from a variety of sources. We can classify them into three

groups: wood, agricultural crops and bacterial cellulose. Nanofibers have been extracted from wood since 1980 when Herrick et al. and Turbak et al. produced MFC from wood pulp via the high pressure homogenization of pulps (Figure 2.6) according to the procedures developed at ITT Rayonnier (Herrick et al., 1983; Turbak et al., 1983). The homogenization process disintegrates the wood pulp and results in a material where the fibers are broken down into their sub-structural microfibrils (Andresen et al., 2006). This resulted in the MFC gels having highly entangled and disordered networks of cellulose nanofiber.

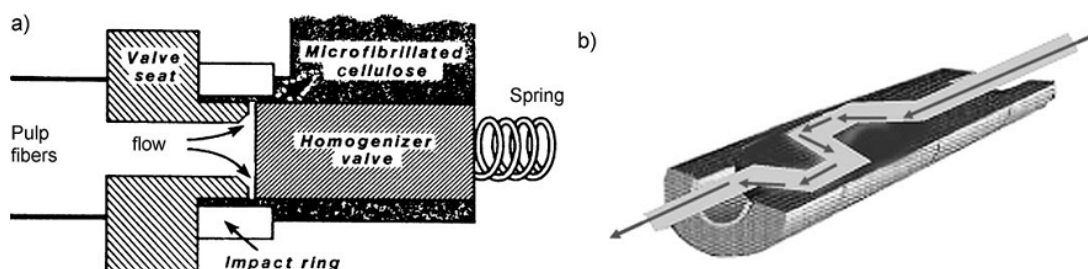


**Figure 2.6:** a) High-pressure homogenizer b) Interior view of a high-pressure microfluidizer (Klemm et. al., 2011).

Even though wood is the most important industrial source of cellulosic fibers, the competition between different sectors such as building products, furniture industries, pulp and paper industry, and combustion of wood for energy makes it difficult to supply wood with a reasonable price to all users. Therefore the fibers from crops such as flax, hemp, sisal and especially from their by-products are likely to become more increasing (Siro and Plackett, 2010).

Bacterial cellulose is produced by bacteria through cellulose biosynthesis and the build-up of bundles of microfibrils, which is the main difference from the existing ways to obtain nanocellulose by mechanical or chemo-mechanical processes (Wagberg et al., 1987). Bacterial cellulose is like a ribbon-shaped fibril, having a diameter of less than 100 nm, which is composed of much smaller 2-4 nm diameter nanofibrils (Brown and Laborie, 2007; Iguchi et al., 2000). These bundles have excellent properties because of their highly crystalline structure (up to 84-89%) (Czaja et al., 2004). It was reported that the 78 GPa elastic

modulus of BC is in the same order of magnitude as glass fibers (70 GPa) and is higher than the recorded values of macro-scale natural fibers (Guhados et al., 2005; Juntaro et al., 2007; Mohanty et al., 2000; Saheb and Jog, 1999). BC also has a high water holding capacity, higher degree of polymerization and better network than celluloses extracted from plants (Barud et al., 2008; Klemm et al., 2006; Wan et al., 2006). In addition to this, BC is produced as a membrane, which means that it is highly hydrated and pure in comparison to plant cellulose, and therefore it does not require chemical treatments to remove lignin and hemicelluloses (Barud et al., 2008; Wan et al., 2006)

### 2.6.1 Preperation of Cellulose Nanocrystal

Among the three types of cellulose in the nano-range, this review will mainly focus on cellulose nanocrystals (CNC). There is a broad range of methods to prepare CNC due to the absence of a standard method to isolate it even from the same source.

CNC can be isolated using specific hydrolysis and separation protocols from different sources. Some of the common sources are ramie (Junior de Menezes et al., 2009), cotton (Araki et al., 2001), sisal (de Rodriguez et al., 2006), wood (Beck-Canedo et al., 2005) and tunicate (Lima et al., 2003). The morphology and the crystallinity of the nanocrystals are similar to the original cellulose fibers; some examples are shown in Figure 2.7.

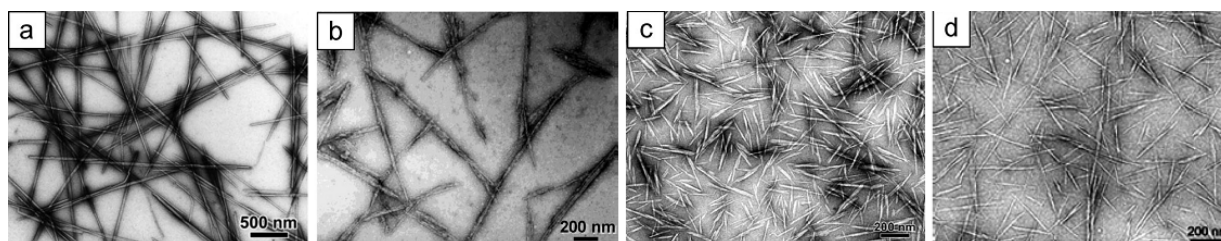


**Figure 2.7:** TEM images of cellulose nanocrystals prepared from (a) tunicate, (b) bacterial, (c) ramie, (d) sisal (Habibi et al., 2010).

Cellulose nanocrystals are prepared via the hydrolysis of cellulosic fibers with mineral acids (Habibi et al., 2010). In sulfuric acid, the hydrolysis of cellulose starts with rapid pro-

tonation of glucosidic oxygen (Figure 2.8/a, path1) or cyclic oxygen (Figure 2.8/a, path2) and it is followed by a slow splitting of glucosidic bonds by the addition of water (Lu and Hsieh, 2010). The acid cleavage stems from the different hydrolysis kinetics of amorphous and crystalline domains. The crystalline domains are stable, whereas amorphous domains are susceptible to acid hydrolysis because they provide an easy access to the interior of the fibrils (Figure 2.9). Aside from the different acid hydrolysis kinetics, the distribution of amorphous and crystalline domains along the fiber is another factor that allows the production of cellulose nanocrystals. In fact, the distribution in bacteria and cotton is more random; therefore higher polydispersity in the size is attained after the hydrolysis (Habibi et al., 2010).

The type of acid used in the hydrolysis step has a major influence on the surface properties of the nanocrystals. Sulfuric and hydrochloric acids have been widely used for cellulose nanocrystal preparation. Nanocrystals generated using HCl show poor colloidal stability and tend to flocculate. However, the nanocrystals prepared with sulfuric acid are stabilized by electrostatic repulsion because the surface hydroxyl groups react with sulfuric acid yielding anionic sulfate ester groups on the surface (Habibi et al., 2010) (Figure 2.8/b).

Acid treatment results in the liberation of crystalline regions of the semicrystalline cellulosic fibers. This process initially removes polysaccharides bound at the fibril surface, followed by the cleavage and destruction of accessible amorphous regions that results in the liberation of rod-like particles. After this treatment the acidic mixture is diluted to remove impurities, which is followed by centrifugation and dialysis. Sonication is also applied after the acid treatment that results in the dispersion of the particles as a uniform stable suspension (Klemm et al., 2011).

The type of acid, its concentration, hydrolysis time, temperature, the power and period of ultrasonic irradiation, cellulose source are the factors that affect the structure, properties, and phase-separation behavior of nanocellulose suspensions (Klemm et al., 2011, Peng et al., 2011). It was demonstrated that the dimensions of cellulose nanocrystals isolated from tunicate and bacteria is usually larger than those isolated from wood and cotton (Heux

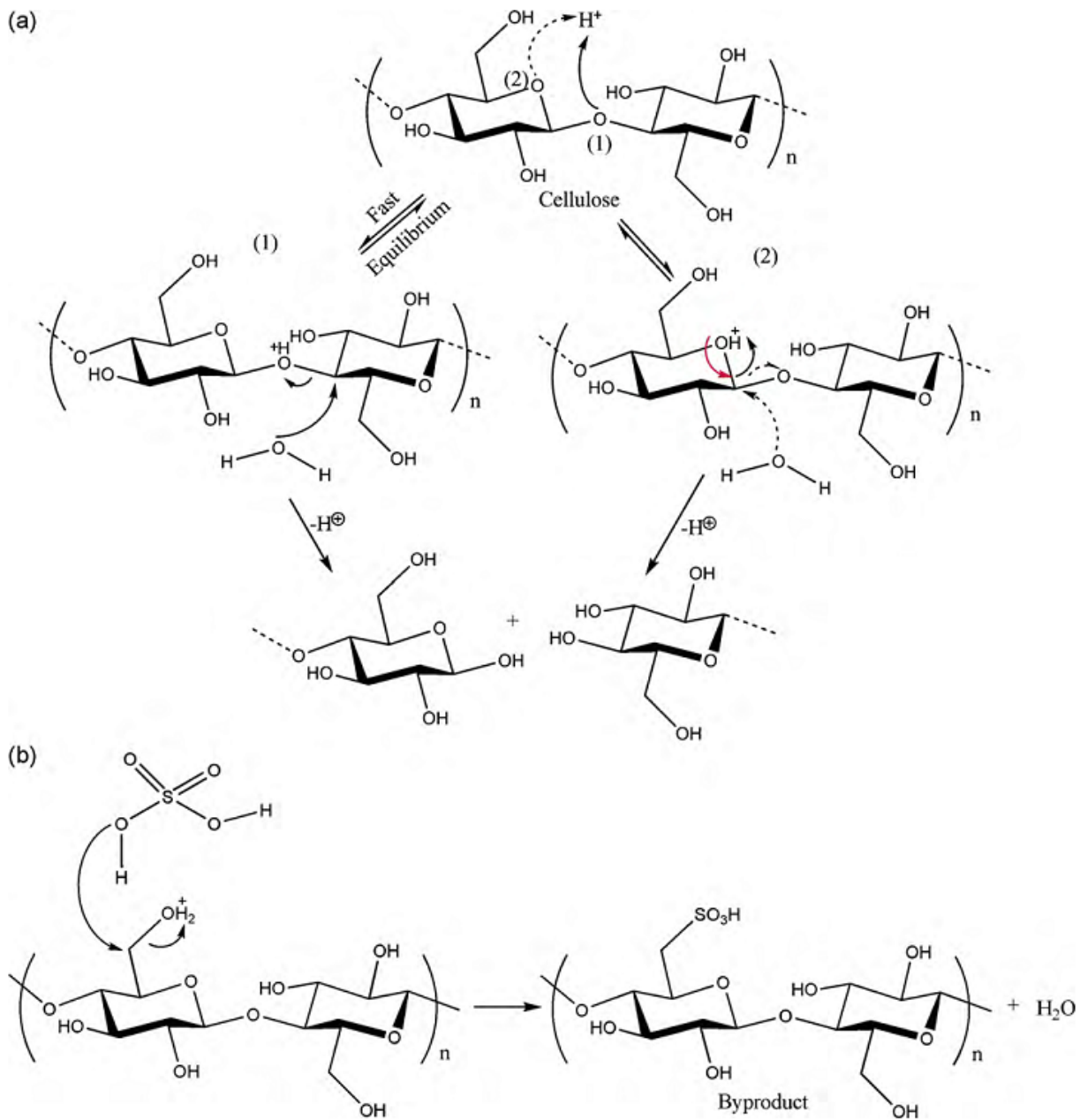


**Figure 2.8:** (a) Hydrolysis mechanism of cellulose (b) Surface esterification of cellulose nanocrystal (Hsieh and Lu, 2010).



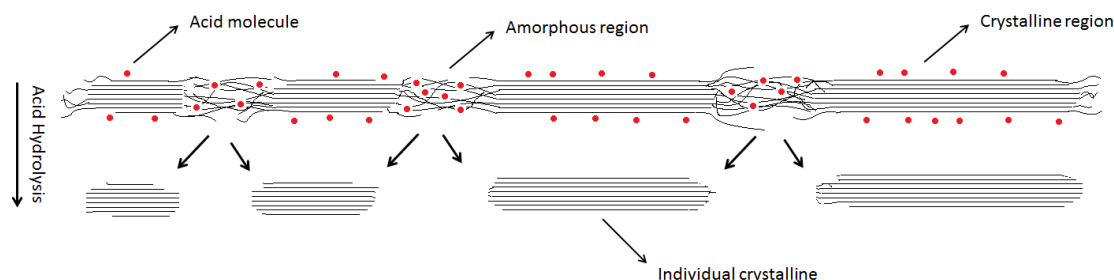


**Figure 2.9:** Model of the formation of individual crystallites.

et al., 2000; Lima et al., 2003). The reason of this is that the bacterial and tunicate cellulose have lower fractions of amorphous regions in their structures (Peng et al., 2011). Beck-Candanedo et al. studied the effect of preparation conditions (reaction time, temperature, and acid-to-pulp ratios) on the properties of CNC isolated from softwood (black spruce) and hardwood (eucalyptus) (Beck-Canedo et al., 2005). They found that for the same reaction conditions the softwood and hardwood CNC suspensions exhibited similar dimensions, surface charge, as well as critical concentrations required to form anisotropic liquid phases. It was also observed that by increasing acid-to-pulp ratio and reaction time, shorter cellulose nanocrystals with narrow polydispersity index (PDI) were prepared and the critical concentration to form an anisotropic phase was increased. Because the cleavage of cellulose chains occurred randomly during the acid hydrolysis process, the dimensions of CNC are not uniform (Peng et al., 2011). Dong et al. also studied the effect of preparation conditions and reported a decrease in the length of nanocrystals and an increase in surface charge with prolonged hydrolysis time (Dong et al., 1998)

## 2.6.2 Properties of CNC Suspensions

When sulfuric acid is used as the hydrolyzing agent to prepare cellulose nanocrystals, the surfaces of nanocrystals are negatively charged with sulfate groups. This promotes a uniform dispersion of nanocrystals because of electrostatic repulsion. In dilute solutions, the nanocrystals are oriented randomly in aqueous phase as an isotropic phase. However,

beyond a critical concentration nanocrystals form a chiral nematic ordering, where suspensions transform from an isotropic to an anisotropic chiral nematic crystalline phase (Figure 2.10) (Revol et al., 1992). CNC suspensions typically have a critical concentration range between 1 and 10% (w/w), which changes with aspect ratio of CNC, charge density and osmolarity (Peng et al., 2011). Stroobants et al. have studied the theories to explain the phenomena (Stroobants et al., 1986).

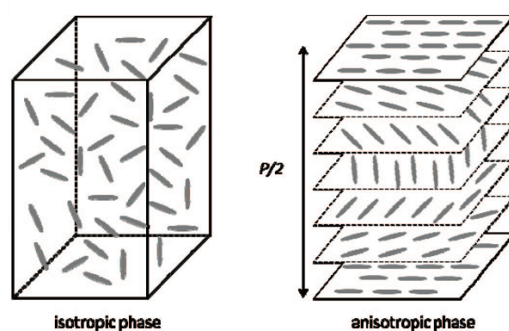


**Figure 2.10:** (a) Orientation of nanocellulose crystals in the isotropic and anisotropic phases (Habibi et al., 2010).

There is equilibrium between the isotropic and anisotropic phase (Figure 2.11) which is sensitive to the presence of electrolytes and its counter ions (Habibi et al., 2010). Dong et al. studied the effect of electrolyte on the phase separation of CNC, and they reported that the volume fraction of the anisotropic phase significantly decreased with the addition of electrolytes, such as HCl, NaCl and KCl (Dong et al., 1996). Dong and Gray also showed the effect of inorganic counterions, weakly basic organic counterions and highly basic organic tetraalkylammonium salts on the phase separation behaviour and stability of CNC suspensions (Dong and Gray, 1997). They observed that the types of counter ions had a significant effect on the phase separation. Macromolecules also strongly affect the phase separation of CNC suspensions. There is a detailed study on the effect of dextran and organic dyes on the phase equilibrium of CNC suspensions (Beck-Candanedo et al., 2006; Beck-Candanedo et al., 2007; Edgar and Gray, 2002).

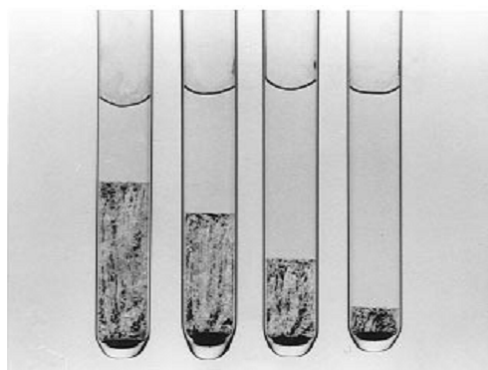


**Figure 2.11:** Phase separation of CNC suspensions. The concentrations are 8.78, 7.75, 6.85 and 5.78 wt% from left to right (Dong et al., 1996).

Cellulose nanocrystals can also self-assemble in an aqueous suspension under an external magnetic or electric field. Habibi et al. studied the effect of AC electrical field (Figure 2.12a) on the alignment and orientation of CNC in aqueous media (Habibi et al., 2008a). It was observed that the application of an AC electric field to the CNC suspensions caused the homogeneous alignment of the cellulose nanocrystals. When the electrical field was increased beyond than 2000 V/cm with a frequency ranging between  $10^4$  and  $10^6$  Hz, the orientation of cellulose nanocrystals became more homogeneous. The previous study done by Revol et al. demonstrated that crystals were able to orient in magnetic field. Figure 2.12b shows the orientation of cholesteric layers in magnetic field (Revol et al., 1994).

### 2.6.3 Modifications of CNC

The abundance of hydroxyl groups on the surface of CNC allows different chemical modifications, such as esterification, etherification, oxidation, silylation, polymer grafting, etc. Noncovalent surface modification is also possible using surfactants. Covalent or non-covalent modifications have been conducted mainly to:

- Transform the hydroxyl groups on the surface of CNC for further modification.

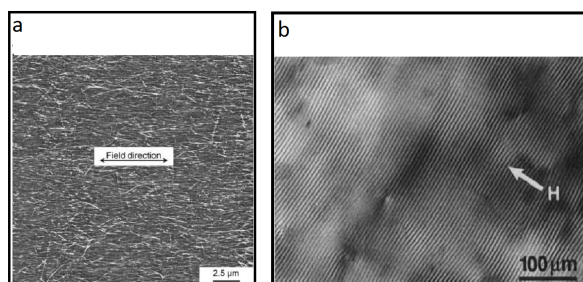


**Figure 2.12:** a) AFM image of CNC films prepared under electrical field at 10 V with a frequency of  $2.5 \times 10^5$  Hz (Habibi et. al, 2008) b) Effect of magnetic field on the orientation of cholesteric layers (Revol et al., 1994).

- Impart positive or negative charges on the surface of CNC to obtain better dispersion.
- Change the surface energy characteristics of CNC to improve compatibility, especially when they are used in hydrophobic matrices in nanocomposites.

The main challenge is to modify only the surface of CNC, while preserving the original morphology of nanocrystal.

### 2.6.3.1 Non-covalent Modification

Noncovalent modification is done via the adsorption of surfactants. Heux et al. used surfactants to obtain stable dispersion of CNC in nonpolar solvents (Heux et al., 2000). Figures 2.13, a and b, display the TEM images of cotton and tunicate suspensions in toluene, respectively.

### 2.6.3.2 Covalent Modification

**2.6.3.2.1 Tempo-Mediated Oxidation:** Hydroxymethyl groups at the surface of the CNC can be converted to carboxylic groups using 2,2,6,6-tetramethylpiperidine-1-oxyl (TEMPO) reagent in the presence of NaBr and NaOCl (Figure 2.14) (Saito and Isogai,

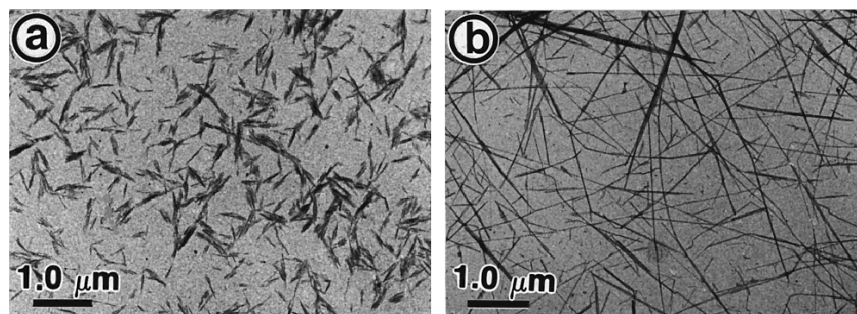


**Figure 2.13:** TEM images of (a) cotton microcrystals and (b) tunicate microcrystals in toluene (Heux et al., 2000).

2004). This technique has been used since it was first reported by de Nooy et al., who showed that only primary hydroxyl groups of polysaccharides were oxidized, while secondary hydroxyl groups were left intact (Denooy et al., 1994). However, all primary hydroxyl groups of CNC are not prone to be oxidized. The morphology and the crystal axis of the CNC are important factors in determining the accessibility of the hydroxymethyl groups. It was reported that only half of the hydroxymethyl groups are available to react because the other half is buried within the crystalline structure of CNC (Figure 2.15) (Habibi et al., 2006).

Tempo-mediated oxidation of cellulose nanocrystalline was first reported by Araki et al. (Araki et al., 2001). It was used as an intermediate step to graft polymeric chains. They demonstrated that CNC maintained its initial morphological integrity after oxidation and formed a homogeneous suspension when dispersed in water due to the permanent charges on the surface of CNC.

Habibi et al. also performed TEMPO-mediated oxidation of CNC isolated from tunicate by HCl hydrolysis (Habibi et al., 2006). They demonstrated that the degree of oxidation could be controlled by using specific amounts of the primary oxidizing agent, NaOCl.

**2.6.3.2.2 Cationization:** Hasani et al. described a single step method to impart positive charges on the surface of CNC by grafting epoxypropyltrimethylammonium chloride

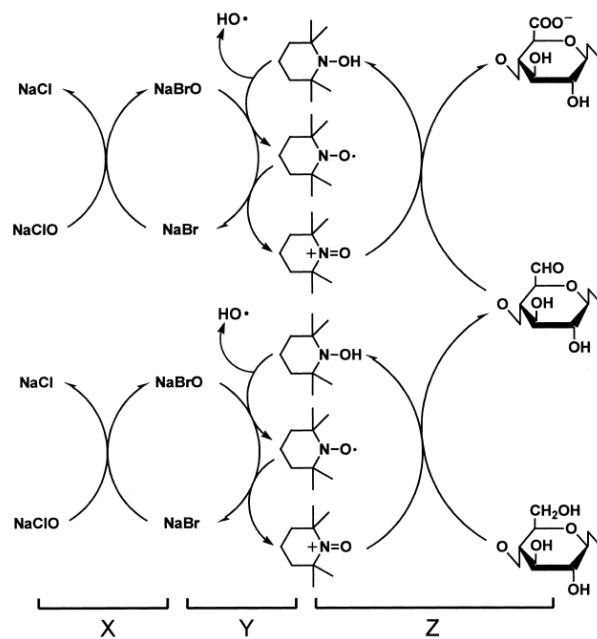


**Figure 2.14:** Scheme of TEMPO-mediated oxidation of cellulose (Shibata and Isogai, 2003).

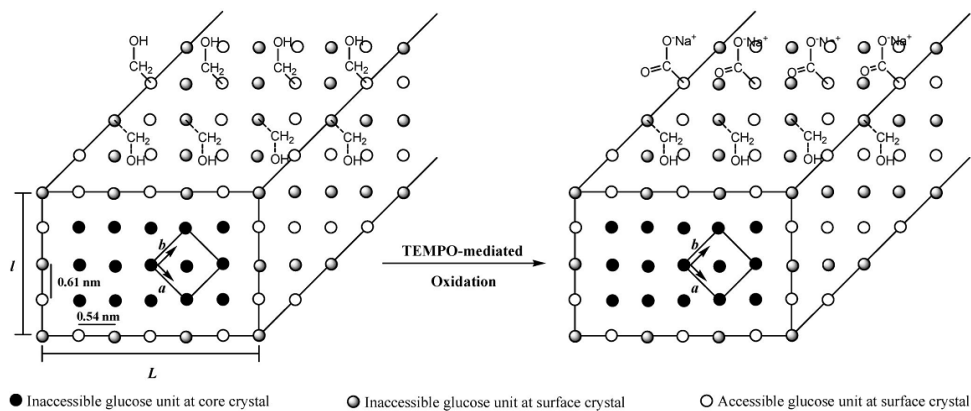


**Figure 2.15:** Cross-sectional representation of CNC showing the available hydroxyl groups for TEMPO-mediated oxidation (Habibi et. al 2006).

(EPTMAC) onto CNC surface (Hasani et al., 2008). Alkali activated surface hydroxyl groups made nucleophilic addition to the epoxy moiety of EPTMAC (Figure 2.16/a). This modification reversed the surface charge and reduced the total surface charge density. These modifications led to the stable aqueous suspensions having unexpected gelling properties (Figure 2.16/b).

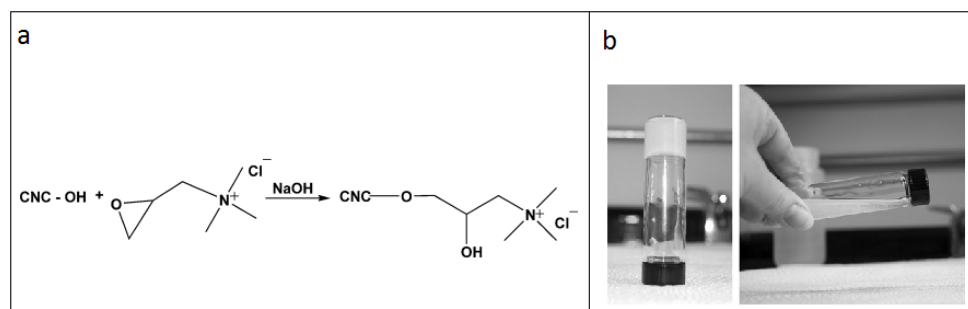


**Figure 2.16:** a)Reaction scheme showing the functionalization of CNC with EPTMAC b)Thixotropic behaviour of HPTMAC-CNC hydrogel (4.9% w/w) before agitation and after agitation (Hasani et al., 2008).

**2.6.3.2.3 Acetylation:** Sassi and Chanzy have studied the homogeneous and heterogeneous acetylation of CNC extracted from valonia and tunicate using acetic anhydride in acetic acid (Sassi and Chanzy, 1995). The TEM imaging (Figure 2.17) and X-ray diffraction showed that the reaction proceeded by a reduction in the diameters of the CNC, however only a small reduction in CNC length was observed. The model for the acetylation of CNC was based on a nonswelling reaction mechanism suggesting that only the cellulose chains on the surface of nanocrystals was affected by the reaction. In the case of homogenous acetylation, the partially acetylated cellulose chains entered the acetylating medium when they were sufficiently soluble, however in the case of heterogeneous acetylation, the cellulose acetate remained insoluble and surrounded the crystalline core of unreacted cellulose chains (Sassi and Chanzy, 1995).

The ultrastructural modifications of cellulose crystals during acetylation can also be observed by TEM images of microcrystals of tunicin before the acetylation (Figure 2.17/a)

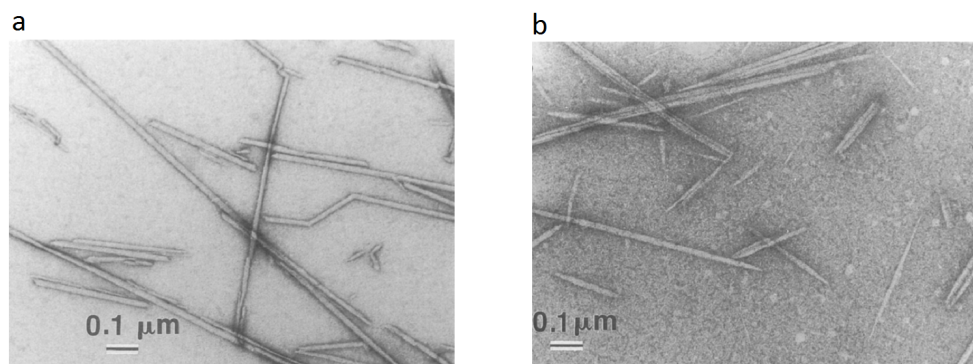


**Figure 2.17:** TEM images of tunicin microcrystals (a) before acetylation (b) after partial acetylation possessing DS value of 0.17 (Sassi and Chanzy, 1995).

and after the reaction, when a DS (degree of substitution) of 0.17 was reached (Figure 2.17/b). The unreacted tunicin are smooth and they have parallel edges, however after the acetylation the crystals are no longer smooth but appeared striated and their tips were frequently pointed.

Yuan et al. reported a simple chemical modification route involving low reagent consumption (Yuan et al., 2006). They mixed alkyenyl succinic anhydride (ASA) emulsion with CNC suspension, freeze dried and heated to 105°C. Highly hydrophobic whiskers were obtained, which could easily be dispersible in solvents with widely different polarities; for example, they were both dispersible in N,N-dimethyl sulfoxide (DMSO) having a very high  $\epsilon$  (dielectric constant) of 46.45 and 1,4-dioxane that has a quite low  $\epsilon$  of 2.21 (Figure 2.18/A). In addition, the whiskers also have good dispersion in polystyrene (Figure 2.18/B).

A one-step methodology for hydrolyzing cellulose and making acetylation of hydroxyl groups simultaneously has been reported (Figure 2.19) (Braun and Dorgan, 2009). A mixture of hydrochloric and organic acid (acetic and butyric acid) was used to carry out the reaction. HCl was used to produce the CNC whiskers and organic acid was used to functionalize the surface of CNC whiskers. The dimensions of the obtained crystals are similar to those obtained by hydrochloric acid hydrolysis alone. More than 50% of the surface hydroxyl groups were substituted under the employed reaction conditions. The



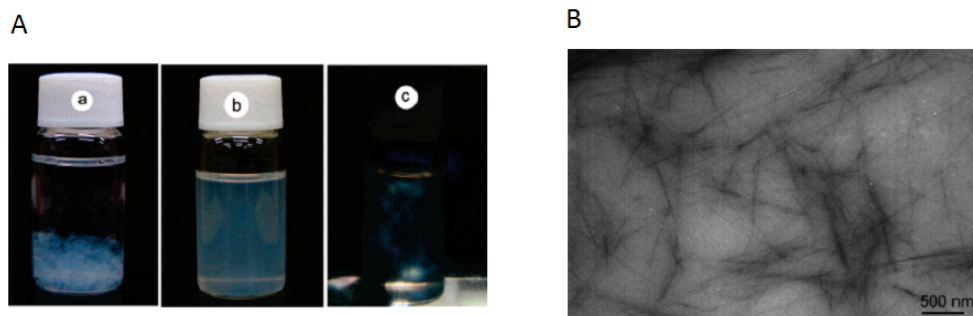


**Figure 2.18:** (A) Dispersibility of (a) unmodified whiskers (b) acetylated whiskers in 1,4-dioxane (c) Suspension of acetylated whiskers viewed through crossed polars (B) TEM image of ASA-modified cellulose whisker ( $DS \approx 0.02$ ) dispersed in thin polystyrene film (Yuan et al., 2006).

obtained nanocrystals were dispersible in ethyl acetate and toluene.

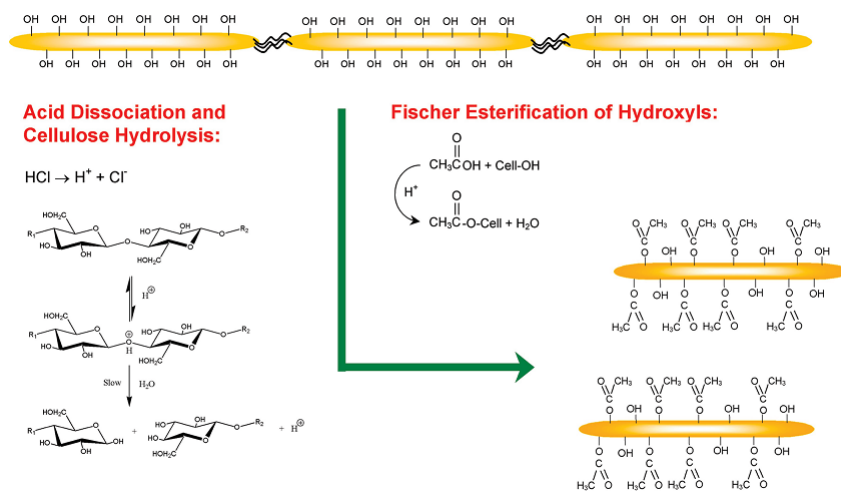


**Figure 2.19:** Reaction scheme representing the simultaneous occurrence of acid hydrolysis and esterification of cellulose (Braun and Dorgan, 2009).

**2.6.3.2.4 Silylation:** Cellulose whiskers isolated from tunicate were silylated by alkyldimethylchlorosilanes, with alkyl groups ranging from isopropyl to *n*-butyl, *n*-octyl and *n*-dodecyl (Gousse et al., 2002). It has been demonstrated that the whiskers became readily dispersible in solvents of low polarity (THF and acetone) with the degree of substitution

(DS) between 0.6 and 1, while their morphological integrity was preserved (Figure 2.20/A). However, when the degree of silylation is high (DS>1) the chains in the core of the crystals became silylated that resulted in the loss of morphology (Figure 2.20/B).

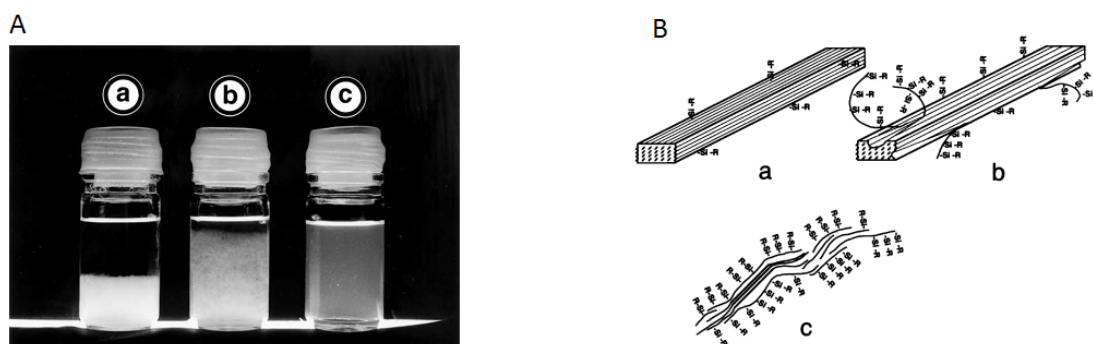


**Figure 2.20:** (A) Suspensions of silylated tunicin whiskers in THF (a) Suspension of original tunicin whisker (b) Suspension of silylated sample possessing DS value of 0.4 (c) Suspension of silylated sample possessing DS value of 0.6 (B) Model of the surface silylation of cellulose whiskers (Gousse et al., 2002).

**2.6.3.2.5 Aldehyde Functionalization:** Drogat et al. used periodate oxidation to generate aldehyde groups on the surface of CNC (Drogat et al., 2011). These aldehyde groups are used as reductive sites, thus avoiding the use of another reducing agent like  $\text{NaBH}_4$  to prepare Ag nanoparticles on the surface of CNC. Periodate oxidation breaks the bond between the carbon atoms possessing secondary hydroxyl groups and gives two aldehyde groups per reacting anhydroglucose unit (Figure 2.21).

**2.6.3.2.6 Polymer Grafting:** There are two main strategies to graft a polymer on the surface of CNC, namely, “grafting-to” and “grafting-from”. The “grafting-to” approach involves the attachment of a pre-synthesized polymer chain to the hydroxyl groups using a coupling agent. In the “grafting-from” approach, the polymer grows from the CNC surface via the atom transfer radical polymerization (ATRP) (Habibi et al. 2010).

Habibi and Dufresne used the “grafting-to” approach to graft different molecular weights

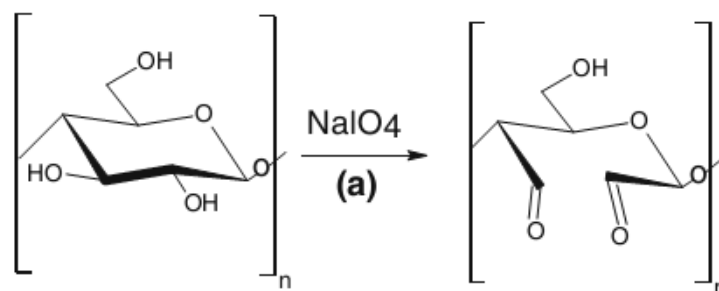


**Figure 2.21:** Aldehyde functionalization of CNC ( Drogat et al.,2011).

of polycaprolactone (PCL) to the CNC via the isocyanate-mediated coupling reaction (Habibi and Dufresne, 2008). It was found that PCL chains at the surface were able to crystallize when the grafting density was sufficiently high. Cao et al. also made a similar effort in the grafting process of pre-synthesized water-borne polyurethane polymers via a one-pot process (Cao et al., 2009). Peptide coupling reaction was also utilized to graft amine-terminated polymer on CNC. Araki et al. used this method to graft poly(ethylene glycol) on CNC particles (Araki et al., 2001). CNC particles were firstly carboxylated by TEMPO-mediated oxidation, and then EDC-NHS carbodiimide reaction was used to couple -COOH groups on CNC with terminal -NH<sub>2</sub> groups of PEG-NH<sub>2</sub>. Mangalam et al. also used the same method to graft DNA oligomers on the surface of TEMPO oxidized CNC (Mangalam et al., 2009). Grafting of DNA to CNC opened a new application area for CNC research. Recently, Azzam et al. grafted thermo-responsive polymers onto CNC via a peptidic coupling reaction (Azzam et al., 2010). They reported that the modified CNC shows unusual properties, such as colloidal stability at high ionic strength, surface activity and thermo reversible aggregation. They also reported a thermo reversible aggregation, which could open a new way to design stimuli-responsive biobased nanocomposite materials.

The “grafting-from” approach uses ATRP technique allows us to produce well-defined monodispersed particles (Wang and Matyjaszewski, 1995). This technique has two steps: the first step is the reaction of surface hydroxyl groups with 2-bromoisobuturyl bromide

(BIBB), which is followed by the polymerisation of monomers (Peng et al., 2011). Morandi et al. used styrene to study surface initiated ATRP, and they reported various grafting products with different grafting densities and molecular weights (Morandi et al., 2009). Yi et al. used N,N-dimethylaminoethyl methacrylate (DMAEMA) as a monomer to study the temperature-induced chiral nematic phase behaviour of PDMAEMA-grafted CNC suspensions (Figure 2.22) (Yi et al., 2009). Habibi et al. reported the first “grafting from” approach by grafting polycaprolactone onto the surface of CNC via ring-opening polymerization (Habibi et al., 2008b). They used stannous octoate ( $\text{Sn}(\text{Oct})_2$ ) as a grafting and polymerization agent. Chen et al. and Lin et al. used microwave radiation to conduct similar grafting reactions with high grafting efficiency (Chen et al., 2009; Lin et al., 2009). Pranger et al. studied in situ polymerization of furfuryl alcohol catalyzed by sulfonic acid residues from the CNC surface (Pranger and Tannenbaum, 2008). The sulfonic acid groups were de-esterified at high temperatures and released into the medium to catalyze in situ the polymerization.

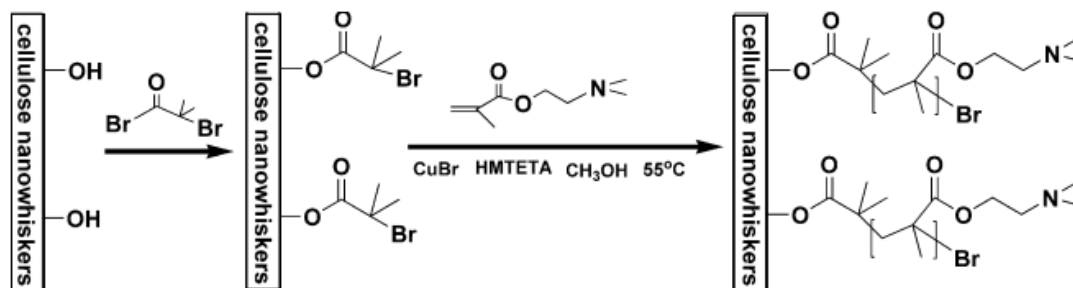


**Figure 2.22:** Growth of PDMAEMA on CNC by surface initiated ATRP (Yi et al., 2009).

# Chapter 3

## Materials and Methods

### 3.1 Materials

Adsorbent, freeze-dried cellulose nanocrystal (CNC), used in this study was provided by FPInnovations. The following chemicals were purchased from Sigma-Aldrich for the carboxylation of CNC: TEMPO (2,2,6,6-Tetramethylpiperidine 1-oxyl, >98%), sodium bromide (NaBr, >99%), sodium hypochlorite (NaOCl, 10-15% available chlorine), hydrochloric acid (standard solution, 1N), sodium hydroxide (standard solution, 1N) and methanol. The cationic dye, methylene blue, used in the study was purchased from Sigma Aldrich. Sodium chloride (NaCl) was used to evaluate the effect of ionic strength on the adsorption properties was purchased from Sigma Aldrich. Calcium chloride ( $\text{CaCl}_2$ ) was purchased from Fisher Chemical. Millipore de-ionized water was used for all the experiments throughout the project.

### 3.2 Carboxylation of CNC

The primary hydroxyl groups on the surface of the CNC were oxidized into carboxyl groups using TEMPO reagent in the presence of NaBr and NaOCl. The reaction conditions

were adapted from Saito and Isogai (2004) and Habibi et al. (2006) (Habibi et al., 2006; Saito and Isogai, 2004). 400 mL of DI water was added to 2 g of CNC. After vigorously mixing, sonication was applied for 15-20 minutes to obtain a homogeneous dispersion. Then, TEMPO (59 mg, 0.376 mmol) and NaBr (0.65 g, 6.3 mmol) were added to the CNC suspension and stirred for 30 min at room temperature until all the TEMPO reagent was dissolved. The pH of the solution was then adjusted to 10 using 0.5 M NaOH. The oxidation was started with the addition of 15% NaOCl solution (14.2 ml) to the CNC suspension over a period of 30 min. The pH of the solution was kept at 10 by adding 0.1/0.5 M NaOH for 4 hours. Then, the solution was continuously stirred overnight. Finally, 22 ml of methanol was added to stop the oxidation and then the solution of pH was adjusted to 7 using 0.1/1.0 M HCl. The solution was dialyzed using cellulose dialysis membrane (spectator, MWCO: 12000-14000) for 1 week.

### **3.3 Characterization of Unmodified and Carboxylated CNC**

#### **3.3.1 Fourier Infrared Transform Spectroscopy**

Infrared spectra of unmodified CNC and carboxylated CNC were recorded on a Bruker Tensor 27 spectrometer with a resolution of  $4\text{ cm}^{-1}$  and a number of scans of 32 from 400 to  $4000\text{ cm}^{-1}$ . Carboxylated CNC was converted to the acid form by adjusting the pH 2 before freeze drying to prevent superposition of carbonyl band with water peak (Lasseguette, 2008). KBr pellets (2% CNC) were dried in a vacuum oven at  $60\text{ }^{\circ}\text{C}$  overnight to remove moisture before the measurement. OPUS software was used to analyze the FT-IR spectra.

### 3.3.2 Potentiometric Titration

Potentiometric titration was used to determine the carboxyl content of oxidized CNC. 0.1 wt % of the carboxylated CNC solution was prepared in a 50 ml jacketed reaction vessel and the pH was adjusted to approximately 3 by adding 100  $\mu\text{L}$  standard HCl solution (1N). The solution was then stirred at 25  $^{\circ}\text{C}$  for 30 minutes under  $\text{N}_2$  purge. Afterwards the solution was titrated with 0.01 M NaOH solution. The pH and conductivity readings were recorded simultaneously, and the data were plotted to calculate the amount of carboxyl groups per g CNC.

Degree of oxidation (DO) represents the number of primary hydroxyl groups that have been converted to carboxyl groups per anhydroglucose unit after oxidation process (Azzam et al., 2010). DO can be calculated using the data ( $V_2$  and  $V_1$ ) from potentiometric titration based on the following equation (Perez et al., 2003):

$$DO = \frac{162(V_2 - V_1)c}{w - 36(V_2 - V_1)c} \quad (3.1)$$

where  $V_1$  and  $V_2$  are the amount of consumed NaOH (in L) in the titration,  $c$  is the concentration of NaOH (mol/L),  $w$  is the weight of the sample. The value of 162 is the molar mass of anhydrous glucose unit (AGU). The difference between the molecular weight of an AGU with that of sodium salt of a glucuronic acid moiety corresponds to 36 (Habibi et al., 2006).

### 3.3.3 Transmission Electron Microscopy

Philips CM10 TEM with 60 keV acceleration voltage was used to record TEM image of CNC. 10  $\mu\text{L}$  of CNC suspension (0.2 wt%) was deposited on a carbon-formvar film on 200 mesh copper grids. The excess solvent was removed from the grid to decrease agglomeration of cellulose nanocrystals and then the grids were dried overnight. To take

clear image of the CNC, the grids were negatively stained with a uranyl acetate solution (2%).

## 3.4 Experimental Setup and Procedure

### 3.4.1 Sampling Procedure

Firstly, stock solutions of dye and CNC and carboxylated CNC (25mg/ml) were prepared to study the adsorption of methylene blue on cellulose nanocrystals. CNC stock solutions (24.34 mg/ml, 24.96 mg/ml) were prepared twice throughout the project, whereas stock solution of dye was prepared before each experiment. For each experiment, 7.5 ml dye and 7.5 ml adsorbent solution was mixed in 20 ml vial and the final solution was mixed using a magnetic stirrer at 500 rpm for 30 minutes. After mixing, the stirrer bar was removed from the vial and the mixture was transferred to a centrifuge flask containing 96.3  $\mu\text{L}$   $\text{CaCl}_2$  (2.16 M). The samples were centrifuged in Heraeus Megafuge at 7500 rpm for 10 minutes to separate the adsorbent from the solution. The experiments were conducted at the pH 9 and 25 °C.

### 3.4.2 Dye Uptake ( $q_e$ )

After centrifugation the concentration of free dye molecules in the supernatant was determined using UV-vis spectrophotometer (Varian Cary 100 Bio). The previously prepared calibration curve was used to convert the absorption values of UV-vis spectrophotometer to the concentration. The amount of dye adsorbed on the surface of CNC was calculated using the following equation:

$$q_e = \frac{(C_0 - C_e)V}{m} \quad (3.2)$$



where  $q_e$  is the amount of dye adsorbed for 1 g of adsorbent (mg/g),  $C_e$  is the equilibrium concentration of free dye molecules in the solution (mg/L),  $C_0$  is the initial dye concentration (mg/L),  $V$  is the volume of solution (L) and  $m$  is the mass of adsorbent (g).

### **3.4.3 Effect of Adsorbent Dosage**

The effect of adsorbent dosage was studied by varying the concentration of CNC from 4 mg/ml to 25 mg/ml while keeping the dye concentration constant at 200 mg/ml. The pH was kept at 9 and the temperature at 25 °C.

### **3.4.4 Effect of Initial Dye Concentration**

The effect of initial dye concentration was evaluated by changing the dye concentration from 100 mg/L to 1500 mg/L while keeping the adsorbent dosage constant at 10 mg/ml. Similar pH and temperature conditions were maintained.

### **3.4.5 Effect of pH**

The effect of pH was studied by maintaining the pH at 2.5, 6.5 and 10 at 25 °C. The dye concentration was 500 mg/L and the adsorbent dosage was 12.17 mg/ml.

### **3.4.6 Effect of Ionic Strength**

The effect of ionic strength was studied in terms of the change in dye removal percentage and dye uptake ( $q_e$ ). The change in dye removal percentage was studied in the presence of 17, 51 and 85 mM NaCl in dye solution (500 mg/L) at the adsorbent dosage of 12.17 mg/ml. The effect of ionic strength on the adsorption of methylene blue per g of CNC was studied by varying the concentration of dye from 600 mg/L to 1600 mg/L in the presence of 34, 82, and 171 mM NaCl. The adsorbent dosage was 12.48 mg/ml.

### **3.4.7 Adsorption Isotherms and Thermodynamic Parameters**

Adsorption isotherms of unmodified CNC were studied at 25 °C and 50 °C to extract thermodynamic parameters of adsorption of methylene blue on the surface of cellulose nanocrystals. However, the adsorption isotherm of carboxylated CNC was studied only at 25 °C to show that activation of CNC with carboxyl groups enhances adsorption capacity.

# Chapter 4

## Results and Discussions

### 4.1 Characterization of Unmodified and Carboxylated CNC

#### 4.1.1 Transmission Electron Microscopy

TEM image (Figure 4.1) shows that CNC possesses rod like structure. It seems that some aggregates were formed during the drying process due to the extensive hydrogen bonding between the nanocrystals (Peng et al., 2012).

#### 4.1.2 Fourier Transform Infrared (FT-IR) Spectroscopy

FT-IR spectra of unmodified CNC and carboxylated CNC are shown in Figure 4.2 and Figure 4.3, respectively. The broad peak between 3600 and 3000  $\text{cm}^{-1}$  in the spectra of CNC (Figure 4.2) is due to the O-H stretching vibrations (Cai and Kim, 2008). The peak bands between 3000-2800  $\text{cm}^{-1}$  and 1500-1250  $\text{cm}^{-1}$  are attributed to the stretching vibrations of aliphatic C-H and bending vibrations of  $\text{CH}_2$ , respectively. The peaks at

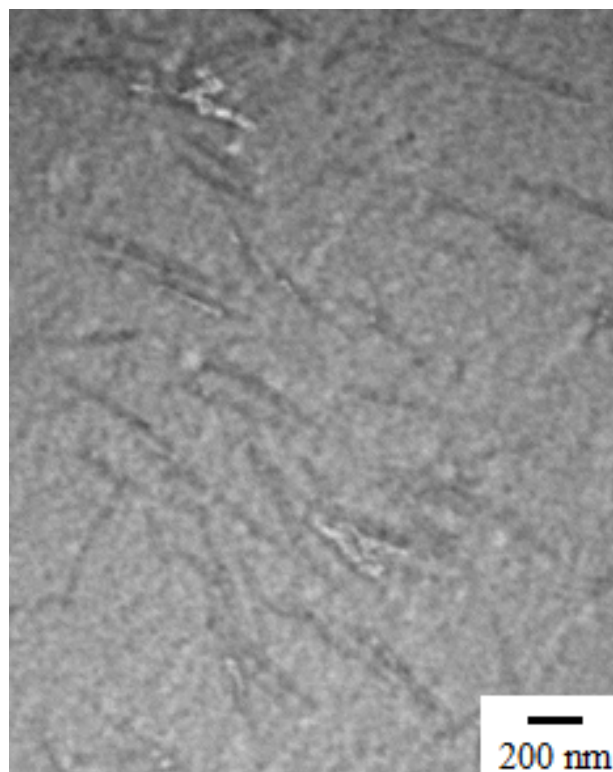


**Figure 4.1:** TEM image of CNC.

1160 and 1070  $\text{cm}^{-1}$  are related to the saccharide structure (de Mesquita et al., 2010). The peak at 1250  $\text{cm}^{-1}$  is attributed to the asymmetrical S=O vibration which shows the presence of sulfate ester groups on the surface of CNC (Gu et al., 2013). The FT-IR spectrum of carboxylated CNC was compared with the spectra of unmodified CNC to show the appearance of new peak at 1730  $\text{cm}^{-1}$  (Figure 4.3). This new peak is attributed to the presence of carboxyl groups in their acidic form, which validates the oxidation process (Azzam et al., 2010).

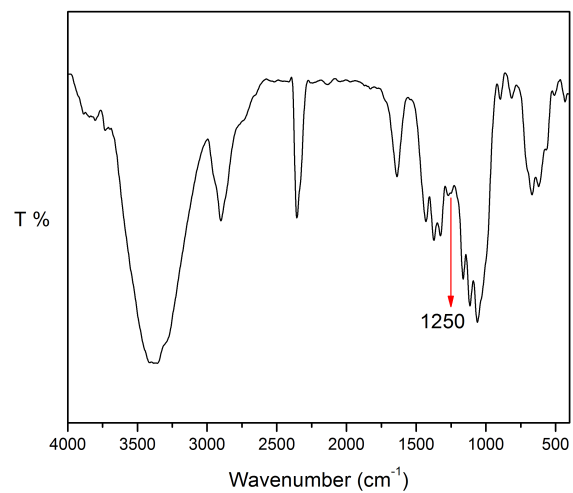


**Figure 4.2:** FTIR spectra of unmodified CNC.

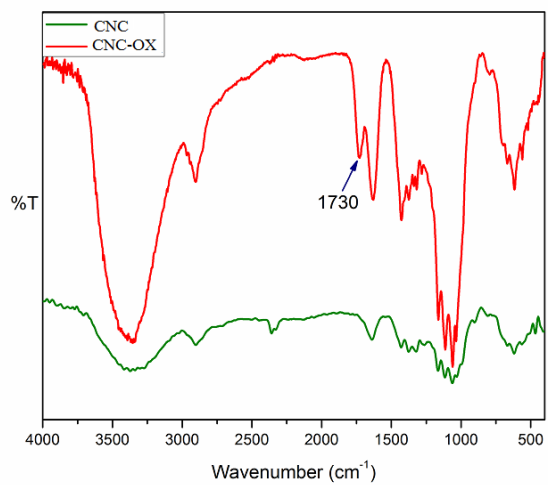


**Figure 4.3:** FTIR spectra of unmodified CNC and carboxylated CNC.

### 4.1.3 Potentiometric Titration (Determination of Carboxyl Acid Content on CNC)

Figures 4.4 and 4.5 show the titration curves of CNC and carboxylated CNC, respectively. Figure 4.4 shows the comparison of the two titration curves, unmodified and modified CNC. There is a sharp increase in the pH due to the absence of weak acid on CNC (Figure 4.4), whereas the gradual increase in pH as seen in Figure 4.5 shows the buffer effect attributed to the presence of weak acids on CNC. There are three regions in the titration curve of carboxylated CNC: strong acid, weak acid and strong base. The amount of carboxyl group per unit mass of the CNC can be determined from the weak acid region of the titration curve.

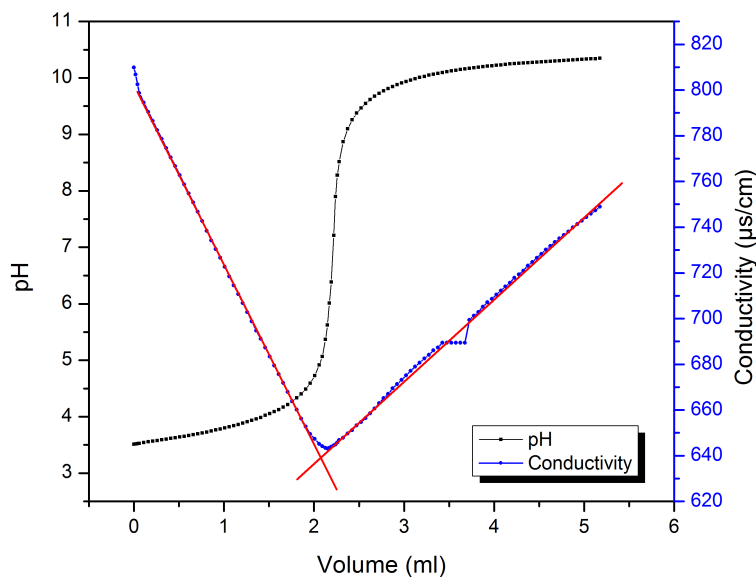


**Figure 4.4:** Potentiometric titration curve for CNC.

It was calculated that there is 2.1 mmol of COOH on the surface of 1g carboxylated CNC, based on the Figure 4.5. Degree of oxidation was calculated using the equation 3.1:

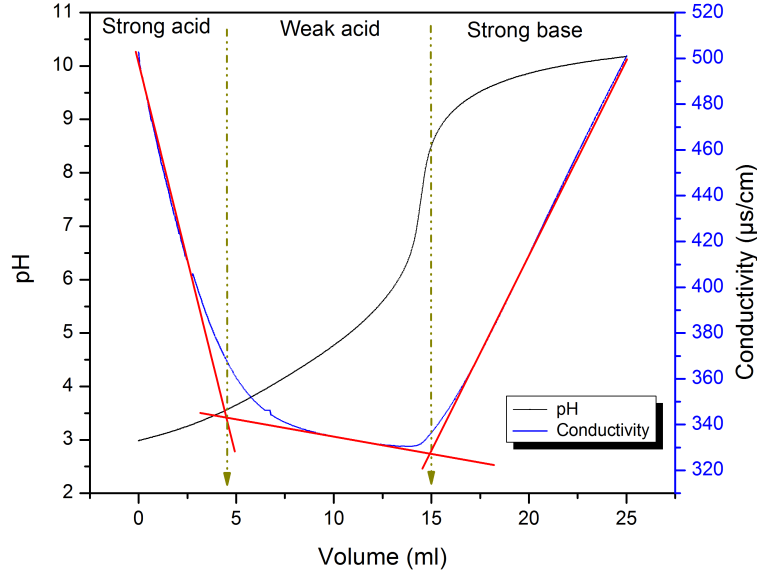


**Figure 4.5:** Potentiometric titration curve for carboxylated CNC.

$$DO = \frac{162 \times 10.4 \times 10^{-3} \times 0.01}{0.05 - (36 \times 10.4 \times 10^{-3} \times 0.01)} = 0.34 \quad (3.1)$$

The degree of oxidation changed with the molar ratio between sodium hypochlorite (NaClO) and anhydrous glucose unit (AGU). The maximum value depended on the crystalline structure and size of CNC (Habibi et al., 2006).

## 4.2 Wavelength of Maximum Absorbance and Calibration Curve

Figure 4.6 shows the absorption spectrum of methylene blue. Maximum absorption was observed around 664 nm, and this particular wavelength was used to determine the concentrations of solutions.

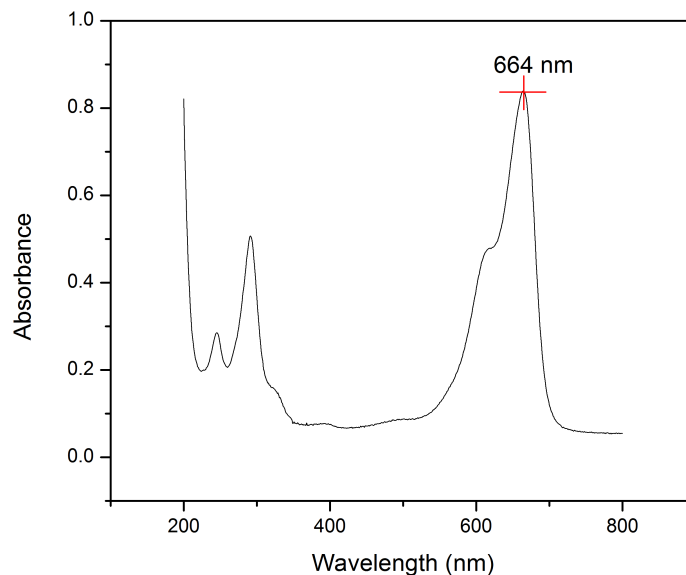


**Figure 4.6:** UV-vis spectrum of methylene blue.

Figure 4.7 represents the calibration curve of methylene blue that was used to calculate the concentration of unknown samples. The high value of regression coefficient ( $R^2$ ) confirmed the strong linear dependence of the absorption and concentrations of samples.

## 4.3 Adsorption of Methylene Blue on Unmodified CNC

### 4.3.1 Effect of Adsorbent Dosage

The effect of adsorbent dosage was investigated by varying the amount of CNC (adsorbent) from 4 to 25 mg/ml at the dye concentration of 200 mg/L.

Figure 4.8 evaluates that the percentage dye removal increased with the increasing amount of adsorbent and it reached a plateau (92.3%) at 20 mg/ml. The increase in dye



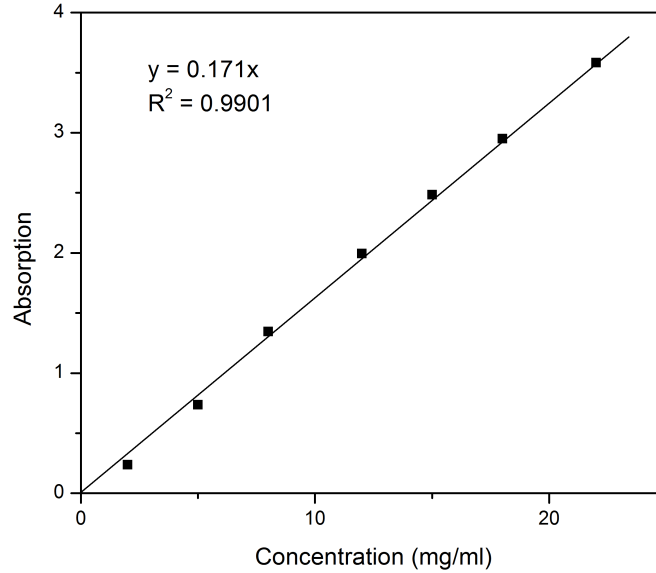


**Figure 4.7:** Calibration curve of methylene blue.

removal at higher adsorbent dosage could be attributed to the presence of more active sites for the same number of dye molecules (Deng et al., 2009).

Although the dye removal percentage increased with the increase in adsorbent dosage, the amount of dye adsorbed per unit mass ( $q_e$ ) decreased as shown in Figure 4.8. This can be attributed to the unsaturation of active sites on adsorbent due to the increase of the ratio of adsorption sites to the dye molecules (Ozacar and Sengil, 2005).

### 4.3.2 Effect of Initial Dye Concentration

For a fixed amount of adsorbent the percentage dye removal initially increased and then gradually decreased with increasing initial dye concentration ( $C_0$ ) as seen in Figure 4.9. The initial increase in the percent removal at low dye concentration could be attributed to the low ratio of initial number of dye molecules to the adsorption sites. Therefore the

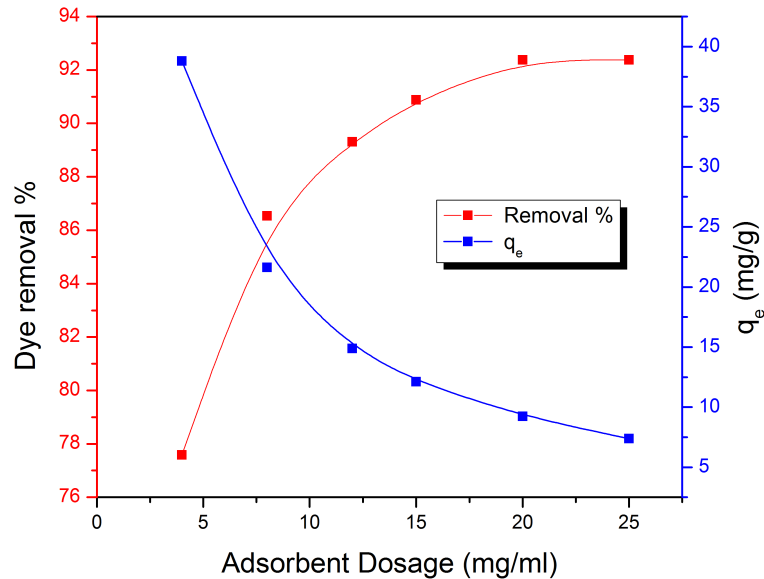


**Figure 4.8:** Effect of adsorbent dosage on the removal of methylene blue (dye concentration=200 mg/L).

removal percentage increased as dye concentration was increased. However, at relatively high dye concentration, the ratio of the increase in dye concentration to the increase in amount of dye adsorbed became lower due to the availability of less adsorption sites (Chaari et al., 2008). This result is consistent with the result of Saha et al. (Saha et al., 2010)

Even though the removal percentage decreased with increasing dye concentration, the amount of adsorbed dye per unit mass ( $q_e$ ) increased because the number of dye molecules available for adsorption was greater for the same number of adsorption sites at high dye concentration. This finding is consistent with the results of Mall et al. (Mall et al., 2005).

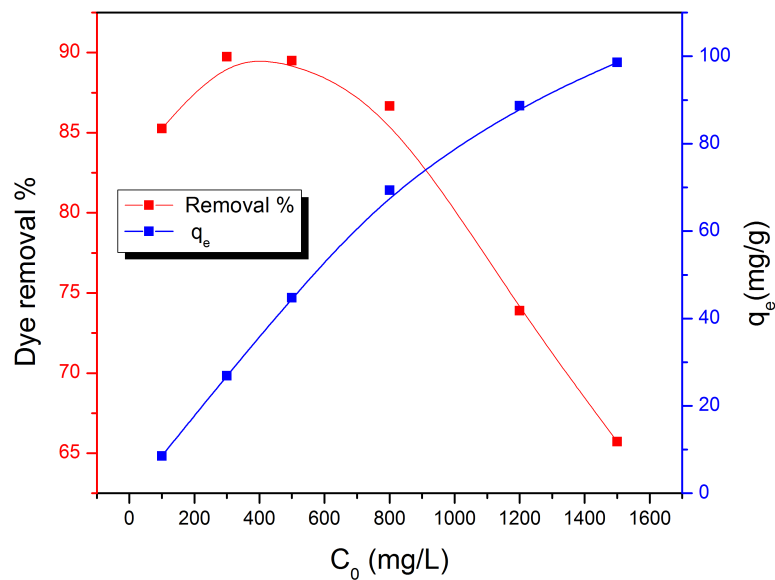


**Figure 4.9:** Effect of initial dye concentration ( $C_0$ ) on the percentage removal of methylene blue (adsorbent dosage=12.17mg/ml).

### 4.3.3 Effect of pH

The pH of the medium affects the surface charge of the adsorbents through the protonation or deprotonation of the functional groups on them. For the adsorbents possessing functional groups such as  $-\text{COO}^-$ ,  $-\text{SO}_3^-$  the negative surface charge decreased as pH approached the pKa of the functional groups. Since the pKa of sulfate groups is around 1.9, the dye removal percentage was not effected at pH range from 2.5 to 10 as observed in the Figure 4.10 (Klemm et al., 2011). This result suggests that CNC can be used to treat textile effluents within a wide range of pH.

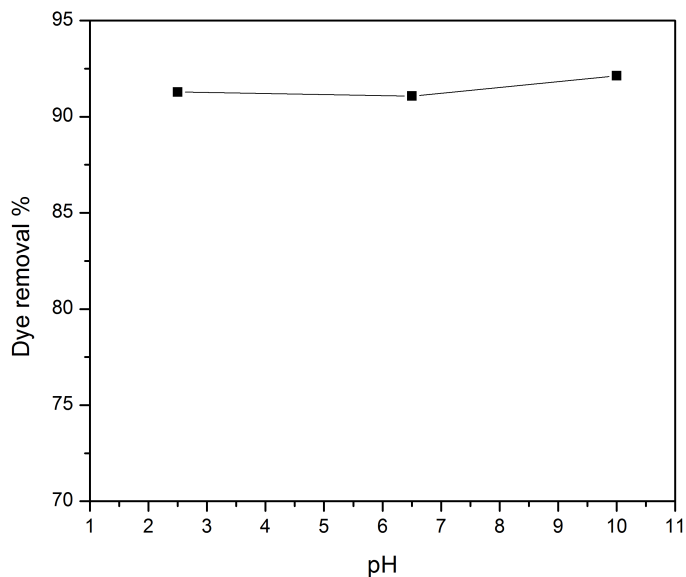


**Figure 4.10:** Effect of pH on the percentage removal of methylene blue (adsorbent dosage=12.17 mg/ml, dye concentration=500 mg/L).

#### 4.3.4 Effect of Inonic Strength

Wastewater from dye industry may contain various impurities such as suspended and dissolved compounds, acids or alkalis, salts, metal ions and other toxic compounds. The presence of ions increases the ionic strength of the solution, which may change the performance of adsorption process (Maurya et al., 2006). The effect of ionic strength on the adsorption of methylene blue was investigated by adding different amounts of NaCl to the solution.  $\text{Na}^+$  and  $\text{Cl}^-$  ions in the solution will screen the electrostatic interaction between the adsorbent and dye molecules (Dogan et al., 2008). As shown in Figure 4.11, the presence of 85 mM NaCl in dye solution (500 mg/L) reduced the removal percentage of methylene blue from 92.3 to 89.8. Figure 4.12 shows the effect of ionic strength on the uptake of methylene blue per g of CNC. It is evaluated that the addition of NaCl to the dye solutions within the concentration range of 600-1600 mg/L did not significantly affect

the removal. These results are consistent with the results of Maurya et al. (Maurya et al., 2006). In the light of these facts, it can be concluded that CNC can be used to remove methylene blue from high ionic strength effluents.

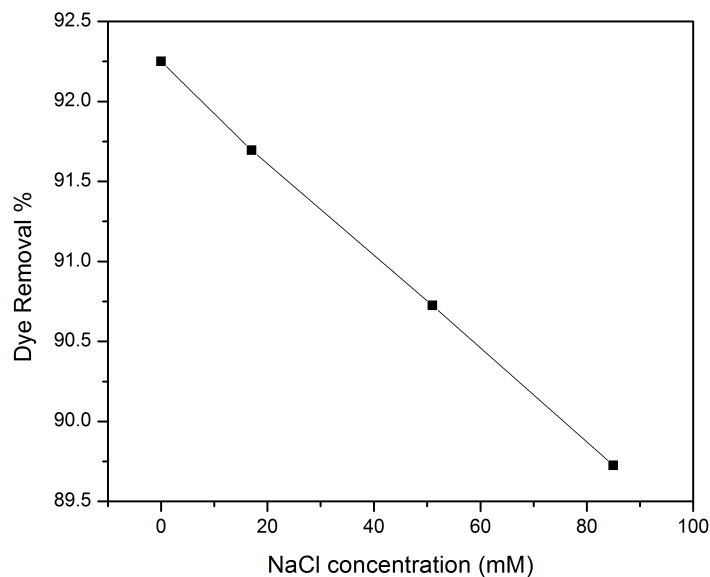


**Figure 4.11:** Effect of ionic strength on percentage dye removal (adsorbent dosage=12.17mg/ml, dye concentration=500 mg/L).

### 4.3.5 Adsorption Isotherms

#### 4.3.5.1 Langmuir Isotherm

The equation of Langmuir isotherm can be represented by Equation 2.1 (Mall et al., 2005):

$$q_e = \frac{q_m K_a C_e}{1 + K_a C_e} \quad (2.1)$$

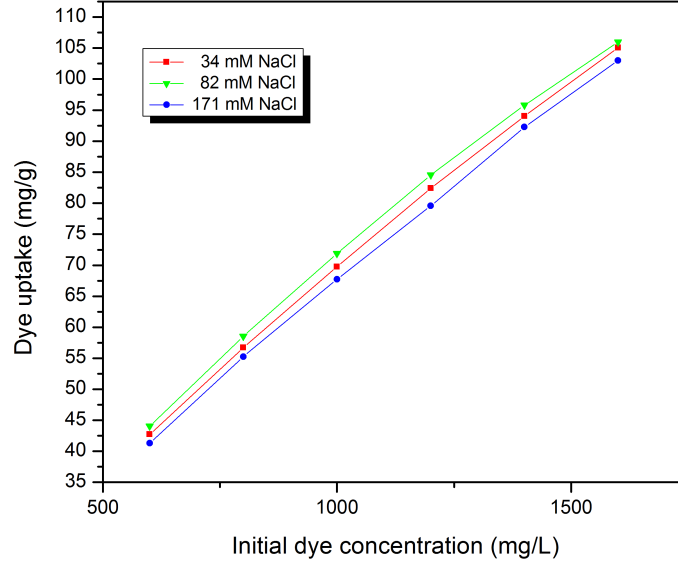


**Figure 4.12:** Effect of ionic strength on dye uptake (mg/g) at various initial dye concentrations.

where  $q_e$  is the amount of dye adsorbed per g of adsorbent (mg/g) in equilibrium,  $q_m$  is the maximum amount of dye which can be adsorbed per g of adsorbent (mg/g) in equilibrium,  $C_e$  is the equilibrium concentration of free dye molecules in the solution (mg/L),  $K_a$  is a constant related to the energy of adsorption (L/mg) which shows the affinity between dye and adsorbent.

The values of  $K_a$  and  $q_m$  can be extracted by using linearized form of Langmuir isotherm.

$$\frac{1}{q_e} = \frac{1}{K_a q_m C_e} + \frac{1}{q_m} \quad (2.2)$$

The linearized form of Langmuir isotherm can be represented a plot of  $1/q_e$  vs.  $1/C_e$ , where  $q_m$  and  $K_a$  can be found from the interception and slope, respectively. Figure 4.13 shows the linearized Langmuir plots of methylene blue at 25 °C and 50 °C. The applicability

of the isotherm model could be judged by the  $R^2$  (determination coefficient) value of each plot. For all temperatures, the  $R^2$  values were 0.99 which confirmed that the experimental data could be described by the Langmuir isotherm. The Langmuir constants ( $q_m$ ,  $K_a$ ) were calculated from the plot and are summarized in Table 4.1.  $K_a$  and  $q_m$  decreased with increasing temperature which indicated a better adsorption at lower temperature. These results are consistent with the results of Bhatnagar and Jain (Bhatnagar and Jain, 2005).

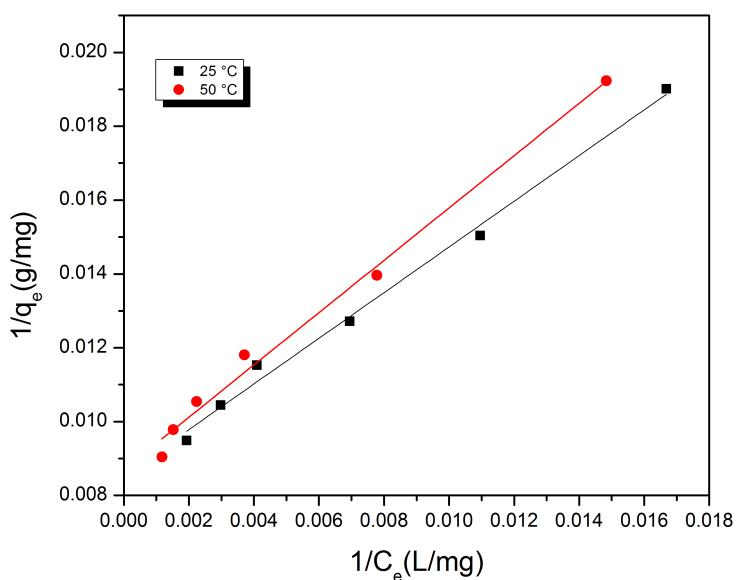


**Figure 4.13:** Linearized Langmuir plots for the adsorption of methylene blue on unmodified CNC at 25 °C and 50 °C.

$R_L$ , a dimensionless separation factor, can be used to determine the favorability and feasibility of adsorption process (Mall et al., 2005). It is given by the following equation.

$$R_L = \frac{1}{1 + K_a C_0} \quad (4.1)$$

where  $C_0$  is the initial dye concentration in solution (mg/L) and  $K_a$  is the Langmuir constant (L/mg). The isotherm is unfavorable if  $R_L > 1$ , linear if  $R_L = 1$ , favorable if  $0 <$

**Table 4.1:** Langmuir constants, equation and regression coefficient of linearized plots for the adsorption of methylene blue on unmodified CNC.

Temperature	$q_m$ (mg/g)	$K_a$ (L/mg)	$K_a$ (L/mol)	Equation	$R^2$
25 °C	118	0.0137	4382	$y = 0.6185x + 0.0085$	0.99
50 °C	115	0.0123	3934	$y = 0.7085x + 0.0087$	0.99

$R_L < 1$  and irreversible if  $R_L = 0$ . In this study for both temperatures the value of  $R_L$  was between 0 and 1 indicating that the adsorption was favorable (Figure 4.14).

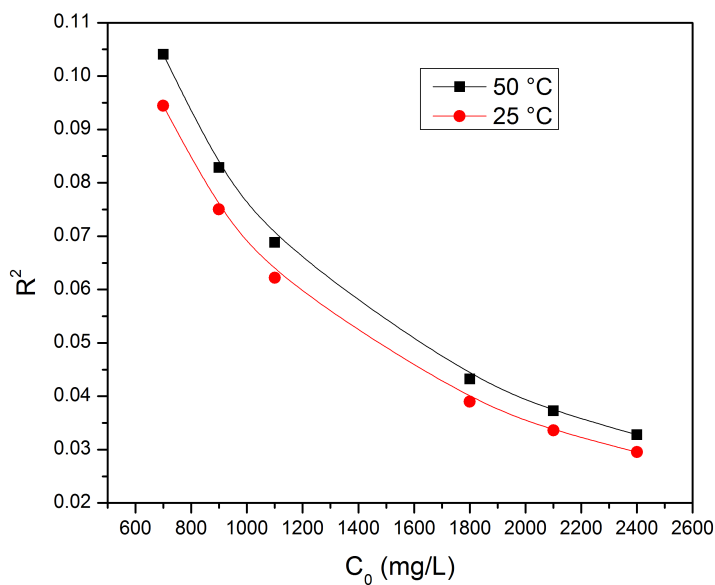


**Figure 4.14:** Plot of separation factor at various dye concentrations.

#### 4.3.5.2 Freundlich Isotherm

Freundlich isotherm model is usually used to describe heterogeneous systems and it involves the formation of multilayer adsorption (Wong et al., 2003). It can be represented



as:

$$q_e = kC_e^{1/n} \quad (2.3)$$

where  $q_e$  is the amount of dye adsorbed per g of adsorbent (mg/g) in equilibrium,  $k$  is related to the adsorption capacity,  $1/n$  is heterogeneity factor which ranges from 0 to 1 and  $C_e$  is the equilibrium concentration of free dye molecules in the solution (mg/L).

The linearized form of Langmuir isotherm is described by the equation below.

$$\log q_e = \log k + \frac{1}{n} \log C_e \quad (2.4)$$

Figure 4.15 shows the linear plot of  $\log q_e$  vs  $\log C_e$  at 25 °C and 50 °C. The values of  $k$  and  $n$  could be obtained from the slope and intercept of this plot (Table 4.2).

The values of  $k$  and  $n$  decreased with increasing temperature, which indicated that better adsorption occurred at lower temperatures (Gupta et al., 2005).

#### 4.3.5.3 Comparison of Isotherms

The regression coefficient values obtained from linearized forms of Langmuir and Freundlich isotherms indicated that both methods could be used to describe the experimental data (Table 4.3). This observation was also reported by other researchers (Sivasamy and Sundarabal, 2011; Široký et al., 2011). The  $R^2$  values of Langmuir model were better than the ones extracted from Freundlich model and experimental datas were more close to

**Table 4.2:** Freundlich constants, equation and regression coefficient of linearized plots for the adsorption of methylene blue on unmodified CNC.

Temperature	n	k	Equation	R <sup>2</sup>
25 °C	3.638	18.56	$y = 0.2749x + 1.269$	0.97
50 °C	3.597	17.27	$y = 0.278x + 1.237$	0.97

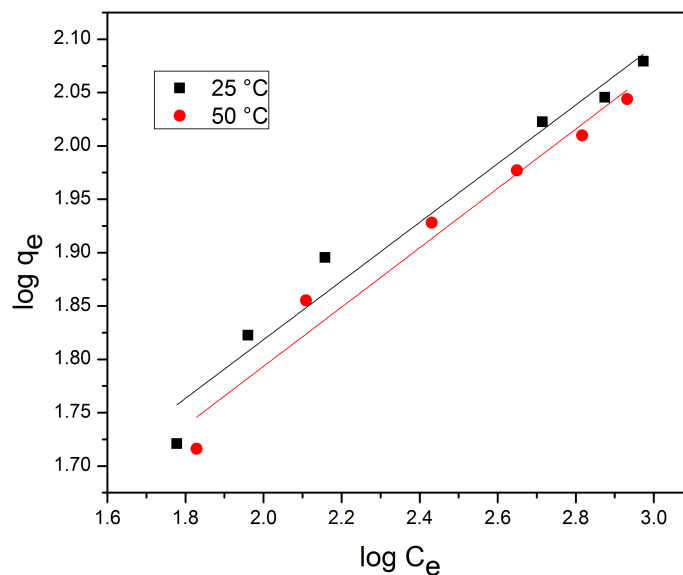


**Figure 4.15:** Linearized Freundlich plot for the adsorption of methylene blue on unmodified CNC at 25 °C and 50 °C.

the non-linearized Langmuir isotherm (Figure 4.16), evaluating the better applicability of Langmuir model to our system.

### 4.3.6 Thermodynamic Parameters

Thermodynamic parameters of the adsorption process such as  $\Delta G$ ,  $\Delta S$  and  $\Delta H$  can be determined using the following equations (Gupta et al., 2005) and they are given in

**Table 4.3:** Freundlich constants, equation and regression coefficient of linearized plots for the adsorption of methylene blue on unmodified CNC.

Temperature	R <sup>2</sup> (Langmuir model)	R <sup>2</sup> (Freundlich model)
25 °C	0.9936	0.9736
50 °C	0.9916	0.9685

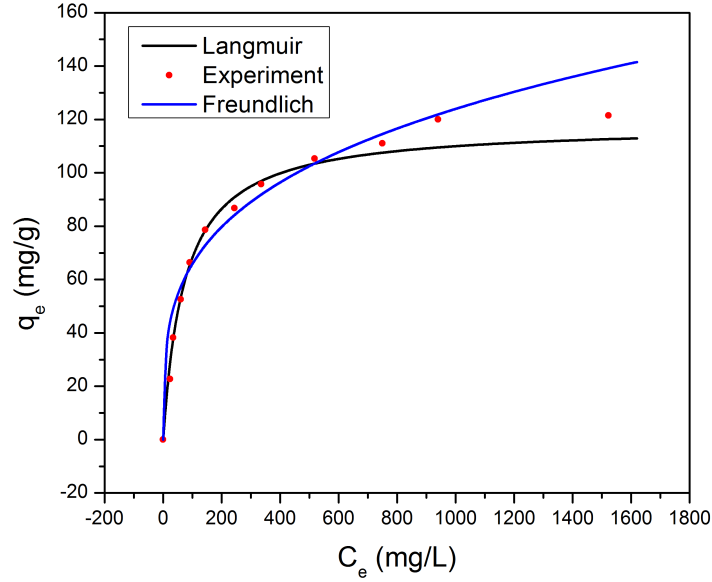


**Figure 4.16:** Comparison of experimental data with Langmuir and Freundlich model.

Table 4.4.

$$\ln \frac{K_{a2}}{K_{a1}} = -\frac{\Delta H}{R} \left( \frac{1}{T_2} - \frac{1}{T_1} \right) \quad (4.2)$$

$$\Delta G = \Delta H - T\Delta S \quad (4.3)$$

$$\Delta G = -RT \ln(K_a) \quad (4.4)$$

where T is the temperature (K), R is gas constant (J/Kmol),  $K_{a1}$  and  $K_{a2}$  are the constants (L/mg) obtained from Langmuir model at 25 °C and 50 °C.

The negative values of  $\Delta G$  shows that methylene blue adsorption on CNC is a spontaneous process. The negative  $\Delta H$  values confirmed the exothermic nature of the adsorption

**Table 4.4:** Thermodynamic parameters for the adsorption of methylene blue on unmodified CNC.

Temperature	$K_a$	$\Delta G(\text{kJ/mol})$	$\Delta H (\text{kJ/mol})$	$\Delta S (\text{kJ/molK})$
25 °C	0.0137	-20.8	-3.45	0.58
50 °C	0.0123	-22.2	-3.45	0.58

process.  $\Delta H$  values were relatively small, which suggested that the adsorption has physical character (Bhatnagar and Jain, 2005). The positive  $\Delta S$  values suggested a good affinity of adsorbent to the methylene blue (Wang et al., 2005). These results are consistent with the results of Bhatnagar and Jain (Bhatnagar and Jain, 2005).

## 4.4 Activation of CNC by Oxidation

Figure 4.17 shows the linearized form of Langmuir isotherm for the adsorption of methylene blue by carboxylated CNC. The Langmuir constants, regression coefficients and the equation are shown in table 4.5 . The adsorption capacity was calculated from the linearized Langmuir model and it possessed a value of 769 mg/g. The increase in  $q_m$  value from 118 to 769 mg/g indicated that the oxidation of CNC increased the adsorption capacity due to the increase in adsorption sites. Before the oxidation of CNC, adsorption occurred due to the presence of sulphate ester groups whereas after the oxidation the carboxyl groups also contributed to the adsorption process. The adsorption capacity of carboxylated CNC is larger than most of the commercially available activated carbons and agricultural wastes (Figure 4.18) (Rafatullah et al., 2010).

**Table 4.5:** Langmuir constants, equations and regression coefficients of linearized plots for the adsorption of methylene blue on carboxylated CNC.

$q_m$ (mg/g)	$K_a$ (L/mg)	Equation	$R^2$
769	0.0091	$y=0.1436x + 0.0013$	0.9923

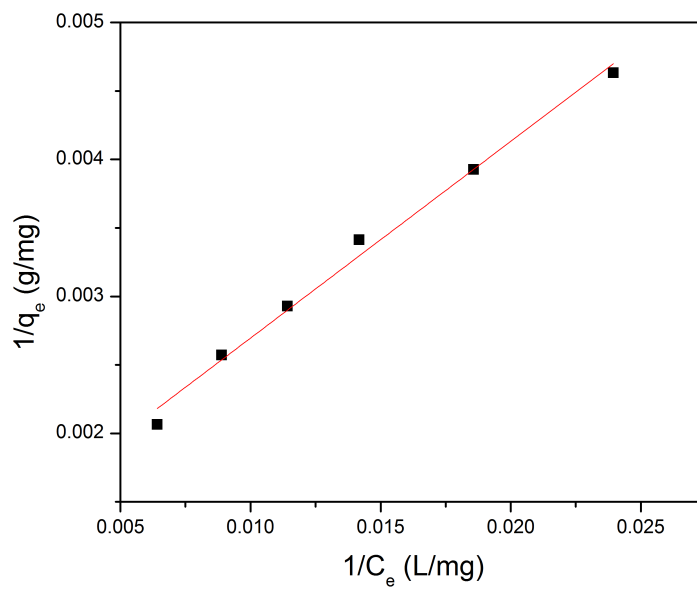


**Figure 4.17:** Linearized Langmuir plot for the adsorption of methylene blue on carboxylated CNC.

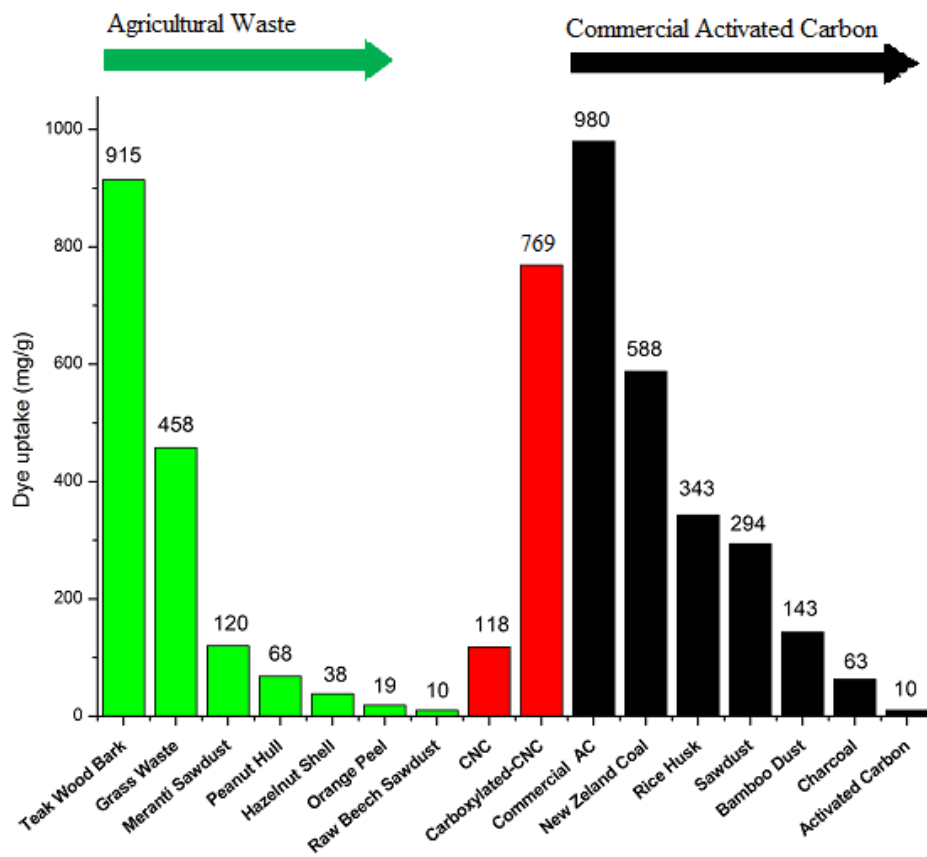


**Figure 4.18:** Comparison of the adsorption capacity of CNC with commercial activated carbons and agricultural wastes (Rafatullah et al., 2010).

# Chapter 5

## Conclusions

### 5.1 Summary

The treatment of dye effluents before discharge to the environment has become an important issue due to the stability and adverse effects of dyes. Among the present methods, adsorption has been preferred to other conventional techniques due to the simple design and operation, low initial investment, effectiveness and insensitivity to toxic substances (Sharma et al., 2011; Unuabonah et al., 2008). Activated carbon is the most widely used adsorbent for water treatment due to its high surface area and excellent adsorption. However, the high cost of activated carbon restricts its widespread use, and this motivates the search of alternative adsorbents for the removal of dyes (Sharma et al., 2011).

The high surface area derived from the nano size of CNC, and the presence of permanent negative charge on the surface makes cellulose nanocrystal an excellent candidate for the adsorption of basic (cationic) dyes. The objective of this project is to demonstrate the adsorption properties of CNC for the removal of methylene blue from aqueous solution by varying the parameters such as adsorbent dosage, initial dye concentration, pH, temperature and salt concentration. It was evaluated that the adsorption is independent of pH, however increase in temperature and ionic strength decreased the removal percentage

slightly. The Langmuir and Freundlich isotherms were used to evaluate the feasibility of the adsorption process, where the Langmuir model described the adsorption better. The adsorption capacity ( $q_m$ ) was determined using the linearized form of Langmuir model. It possessed a value of 118 mg/g at pH 9 and 25 °C. To increase the adsorption capacity, CNC was oxidized with TEMPO reagent that converts primary hydroxyl groups to carboxyl groups. The adsorption capacity increased from 118 to 769 mg/g. In the light of these facts, it could be concluded that the use of unmodified CNC for the removal of methylene blue is feasible and the promising adsorption capacity of carboxylated CNC implies that surface modifications can enhance the potentials of CNC in this application.

## 5.2 Future Direction

The use of CNC for adsorption of methylene blue results in sludge formation. This increases the cost of disposal. Instead of using CNC dispersed in solution, incorporating inside the beads of biomolecules such as alginate or chitosan could make operation and separation easier. Incorporation of CNC could increase the mechanical strength of beads, which can be used in column studies. Therefore one of the further steps of this project could be the incorporation of CNC inside the beads and to study adsorption properties.

In this study the negative permanent charge ( $-\text{OSO}_3^-$ ) on the surface of CNC was utilized for the adsorption of cationic dye. The surface of CNC could be also positively charged which allows studying the adsorption of anionic dyes. This could be another approach for future study arising from this project.

Finally, the cost analysis of raw material (CNC), chemical treatment and operation can be very beneficial to compare its feasibility with commercially available adsorbents.



# References

Acemioglu, B., "Adsorption of Congo red from aqueous solution onto calcium-rich fly ash," *J. Colloid Interface Sci.* 274 (2004).

Ahmad, A., M. Rafatullah, O. Sulaiman, M.H. Ibrahim and R. Hashim, "Scavenging behaviour of meranti sawdust in the removal of methylene blue from aqueous solution," *J. Hazard. Mater.* 170, 357-365 (2009).

Ahuja, S., "Handbook of Water Purity and Quality," IWA Publishing, Great Britain (2009).

Aksu, Z., "Application of biosorption for the removal of organic pollutants: A review," *Process Biochemistry.* 40 (2005).

Aksu, Z., "Reactive dye bioaccumulation by *Saccharomyces cerevisiae*," *Process Biochemistry.* 38, 1437-1444 (2003).

Aksu, Z. and S. Tezer, "Equilibrium and kinetic modelling of biosorption of Remazol Black B by *Rhizopus arrhizus* in a batch system: effect of temperature," *Process Biochemistry.*

36, 431-439 (2000).

Al-Asheh, S., F. Banat and L. Abu-Aitah, "Adsorption of phenol using different types of activated bentonites," *Separation and Purification Technology*. 33, 1-10 (2003).

Alaton, I.A., I.A. Balcioglu and D.W. Bahnemann, "Advanced oxidation of a reactive dye bath effluent: comparison of O<sub>3</sub>, H<sub>2</sub>O<sub>2</sub>/UV-C and TiO<sub>2</sub>/UV-A processes," *Water Res.* 36, 1143-1154 (2002).

Alkan, M., S. Celikcapa, O. Demirbas and M. Dogan, "Removal of reactive blue 221 and acid blue 62 anionic dyes from aqueous solutions by sepiolite," *Dyes and Pigments*. 65, 251-259 (2005).

Allen, R.L.M., "Colour Chemistry," Appleton-Century-Crofts, Educational Division, New York (1971).

Alpat, S., O. Ozbayrak, S. Alpat and H. Akcay, "The adsorption kinetics and removal of cationic dye, Toluidine Blue O, from aqueous solution with Turkish zeolite," *J. Hazard. Mater.* 151, 213-220 (2008).

Andrade, L.S., L.A.M. Ruotolo, R.C. Rocha-Filho, N. Bocchi, S.R. Biaggio, J. Iniesta, V. Garcia-Garcia and V. Montiel, "On the performance of Fe and Fe,F doped Ti-Pt/PbO<sub>2</sub> electrodes in the electrooxidation of the Blue Reactive 19 dye in simulated textile wastewater," *Chemosphere*. 66, 2035-2043 (2007).

Andresen, M., L. Johansson, B.S. Tanem and P. Stenius, "Properties and characterization of hydrophobized microfibrillated cellulose," *Cellulose*. 13, 665-677 (2006).

Angles, M.N. and A. Dufresne, "Plasticized starch/tunicin whiskers nanocomposite mate-

rials. 2. Mechanical behavior,” *Macromolecules*. 34, 2921-2931 (2001).

Anjaneyulu, Y., N. Sreedhara Chary and D. Samuel Suman Raj, “Decolourization of Industrial Effluents - Available Methods and Emerging Technologies - A Review,” *Rev Environ Sci Biotechnol*. 4, 245-273 (2005).

Anliker, R., “Ecotoxicology of dyestuffs-A joint effort by industry,” *Ecotoxicol. Environ. Saf.* 3, 59-74 (1979).

Annadurai, G., R. Juang and D. Lee, “Use of cellulose-based wastes for adsorption of dyes from aqueous solutions,” *J. Hazard. Mater.* 92, 263-274 (2002).

Araki, J., M. Wada and S. Kuga, “Steric stabilization of a cellulose microcrystal suspension by poly(ethylene glycol) grafting,” *Langmuir*. 17, 21-27 (2001).

Atalla, R.H. and D.L. VanderHart, “The role of solid state C-13 NMR spectroscopy in studies of the nature of native celluloses,” *Solid State Nucl. Magn. Reson.* 15, 1-19 (1999).

Awad, H.S. and N.A. Galwa, “Electrochemical degradation of Acid Blue and Basic Brown dyes on Pb/PbO<sub>2</sub> electrode in the presence of different conductive electrolyte and effect of various operating factors,” *Chemosphere*. 61, 1327-1335 (2005).

Aygün, A., S. Yenisoy-Karakaş and I. Duman, “Production of granular activated carbon from fruit stones and nutshells and evaluation of their physical, chemical and adsorption properties,” *Microporous and Mesoporous Materials*. 66, 189-195 (2003).

Azmi, W. and U.C. Banerjee, “Biological decolorization of crystal violet by a newly isolated *Bacillus* sp. and microbial assessment of toxicity of untreated and treated dye,” *Sci. Iranica*. 8, 171-178 (2001).

Azzam, F., L. Heux, J. Putaux and B. Jean, "Preparation By Grafting Onto, Characterization, and Properties of Thermally Responsive Polymer-Decorated Cellulose Nanocrystals," *Biomacromolecules*. 11, 3652-3659 (2010).

Bailey, S.E., T.J. Olin, R.M. Bricka and D.D. Adrian, "A review of potentially low-cost sorbents for heavy metals," *Water Res.* 33, 2469-2479 (1999).

Banat, F., S. Al-Asheh and L. Al-Makhadmeh, "Evaluation of the use of raw and activated date pits as potential adsorbents for dye containing waters," *Process Biochemistry*. 39, 193-202 (2003).

Barud, H.S., C. Barrios, T. Regiani, R.F.C. Marques, M. Verelst, J. Dexpert-Ghys, Y. Messaddeq and S.J.L. Ribeiro, "Self-supported silver nanoparticles containing bacterial cellulose membranes," *Materials Science & Engineering C-Biomimetic and Supramolecular Systems*. 28, 515-518 (2008).

Basar, C.A., "Applicability of the various adsorption models of three dyes adsorption onto activated carbon prepared waste apricot," *J. Hazard. Mater.* 135, 232-241 (2006).

Basava Rao, V.V. and S. Ram Mohan Rao, "Adsorption studies on treatment of textile dyeing industrial effluent by flyash," *Chem. Eng. J.* 116, 77-84 (2006).

Batzias, F., D. Sidiras, E. Schroeder and C. Weber, "Simulation of dye adsorption on hydrolyzed wheat straw in batch and fixed-bed systems," *Chem. Eng. J.* 148, 459-472 (2009).

Beck-Candanedo, S., D. Viet and D.G. Gray, "Triphase equilibria in cellulose nanocrystal suspensions containing neutral and charged macromolecules," *Macromolecules*. 40, 3429-

3436 (2007).

Beck-Candanedo, S., D. Viet and D.G. Gray, "Induced phase separation in cellulose nanocrystal suspensions containing ionic dye species," *Cellulose*. 13, 629-635 (2006).

Beck-Canedo, S., M. Roman and D.G. Gray, "Effect of Reaction Conditions on the Properties and Behavior of Wood Cellulose Nanocrystal Suspensions," *Biomacromolecules*. 6, 1048-1054 (2005).

Bhatnagar, A. and A.K. Jain, "A comparative adsorption study with different industrial wastes as adsorbents for the removal of cationic dyes from water," *J. Colloid Interface Sci.* 281, 49-55 (2005).

Bhattacharyya, K.G. and A. Sarma, "Adsorption characteristics of the dye, Brilliant Green, on Neem leaf powder," *Dyes and Pigments*. 57, 211-222 (2003).

Bhatti, H.N., N. Akram and M. Asgher, "Optimization of culture conditions for enhanced decolorization of cibacron red FN-2BL by *Schizophyllum commune* IBL-6," *Appl. Biochem. Biotechnol.* 149, 255-264 (2008).

Blumel, S., M. Contzen, M. Lutz, A. Stolz and H.J. Knackmuss, "Isolation of a bacterial strain with the ability to utilize the sulfonated azo compound 4-carboxy-4'-sulfoazobenzene as the sole source of carbon and energy," *Appl. Environ. Microbiol.* 64, 2315-2317 (1998).

Braun, B. and J.R. Dorgan, "Single-Step Method for the Isolation and Surface Functionalization of Cellulosic Nanowhiskers," *Biomacromolecules*. 10, 334-341 (2009).

Bromley-Challenor, K.C.A., J.S. Knapp, Z. Zhang, N.C.C. Gray, M.J. Hetheridge and M.R. Evans, "Decolorization of an azo dye by unacclimated activated sludge under anaer-

obic conditions,” *Water Res.* 34, 4410-4418 (2000).

Brown, E.E. and M.G. Laborie, “Bioengineering bacterial cellulose/poly(ethylene oxide) nanocomposites,” *Biomacromolecules.* 8, 3074-3081 (2007).

Brown, J.P., “Reduction of Polymeric Azo and Nitro Dyes by Intestinal Bacteria,” *Appl. Environ. Microbiol.* 41, 1283-1286 (1981).

Cai, Z. and J. Kim, “Characterization and electromechanical performance of cellulose-chitosan blend electro-active paper,” *Smart Mater Struct.* 17, 1-8 (2008).

Cameselle, C., M. Pazos and M.A. Sanroman, “Selection of an electrolyte to enhance the electrochemical decolourisation of indigo. Optimisation and scale-up,” *Chemosphere.* 60, 1080-1086 (2005).

Campos, R., A. Kandelbauer, K.H. Robra, A. Cavaco-Paulo and G.M. Gubitz, “Indigo degradation with purified laccases from *Trametes hirsuta* and *Sclerotium rolfsii*,” *J. Biotechnol.* 89, 131-139 (2001).

Can, O.T., M. Bayramoglu and M. Kobya, “Decolorization of Reactive Dye Solutions by Electrocoagulation Using Aluminum Electrodes,” *Ind Eng Chem Res.* 42, 3391-3396 (2003).

Cao, X., Y. Habibi and L.A. Lucia, “One-pot polymerization, surface grafting, and processing of waterborne polyurethane-cellulose nanocrystal nanocomposites,” *Journal of Materials Chemistry.* 19, 7137-7145 (2009).

Capalash, N. and P. Sharma, “Biodegradation of textile azo-dyes by *Phanerochaete chrysosporium*,” *World J. Microbiol. Biotechnol.* 8, 309-312 (1992).

Carliell, C.M., S.J. Barclay, C. Shaw, A.D. Wheatley and C.A. Buckley, "The Effect of Salts Used in Textile Dyeing on Microbial Decolourisation of a Reactive Azo Dye," *Environ. Technol.* 19, 1133-1137 (1998).

Carliell, C.M., S.J. Barclay, N. Naidoo, C.A. Buckley, D.A. Mulholland and E. Senior, "Microbial Decolorization of a Reactive Azo-Dye Under Anaerobic Conditions," *Water Sa.* 21, 61-69 (1995).

Chaari, I., E. Fakhfakh, S. Chakroun, J. Bouzid, N. Boujelben, M. Feki, F. Rocha and F. Jamoussi, "Lead removal from aqueous solutions by a Tunisian smectitic clay," *J. Hazard. Mater.* 156, 545-551 (2008).

Chao, A., S. Shyu, Y. Lin and F. Mi, "Enzymatic grafting of carboxyl groups on to chitosan—to confer on chitosan the property of a cationic dye adsorbent," *Bioresour. Technol.* 91, 157-162 (2004).

Chen, G., A. Dufresne, J. Huang and P.R. Chang, "A Novel Thermoformable Bionanocomposite Based on Cellulose Nanocrystal-graft-Poly(epsilon-caprolactone)," *Macromolecular Materials and Engineering.* 294, 59-67 (2009).

Chen, X., G. Chen, F. Gao and P.L. Yue, "High-Performance Ti/BDD Electrodes for Pollutant Oxidation," *Environ. Sci. Technol.* 37, 5021-5026 (2003)

Chiou, M. and H. Li, "Equilibrium and kinetic modeling of adsorption of reactive dye on cross-linked chitosan beads," *J. Hazard. Mater.* 93, 233-248 (2002).

Chiou, M., P. Ho and H. Li, "Adsorption of anionic dyes in acid solutions using chemically cross-linked chitosan beads," *Dyes and Pigments.* 60, 69-84 (2004).

Chrisite, R.M., "Environmental Aspects of Textile Dyeing," Woodhead, Cambridge, Boca Raton (2007).

Cooper, P., "Colour in Dyehouse Effluent," Society of Dyers and Colourists, Bradford (1995).

Costerton, J.W., Z. Lewandowski, D. Debeer, D. Caldwell, D. Korber and G. James, "Biofilms, the Customized Microniche," J. Bacteriol. 176, 2137-2142 (1994).

Coughlin, M.F., B.K. Kinkle and P.L. Bishop, "Degradation of azo dyes containing aminonaphthol by *Sphingomonas* sp strain 1CX," J Ind Microbiol Biotech. 23, 341-346 (1999).

Coughlin, M.F., B.K. Kinkle, A. Tepper and P.L. Bishop, "Characterization of aerobic azo dye-degrading bacteria and their activity in biofilms," Water Science and Technology. 36, 215-220 (1997).

Crini, G., "Non-conventional low-cost adsorbents for dye removal: A review," Bioresour. Technol. 97 (2006).

Cripps, C., J.A. Bumpus and S.D. Aust, "Biodegradation of Azo and Heterocyclic Dyes by *Phanerochaete-Chrysosporium*," Appl. Environ. Microbiol. 56, 1114-1118 (1990).

Czaja, W., D. Romanovicz and R.M. Brown, "Structural investigations of microbial cellulose produced in stationary and agitated culture," Cellulose. 11, 403-411 (2004).

Czímerová, A., J. Bujdák and A. Gáplovský, "The aggregation of thionine and methylene blue dye in smectite dispersion," Colloids Surf. Physicochem. Eng. Aspects. 243, 89-96 (2004).



Damardji, B., H. Khalaf, L. Duclaux and B. David, "Preparation of TiO<sub>2</sub>-pillared montmorillonite as photocatalyst Part II Photocatalytic degradation of a textile azo dye," *Appl. Clay. Sci.* 45, 98-104 (2009).

Daneshvar, N., A.R. Khataee, A.R. Amani Ghadim and M.H. Rasoulifard, "Decolorization of C.I. Acid Yellow 23 solution by electrocoagulation process: Investigation of operational parameters and evaluation of specific electrical energy consumption (SEEC)," *J. Hazard. Mater.* 148, 566-572 (2007).

de Mesquita, J.P., C.L. Donnici and F.V. Pereira, "Biobased Nanocomposites from Layer-by-Layer Assembly of Cellulose Nanowhiskers with Chitosan," *Biomacromolecules.* 11, 473-480 (2010).

de Rodriguez, N.L.G., W. Thielemans and A. Dufresne, "Sisal cellulose whiskers reinforced polyvinyl acetate nanocomposites," *Cellulose.* 13, 261-270 (2006).

Deng, H., L. Yang, G. Tao and J. Dai, "Preparation and characterization of activated carbon from cotton stalk by microwave assisted chemical activation—Application in methylene blue adsorption from aqueous solution," *J. Hazard. Mater.* 166, 1514-1521 (2009).

Denooy, A.E.J., A.C. Besemer and H. Vanbekkum, "Highly Selective Tempo Mediated Oxidation of Primary Alcohol Groups in Polysaccharides," *Recueil Des Travaux Chimiques Des Pays-Bas-Journal of the Royal Netherlands Chemical Society.* 113, 165-166 (1994).

Doğan, M., M. Alkan, A. Türkyilmaz and Y. Özdemir, "Kinetics and mechanism of removal of methylene blue by adsorption onto perlite," *J. Hazard. Mater.* 109, 141-148 (2004).

Dogan, M., H. Abak and M. Alkan, "Biosorption of methylene blue from aqueous so-

lutions by hazelnut shells: Equilibrium, parameters and isotherms,” *Water Air and Soil Pollution*. 192, 141-153 (2008).

Dong, X.M. and D.G. Gray, “Effect of counterions on ordered phase formation in suspensions of charged rodlike cellulose crystallites,” *Langmuir*. 13, 2404-2409 (1997).

Dong, X.M., J.F. Revol and D.G. Gray, “Effect of microcrystallite preparation conditions on the formation of colloid crystals of cellulose,” *Cellulose*. 5, 19-32 (1998).

Dong, X.M., T. Kimura, J.F. Revol and D.G. Gray, “Effects of ionic strength on the isotropic-chiral nematic phase transition of suspensions of cellulose crystallites,” *Langmuir*. 12, 2076-2082 (1996).

dos Santos, A.B., F.J. Cervantes and J.B. van Lier, “Review paper on current technologies for decolourisation of textile wastewaters: Perspectives for anaerobic biotechnology,” *Bioresour. Technol.* 98, 2369-2385 (2007).

Drogat, N., R. Granet, V. Sol, A. Memmi, N. Saad, C.K. Koerkamp, P. Bressollier and P. Krausz, “Antimicrobial silver nanoparticles generated on cellulose nanocrystals,” *Journal of Nanoparticle Research*. 13, 1557-1562 (2011).

Edgar, C.D. and D.G. Gray, “Influence of dextran on the phase behavior of suspensions of cellulose nanocrystals,” *Macromolecules*. 35, 7400-7406 (2002).

Eichlerova, I., L. Homolka and F. Nerud, “Decolorization of high concentrations of synthetic dyes by the white rot fungus *Bjerkandera adusta* strain CCBAS 232,” *Dyes and Pigments*. 75, 38-44 (2007).

El Qada, E.N., S.J. Allen and G.M. Walker, “Adsorption of basic dyes from aqueous

solution onto activated carbons,” *Chem. Eng. J.* 135, 174-184 (2008).

Eren, Z. and F.N. Acar, “Effect of Fenton’s reagent on the degradability of CI reactive yellow 15,” *Coloration Technology.* 122, 259-263 (2006).

Fan, L., Y. Zhou, W. Yang, G. Chen and F. Yang, “Electrochemical degradation of Amaranth aqueous solution on ACF,” *J. Hazard. Mater.* 137, 1182-1188 (2006).

Forgacs, E., T. Cserhati and G. Oros, “Removal of synthetic dyes from wastewaters: a review,” *Environ. Int.* 30, 953-971 (2004).

Freundlich, H., “Concerning adsorption in solutions.” *Zeitschrift Fur Physikalische Chemie–Stoichiometrie Und Verwandtschaftslehre.* 57, 385-470 (1906).

Fu, Y.Z. and T. Viraraghavan, “Fungal decolorization of dye wastewaters: a review,” *Bioresour. Technol.* 79, 251-262 (2001).

Fu, Y.Z. and T. Viraraghavan, “Removal of CI Acid Blue 29 from an aqueous solution by *Aspergillus niger*,” *Aatcc Review.* 1, 36-40 (2001b).

Garg, V.K., R. Gupta, A. Bala Yadav and R. Kumar, “Dye removal from aqueous solution by adsorption on treated sawdust,” *Bioresour. Technol.* 89, 121-124 (2003).

Gingell, R. and R. Walker, “Mechanisms of Azo Reduction by *Streptococcus faecalis* II. The Role of Soluble Flavins,” *Xenobiotica.* 1, 231-239 (1971).

Glenn, J.K. and M.H. Gold, “Decolorization of several Polymeric Dyes by the Lignin-Degrading Basidiomycete *Phanerochaete-Chrysosporium*,” *Appl. Environ. Microbiol.* 45, 1741-1747 (1983).

- Gordon, P.F. and P. Gregory, "Organic Chemistry in Colour," Springer, Berlin (1983).
- Gousse, C., H. Chanzy, G. Excoffier, L. Soubeyrand and E. Fleury, "Stable suspensions of partially silylated cellulose whiskers dispersed in organic solvents," *Polymer*. 43, 2645-2651 (2002).
- Greenleaf, J.E., J. Lin and A.K. Sengupta, "Two novel applications of ion exchange fibers: Arsenic removal and chemical-free softening of hard water," *Environ. Prog.* 25, 300-311 (2006).
- Gu, J., J.M. Catchmark, E.Q. Kaiser and D.D. Archibald, "Quantification of cellulose nanowhiskers sulfate esterification levels," *Carbohydr. Polym.* 92, 1809-1816 (2013).
- Guhados, G., W.K. Wan and J.L. Hutter, "Measurement of the elastic modulus of single bacterial cellulose fibers using atomic force microscopy," *Langmuir*. 21, 6642-6646 (2005).
- Guibal, E., "Interactions of metal ions with chitosan-based sorbents: a review," *Separation and Purification Technology*. 38, 43-74 (2004).
- Gul, S., O. Ozcan and O. Erbatur, "Ozonation of C.I. Reactive Red 194 and C.I. Reactive Yellow 145 in aqueous solution in the presence of granular activated carbon," *Dyes and Pigments*. 75, 426-431 (2007).
- Gulnaz, O., A. Kaya, F. Matyar and B. Arıkan, "Sorption of basic dyes from aqueous solution by activated sludge," *J. Hazard. Mater.* 108, 183-188 (2004).
- Gupta, V.K. and Suhas, "Application of low-cost adsorbents for dye removal - A review,"

J. Environ. Manage. 90 (2009).

Gupta, V.K., I. Ali, V.K. Saini, T.V. Gerven, B.V.d. Bruggen and C. Vecastele, "Removal of Dyes from Wastewater Using Bottom Ash," *Ind Eng Chem Res.* 44, 3655-3664 (2005).

Gürses, A., S. Karaca, Ç. Doğar, R. Bayrak, M. Açıkyıldız and M. Yalçın, "Determination of adsorptive properties of clay/water system: methylene blue sorption," *J. Colloid Interface Sci.* 269, 310-314 (2004).

Gurses, A., C. Dogar, S. Karaca, M. Acikyildiz and R. Bayrak, "Production of granular activated carbon from waste *Rosa canina* sp seeds and its adsorption characteristics for dye," *J. Hazard. Mater.* 131, 254-259 (2006).

Habibi, Y., H. Chanzy and M.R. Vignon, "TEMPO-mediated surface oxidation of cellulose whiskers," *Cellulose.* 13, 679-687 (2006).

Habibi, Y. and A. Dufresne, "Highly Filled Bionanocomposites from Functionalized Polysaccharide Nanocrystals," *Biomacromolecules.* 9, 1974-1980 (2008).

Habibi, Y., L.A. Lucia and O.J. Rojas, "Cellulose Nanocrystals: Chemistry, Self-Assembly, and Applications," *Chem. Rev.* 110, 3479-3500 (2010).

Habibi, Y., T. Heim and R. Douillard, "AC electric field-assisted assembly and alignment of cellulose nanocrystals," *Journal of Polymer Science Part B-Polymer Physics.* 46, 1430-1436 (2008a).

Habibi, Y., A. Goffin, N. Schiltz, E. Duquesne, P. Dubois and A. Dufresne, "Bionanocomposites based on poly(epsilon-caprolactone)-grafted cellulose nanocrystals by ring-opening polymerization," *Journal of Materials Chemistry.* 18, 5002-5010 (2008b).

Hai, F.I., K. Yamamoto and K. Fukushi, "Hybrid treatment systems for dye wastewater," *Crit. Rev. Environ. Sci. Technol.* 37 (2007).

Hamdaoui, O., "Batch study of liquid-phase adsorption of methylene blue using cedar sawdust and crushed brick," *J. Hazard. Mater.* 135, 264-273 (2006).

Hameed, B.H., A.T.M. Din and A.L. Ahmad, "Adsorption of methylene blue onto bamboo-based activated carbon: Kinetics and equilibrium studies," *J. Hazard. Mater.* 141, 819-825 (2007).

Hasani, M., E.D. Cranston, G. Westman and D.G. Gray, "Cationic surface functionalization of cellulose nanocrystals," *Soft Matter*. 4, 2238-2244 (2008).

Hattori, S., M. Doi, E. Takahashi, T. Kurosu, M. Nara, S. Nakamatsu, Y. Nishiki, T. Furuta and M. Iida, "Electrolytic decomposition of amaranth dyestuff using diamond electrodes," *J. Appl. Electrochem.* 33, 85-91 (2003).

Haug, W., A. Schmidt, B. Nortemann, D.C. Hempel, A. Stolz and H.J. Knackmuss, "Mineralization of the Sulfonated Azo Dye Mordant Yellow-3 by a 6-Aminonaphthalene-2-Sulfonate-Degrading Bacterial Consortium," *Appl. Environ. Microbiol.* 57, 3144-3149 (1991).

Herrick, F.W., R.L. Casebier, J.K. Hamilton and K.R. Sandberg, "Microfibrillated cellulose: morphology and accessibility," *J. Appl. Polym. Sci. : Appl. Polym. Symp.* 37, 797-813 (1983).

Heux, L., G. Chauve and C. Bonini, "Nonflocculating and chiral-nematic self-ordering of cellulose microcrystals suspensions in nonpolar solvents," *Langmuir*. 16, 8210-8212 (2000).

Ho, Y.S. and G. McKay, "Sorption of dyes and copper ions onto biosorbents," *Process Biochemistry*. 38, PII S0032-9592(02)00239-X (2003).

Ho, Y.S. and G. McKay, "Kinetic models for the sorption of dye from aqueous solution by wood," *Process Saf. Environ. Prot.* 76, 183-191 (1998).

Hu, T.L., "Decolourization of Reactive Azo Dyes by Transformation with *Pseudomonas-Luteola*," *Bioresour. Technol.* 49, 47-51 (1994).

Huang, Y.H., Y.F. Huang, P.S. Chang and C.Y. Chen, "Comparative study of oxidation of dye-Reactive Black B by different advanced oxidation processes: Fenton, electro-Fenton and photo-Fenton," *J. Hazard. Mater.* 154, 655-662 (2008).

Hubbe, M.A., K.R. Beck, W.G. O'Neal and Y.C. Sharma, "Cellulosic Substrates for Removal of Pollutants from Aqueous Systems: a Review. 2. Dyes," *Bioresources*. 7 (2012).

Humphreys, L.R., "Crawford Munro: A Vision for Australia's Water," *Engineers Media* (2009).

Hunger, K., "Industrial Dyes: Chemistry, Properties, Applications," Wiley-VCH, Cambridge, Weinheim (2003).

Husain, Q., "Potential applications of the oxidoreductive enzymes in the decolorization and detoxification of textile and other synthetic dyes from polluted water: A review," *Crit. Rev. Biotechnol.* 26 (2006).

Idaka, E., T. Ogawa, H. Horitsu and M. Tomoyeda, "Degradation of Azo-Compounds by *Aeromonas-Hydrophila* Var 24b," *Journal of the Society of Dyers and Colourists*. 94,

91-94 (1978).

Iguchi, M., S. Yamanaka and A. Budhiono, "Bacterial cellulose - a masterpiece of nature's arts," *J. Mater. Sci.* 35, 261-270 (2000).

Jain, A.K., V.K. Gupta, A. Bhatnagar and Suhas, "Utilization of industrial waste products as adsorbents for the removal of dyes," *J. Hazard. Mater.* 101 (2003a).

Jain, R., M. Bhargava and N. Sharma, "Electrochemical Studies on a Pharmaceutical Azo Dye: Tartrazine," *Ind Eng Chem Res.* 42, 243-247 (2003b).

Janoš, P., H. Buchtová and M. Rýznarová, "Sorption of dyes from aqueous solutions onto fly ash," *Water Res.* 37, 4938-4944 (2003).

Jiang, H. and P.L. Bishop, "Aerobic Biodegradation of Azo Dyes in Biofilms," *Water Science and Technology.* 29, 525-530 (1994).

Josji, M. and R. Purwar, "Developments in new processes for colour removal from effluent," *Coloration Technology.* 34, 58-71 (2004).

Junior de Menezes, A., G. Siqueira, A.A.S. Curvelo and A. Dufresne, "Extrusion and characterization of functionalized cellulose whiskers reinforced polyethylene nanocomposites," *Polymer.* 50, 4552-4563 (2009).

Juntaro, J., M. Pommet, A. Mantalaris, M. Shaffer and A. Bismarck, "Nanocellulose enhanced interfaces in truly green unidirectional fibre reinforced composites," *Composite Interfaces.* 14, 753-762 (2007).

Kannan, N. and M.M. Sundaram, "Kinetics and mechanism of removal of methylene blue



by adsorption on various carbons-a comparative study,” *Dyes and Pigments*. 51, 25-40 (2001).

Kaushik, P. and A. Malik, “Fungal dye decolourization: Recent advances and future potential,” *Environ. Int.* 35, 127-141 (2009).

Khadhraoui, M., H. Trabelsi, M. Ksibi, S. Bouguerra and B. Elleuch, “Discoloration and detoxification of a Congo red dye solution by means of ozone treatment for a possible water reuse,” *J. Hazard. Mater.* 161, 974-981 (2009).

Khatti, S.D. and M.K. Singh, “Colour removal from synthetic dye wastewater using a bioadsorbent,” *Water Air and Soil Pollution*. 120, 283-294 (2000).

Klemm, D., B. Heublein, H.P. Fink and A. Bohn, “Cellulose: Fascinating biopolymer and sustainable raw material,” *Angewandte Chemie-International Edition*. 44, 3358-3393 (2005).

Klemm, D., P. Bertram, H. Thomas, H. Ute and W. Wagenknecht, “Comprehensive Cellulose Chemistry: Functionalization of Cellulose (Volume 2),” Wiley-WCH, Weinheim (1998).

Klemm, D., F. Kramer, S. Moritz, T. Lindstrom, M. Ankerfors, D. Gray and A. Dorris, “Nanocelluloses: A New Family of Nature-Based Materials,” *Angewandte Chemie-International Edition*. 50, 5438-5466 (2011).

Klemm, D., D. Schumann, F. Kramer, N. Hessler, M. Hornung, H. Schmauder and S. Marsch, “Nanocelluloses as innovative polymers in research and application,” *Polysaccharides II*. 205, 49-96 (2006).

Korzoun, V. and A. Sokolov, “World water balance and water resources of the earth,”

(1978).

Kulla, H.G., F. Klausener, U. Meyer, B. Ludeke and T. Leisinger, "Interference of Aromatic Sulfo Groups in the Microbial-Degradation of the Azo Dyes Orange-I and Orange-II," *Arch. Microbiol.* 135, 1-7 (1983).

Landry, V., A. Alemdar and P. Blanchet, "Nanocrystalline cellulose: morphological, physical, and mechanical properties," *For. Prod. J.* 61, 104-112 (2011).

Langmuir, I., "The Adsorption of Gases on Plane Surfaces of Glass, Mica and Platinum." *J. Am. Chem. Soc.* 40, 1361-1403 (1918).

Lasseguette, E., "Grafting onto microfibrils of native cellulose," *Cellulose.* 15, 571-580 (2008).

Letterman, R.D., "Water quality and treatment : a handbook of community water supplies," McGraw-Hill, New York (1999).

Liakou, S., M. Kornaros and G. Lyberatos, "Pretreatment of azo dyes using ozone," *Water Science and Technology.* 36, 155-163 (1997).

Lima, A.M.D., J.T. Wong, M. Paillet, R. Borsali and R. Pecora, "Translational and rotational dynamics of rodlike cellulose whiskers," *Langmuir.* 19, 24-29 (2003).

Lin, N., G. Chen, J. Huang, A. Dufresne and P.R. Chang, "Effects of Polymer-Grafted Natural Nanocrystals on the Structure and Mechanical Properties of Poly(lactic acid): A Case of Cellulose Whisker-graft-Polycaprolactone," *J Appl Polym Sci.* 113, 3417-3425 (2009).

Lu, P. and Y. Hsieh, "Preparation and properties of cellulose nanocrystals: Rods, spheres, and network," *Carbohydr. Polym.* 82, 329-336 (2010).

Mall, I.D., V.C. Srivastava, N.K. Agarwal and I.M. Mishra, "Adsorptive removal of malachite green dye from aqueous solution by bagasse fly ash and activated carbon-kinetic study and equilibrium isotherm analyses," *Colloids and Surfaces, A: Physicochem. and Eng. Asp.* 264, 17-28 (2005).

Mangalam, A.P., J. Simonsen and A.S. Benight, "Cellulose/DNA Hybrid Nanomaterials," *Biomacromolecules.* 10, 497-504 (2009).

Manz, O.E., "Coal fly ash: a retrospective and future look," *Fuel.* 78, 133-136 (1999).

Martínez-Huitle, C.A. and E. Brillas, "Decontamination of wastewaters containing synthetic organic dyes by electrochemical methods: A general review," *Applied Catalysis B, Environmental.* 87, 105-145 (2009).

Marungrueng, K. and P. Pavasant, "High performance biosorbent (*Caulerpa lentillifera*) for basic dye removal," *Bioresour. Technol.* 98, 1567-1572 (2007).

Maurya, N.S., A.K. Mittal, P. Cornel and E. Rother, "Biosorption of dyes using dead macro fungi: Effect of dye structure, ionic strength and pH," *Bioresour. Technol.* 97, 512-521 (2006).

McKay, G., J.F. Porter and G.R. Prasad, "The removal of dye colours from aqueous solutions by adsorption on low-cost materials," *Water Air and Soil Pollution.* 114, 423-438 (1999).

McKay, G., G. Ramprasad and P. Pratapa Mowli, "Equilibrium studies for the adsorption

of dyestuffs from aqueous solutions by low-cost materials,” *Water Air Soil Pollut.* 29, 273-283 (1986).

McKay, G., “Use of adsorbents for the removal of pollutants from wastewaters,” CRC Press, Boca Raton, Fla. (1996).

Métivier-Pignon, H., C. Faur-Brasquet and P. Le Cloirec, “Adsorption of dyes onto activated carbon cloths: approach of adsorption mechanisms and coupling of ACC with ultrafiltration to treat coloured wastewaters,” *Separation and Purification Technology.* 31, 3-11 (2003).

Mohanty, A.K., M. Misra and G. Hinrichsen, “Biofibres, biodegradable polymers and biocomposites: An overview,” *Macromolecular Materials and Engineering.* 276, 1-24 (2000).

Moldes, D., P.P. Gallego, S.R. Couto and A. Sanroman, “Grape seeds: the best lignocellulosic waste to produce laccase by solid state cultures of *Trametes hirsuta*,” *Biotechnol. Lett.* 25, 491-495 (2003).

Monvisade, P. and P. Siriphannon, “Chitosan intercalated montmorillonite: Preparation, characterization and cationic dye adsorption,” *Appl. Clay. Sci.* 42, 427-431 (2009).

Morandi, G., L. Heath and W. Thielemans, “Cellulose Nanocrystals Grafted with Polystyrene Chains through Surface-Initiated Atom Transfer Radical Polymerization (SI-ATRP),” *Langmuir.* 25, 8280-8286 (2009).

Namasivayam, C. and S. Sumithra, “Removal of direct red 12B and methylene blue from water by adsorption onto Fe (III)/Cr (III) hydroxide, an industrial solid waste,” *J. Environ. Manage.* 74, 207-215 (2005).

Namasivayam, C. and D.J.S.E. Arasi, "Removal of congo red from wastewater by adsorption onto waste red mud," *Chemosphere*. 34, 401-417 (1997).

Namasivayam, C., R.T. Yamuna and D.J.S.E. Arasi, "Removal of procion orange from wastewater by adsorption on waste red mud," *Sep. Sci. Technol.* 37, 2421-2431 (2002).

Nandi, B.K., A. Goswami and M.K. Purkait, "Removal of cationic dyes from aqueous solutions by kaolin: Kinetic and equilibrium studies," *Appl. Clay. Sci.* 42, 583-590 (2009).

Netpradit, S., P. Thiravetyan and S. Towprayoon, "Application of 'waste' metal hydroxide sludge for adsorption of azo reactive dyes," *Water Res.* 37, 763-772 (2003).

O'Neill, C., F.R. Hawkes, D.L. Hawkes, N.D. Lourenco, H.M. Pinheiro and W. Delee, "Colour in textile effluents—sources, measurement, discharge consents and simulation: a review," *Journal of Chemical Technology and Biotechnology*. 74, 1009-1018 (1999).

Ozacar, M. and I.A. Sengil, "Adsorption of metal complex dyes from aqueous solutions by pine sawdust," *Bioresour. Technol.* 96, 791-795 (2005).

Ozcan, A., C. Omeroglu, Y. Erdogan and A.S. Ozcan, "Modification of bentonite with a cationic surfactant: An adsorption study of textile dye Reactive Blue 19," *J. Hazard. Mater.* 140, 173-179 (2007).

Ozcan, A.S. and A. Ozcan, "Adsorption of acid dyes from aqueous solutions onto acid-activated bentonite," *J. Colloid Interface Sci.* 276 (2004).

Pagga, U. and D. Brown, "The degradation of dyestuffs: Part II Behaviour of dyestuffs in aerobic biodegradation tests," *Chemosphere*. 15, 479-491 (1986).

Panizza, M. and G. Cerisola, "Electrocatalytic materials for the electrochemical oxidation of synthetic dyes," *Applied Catalysis B, Environmental*. 75, 95-101 (2007).

Paszczynski, A., V.B. Huynh and R. Crawford, "Comparison of Ligninase-i and Peroxidase-M2 from the White-Rot Fungus *Phanerochaete-Chrysosporium*," *Arch. Biochem. Biophys.* 244, 750-765 (1986).

Peng, B.L., N. Dhar, H.L. Liu and K.C. Tam, "Chemistry and Applications of Nanocrystalline Cellulose and its Derivatives: a Nanotechnology Perspective," *Can. J. Chem. Eng.* 89, 1191-1206 (2011).

Paszczynski, A., M.B. Pastigrigsby, S. Goszczynski, R.L. Crawford and D.L. Crawford, "Mineralization of Sulfonated Azo Dyes and Sulfanilic Acid by *Phanerochaete-Chrysosporium* and *Streptomyces-Chromofuscus*," *Appl. Environ. Microbiol.* 58, 3598-3604 (1992).

Peng, Y., D. Gardner and Y. Han, "Drying cellulose nanofibrils: in search of a suitable method," *Cellulose*. 19, 91-102 (2012).

Perez, D.d.S., S. Montanari and M.R. Vignon, "TEMPO-Mediated Oxidation of Cellulose III," *Biomacromolecules*. 4, 1417-1425 (2003).

Petricic, I., N.P.R. Andersen, S. Sostar-Turk and A.M. Le Marechal, "The removal of reactive dye printing compounds using nanofiltration," *Dyes and Pigments*. 74, 512-518 (2007).

Pranger, L. and R. Tannenbaum, "Biobased Nanocomposites Prepared by In Situ Polymerization of Furfuryl Alcohol with Cellulose Whiskers or Montmorillonite Clay," *Macromolecules*. 41, 8682-8687 (2008).

Purkait, M.K., A. Maiti, S. DasGupta and S. De, "Removal of congo red using activated carbon and its regeneration," *J. Hazard. Mater.* 145, 287-295 (2007).

QU, J., "Research progress of novel adsorption processes in water purification: A review," *Journal of Environmental Sciences.* 20, 1-13 (2008).

Rafatullah, M., O. Sulaiman, R. Hashim and A. Ahmad, "Adsorption of methylene blue on low-cost adsorbents: A review," *J. Hazard. Mater.* 177, 70-80 (2010).

Rai, H.S., M.S. Bhattacharyya, J. Singh, T.K. Bansal, P. Vats and U.C. Banerjee, "Removal of dyes from the effluent of textile and dyestuff manufacturing industry: A review of emerging techniques with reference to biological treatment," *Crit. Rev. Environ. Sci. Technol.* 35 (2005).

Ravi Kumar, M.N.V., "A review of chitin and chitosan applications," *React Funct Polym.* 46, 1-27 (2000).

Reife, A. and H.S. Freeman, "Environmental chemistry of dyes and pigments," Wiley, New York (1996).

Revol, J.F., H. Bradford, J. Giasson, R.H. Marchessault and D.G. Gray, "Helicoidal Self-Ordering of Cellulose Microfibrils in Aqueous Suspension," *Int. J. Biol. Macromol.* 14, 170-172 (1992).

Revol, J.F., L. Godbout, X.M. Dong, D.G. Gray, H. Chanzy and G. Maret, "Chiral Nematic Suspensions of Cellulose Crystallites - Phase-Separation and Magnetic-Field Orientation," *Liquid Crystals.* 16, 127-134 (1994).

Rijsberman, F.R., "Water scarcity: Fact or fiction?" *Agric. Water Manage.* 80, 5-22

(2006).

Rinaudo, M., "Chitin and chitosan: Properties and applications," *Progress in Polymer Science*. 31, 603-632 (2006).

Robinson, T., G. McMullan, R. Marchant and P. Nigam, "Remediation of dyes in textile effluent: a critical review on current treatment technologies with a proposed alternative," *Bioresour. Technol.* 77 (2001).

Saha, P., S. Chowdhury, S. Gupta, I. Kumar and R. Kumar, "Assessment on the Removal of Malachite Green Using Tamarind Fruit Shell as Biosorbent," *Clean-Soil Air Water*. 38, 437-445 (2010).

Saheb, D.N. and J.P. Jog, "Natural fiber polymer composites: A review," *Adv. Polym. Technol.* 18, 351-363 (1999).

Saito, T. and A. Isogai, "TEMPO-Mediated Oxidation of Native Cellulose. The Effect of Oxidation Conditions on Chemical and Crystal Structures of the Water-Insoluble Fractions," *Biomacromolecules*. 5, 1983-1989 (2004).

Samir, M.A.S.A., F. Alloin and A. Dufresne, "Review of recent research into cellulosic whiskers, their properties and their application in nanocomposite field," *Biomacromolecules*. 6, 612-626 (2005).

Sassi, J.F. and H. Chanzy, "Ultrastructural Aspects of the Acetylation of Cellulose," *Cellulose*. 2, 111-127 (1995).

Sharma, P., H. Kaur, M. Sharma and V. Sahore, "A review on applicability of naturally available adsorbents for the removal of hazardous dyes from aqueous waste," *Environ.*



Monit. Assess. 183, 151-195 (2011).

Shibata, I. and A. Isogai, "Depolymerization of cellouronic acid during TEMPO-mediated oxidation," *Cellulose*. 10, 151-158 (2003).

Shore, J., "Advances in direct dyes," *Indian Journal of Fibre & Textile Research*. 21 (1996).

Shukla, A., Y. Zhang, P. Dubey, J.L. Margrave and S.S. Shukla, "The role of sawdust in the removal of unwanted materials from water," *J. Hazard. Mater.* 95, 137-152 (2002).

Singh, K. and S. Arora, "Removal of Synthetic Textile Dyes From Wastewaters: A Critical Review on Present Treatment Technologies," *Crit. Rev. Environ. Sci. Technol.* 41, 807-878 (2011).

Siro, I. and D. Plackett, "Microfibrillated cellulose and new nanocomposite materials: a review," *Cellulose*. 17, 459-494 (2010).

Široký, J., R.S. Blackburn, T. Bechtold, J. Taylor and P. White, "Alkali treatment of cellulose II fibres and effect on dye sorption," *Carbohydr. Polym.* 84, 299-307 (2011).

Sivasamy, A. and N. Sundarabal, "Biosorption of an Azo Dye by *Aspergillus niger* and *Trichoderma* sp. Fungal Biomasses," *Curr. Microbiol.* 62, 351-357 (2011).

Slokar, Y.M. and A.M. Le Marechal, "Methods of Decoloration of Textile Wastewaters," *Dyes and Pigments*. 37, 335-356 (1998).

Socha, A., E. Sochocka, R. Podsiadly and J. Sokolowska, "Electrochemical and photo-electrochemical degradation of direct dyes," *Coloration Technology*. 122, 207-212 (2006).

Song, Y., J. Li and H. Chen, "Degradation of CI Acid Red 88 aqueous solution by combination of Fenton's reagent and ultrasound irradiation," *Journal of Chemical Technology and Biotechnology*. 84 (2009).

Sotero-Santos, R.B., O. Rocha and J. Povinelli, "Toxicity of ferric chloride sludge to aquatic organisms," *Chemosphere*. 68, 628-636 (2007).

Stroobants, A., H.N.W. Lekkerkerker and T. Odijk, "Effect of Electrostatic Interaction on the Liquid-Crystal Phase-Transition in Solutions of Rodlike Polyelectrolytes," *Macromolecules*. 19, 2232-2238 (1986).

Tang, C. and V. Chen, "Nanofiltration of textile wastewater for water reuse," *Desalination*. 143, 11-20 (2002).

Thurston, C.F., "The Structure and Function of Fungal Laccases," *Microbiology-Sgm*. 140, 19-26 (1994).

Tor, A. and Y. Cengelolu, "Removal of congo red from aqueous solution by adsorption onto acid activated red mud," *J. Hazard. Mater.* 138, 409-415 (2006).

Turbak, A.F., F.W. Snyder, K.R. Sandberg, S. ITT Rayonier Inc. WA and Conference: 9. cellulose conference, Syracuse, NY, USA, 24 May 1982, "Microfibrillated cellulose, a new cellulose product: properties, uses, and commercial potential," *J.Appl.Polym.Sci.: Appl.Polym.Symp.* 37, 815-827 (1983).

Unuabonah, E.I., K.O. Adebowale and F.A. Dawodu, "Equilibrium, kinetic and sorber design studies on the adsorption of Aniline blue dye by sodium tetraborate-modified Kaolinite clay adsorbent," *J. Hazard. Mater.* 157, 397-409 (2008).

Uygur, A., "An overview of oxidative and photooxidative decolorisation treatments of textile waste waters," *Journal of the Society of Dyers and Colourists*. 113, 211-217 (1997).

Vadivelan, V. and K.V. Kumar, "Equilibrium, kinetics, mechanism, and process design for the sorption of methylene blue onto rice husk," *J. Colloid Interface Sci.* 286, 90-100 (2005).

van der Zee, F.P., G. Lettinga and J.A. Field, "The role of (auto)catalysis in the mechanism of an anaerobic azo reduction," *Water Science and Technology*. 42, 301-308 (2000).

Varma, A.J., S.V. Deshpande and J.F. Kennedy, "Metal complexation by chitosan and its derivatives: a review," *Carbohydr. Polym.* 55, 77-93 (2004).

Venkataraman, K., "The Chemistry of Synthetic Dyes," Academic Press Inc., New York (1965).

Verma, A.K., R.R. Dash and P. Bhunia, "A review on chemical coagulation/flocculation technologies for removal of colour from textile wastewaters," *J. Environ. Manage.* 93, 154-168 (2012).

Vishnu, G. and K. Joseph, "Nanofiltration and ozonation for decolorisation and salt recovery from reactive dyebath," *Coloration Technology*. 123, 260-266 (2007).

Wagberg, L., L. Winter, L. Odberg and T. Lindstrom, "On the Charge Stoichiometry upon Adsorption of a Cationic Polyelectrolyte on Cellulosic Materials," *Colloids and Surfaces*. 27, 163-173 (1987).

Walker, R. and A.J. Ryan, "Some molecular parameters influencing rate of reduction of azo compounds by intestinal microflora." *Xenobiotica*. 1, 483-6 (1971).

Wan, W.K., J.L. Hutter, L. Millon and G. Guhados, "Bacterial cellulose and its nanocomposites for biomedical applications," *Cellulose Nanocomposites: Processing, Characterization, and Properties*. 938, 221-241 (2006).

Wang, J.S. and K. Matyjaszewski, "Controlled Living Radical Polymerization - Atom-Transfer Radical Polymerization in the Presence of Transition-Metal Complexes," *J. Am. Chem. Soc.* 117, 5614-5615 (1995).

Wang, S., H. Li and L. Xu, "Application of zeolite MCM-22 for basic dye removal from wastewater," *J. Colloid Interface Sci.* 295, 71-78 (2006).

Wang, S., Y. Boyjoo, A. Choueib and Z.H. Zhu, "Removal of dyes from aqueous solution using fly ash and red mud," *Water Res.* 39, 129-138 (2005).

Wong, Y., Y. Szeto, W. Cheung and G. McKay, "Adsorption of acid dyes on chitosan—equilibrium isotherm analyses," *Process Biochemistry*. 39, 695-704 (2004).

Wong, Y.C., Y.S. Szeto, W.H. Cheung and G. McKay, "Equilibrium Studies for Acid Dye Adsorption onto Chitosan," *Langmuir*. 19, 7888-7894 (2003).

Wong, Y. and J. Yu, "Laccase-catalyzed decolorization of synthetic dyes," *Water Res.* 33, 3512-3520 (1999).

Wu, F., R. Tseng and R. Juang, "Comparative adsorption of metal and dye on flake- and bead-types of chitosans prepared from fishery wastes," *J. Hazard. Mater.* 73, 63-75 (2000).

Wuhrmann, K., K. Mechsner and T. Kappeler, "Investigation on Rate-Determining Factors in the Microbial Reduction of Azo Dyes," *Eur. J. Appl. Microb. Biotechnol.* 9, 325-338

(1980).

Xia, F., E. Ou, L. Wang and J. Wang, "Photocatalytic degradation of dyes over cobalt doped mesoporous SBA-15 under sunlight," *Dyes and Pigments*. 76, 76-81 (2008).

Xu, X.R., H.B. Li, W.H. Wang and J.D. Gu, "Decolorization of dyes and textile wastewater by potassium permanganate," *Chemosphere*. 59, 893-898 (2005).

Xu, X.R., H.B. Li, W.H. Wang and J.D. Gu, "Degradation of dyes in aqueous solutions by the Fenton process," *Chemosphere*. 57, 595-600 (2004).

Yang, T., X.D. Wen, J. Li and L. Yang, "Theoretical and experimental investigations on the structures of purified clay and acid-activated clay," *Appl. Surf. Sci.* 252, 6154-6161 (2006).

Yi, J., Q. Xu, X. Zhang and H. Zhang, "Temperature-induced chiral nematic phase changes of suspensions of poly(N,N-dimethylaminoethyl methacrylate)-grafted cellulose nanocrystals," *Cellulose*. 16, 989-997 (2009).

Young, L. and J. Yu, "Ligninase-catalysed decolorization of synthetic dyes," *Water Res.* 31, 1187-1193 (1997).

Yuan, H.H., Y. Nishiyama, M. Wada and S. Kuga, "Surface acylation of cellulose whiskers by drying aqueous emulsion," *Biomacromolecules*. 7, 696-700 (2006).

Zhang, F., A. Yediler, X. Liang and A. Kettrup, "Effects of dye additives on the ozonation process and oxidation by-products: a comparative study using hydrolyzed C.I. Reactive Red 120," *Dyes and Pigments*. 60, 1-7 (2004).

Zhao, X. and I.R. Hardin, "HPLC and spectrophotometric analysis of biodegradation of azo dyes by *Pleurotus ostreatus*," *Dyes and Pigments*. 73, 322-325 (2007).

Zhen, Z.M. and J. Yu, "Stresses on immobilized *Phanerochaete chrysosporium* hyphae in submerged cultures for ligninase production," *Can. J. Chem. Eng.* 76, 784-789 (1998).

Zollinger, H., "Color Chemistry: Syntheses, Properties, and Applications of Organic Dyes and Pigmentss," VCH Publications, New York (1991).